A Szilikátipari Tudományos Egyesület lapja

építőanyag

Journal of Silicate Based and Composite Materials

A TARTALOMBÓL:

- Rheological investigation of SBR/CW/CB tricomposite used to create a sustainable procedure for idler rollers production
- The effect of mechanical activation on the compressive strength of landfilled fly ash geopolymers
- Rheological properties of blended metakaolin self-compacting concrete containing recycled CRT funnel glass aggregate
- Rheological characterization of the curing process for a water-based epoxy added with polythiol crosslinking agent
- Student hostel for Turkish students
- Two approaches to the modelling of chip formation: rheological models and finite element analysis

2019/5

ESCM
EUROPEAN SOCIETY
FOR COMPOSITE MATERIALS

THE SCIENTIFIC,
ENGIEERING
AND INDUSTRIAL
COMMNITY
INVOLVED WITH
COMPOSITE
MATERIALS

THE SOCIETY

OBJECTIVES OF THE SOCIETY

ESCM is a European, non-governmental, non-profit scientific and engineering organisation with the following objectives:

- To encourage the free interchange of information on all those aspects related to composite materials which of are interest to the scientific and engineering community.
- To provide a Europe-wide forum for the discussion of such topics, e.g. by organising the ECCM (European Conference on Composite Materials) and more specialised symposia related to composites.
- To guide and foster the understanding and utilisation of the science and technology of composite materials.
- To promote European co-operation in the study of topics in composite materials science and technology.
- To promote liaison with engineering and scientific bodies throughout Europe with similar aims and to serve as a facilitator for communication between such bodies.
- To foster an environment for timely and cost-effective research, development and implementation of advanced technology in composites.
- To encourage the education of young specialists in the disciplines supporting composite materials science and technology.
- To recognise individuals of outstanding achievement in the science, technology, engineering, and application of composite materials.

építőanyag

2019/5

Journal of Silicate Based and Composite Materials

TARTALOM

144 Feszítőgörgők fenntartható előállítására szolgáló SBR/CW/CB háromkomponensű rendszer reológiai vizsgálata
Mohammed H. AL-MAAMORI ▪ Abbass A. HASHIM ▪ Ali I. AL-MOSAWI ▪ Shaymaa Abbas ABDULSADA ▪ MAROSSY Kálmán

148 Mechanikai aktiválás hatása deponált pernye alapú geopolimerek nyomószilárdságára
AMBRUS Mária

154 Újrahasznosított CRT tölcsérüveg adalékanyag és metakaolin kiegészítő anyag tartalmú öntömörödő beton reológiai tulajdonságai
Younes OULDKHAOUA ▪ Benchaa BENABED ▪ Rajab ABOUSNINA ▪ El-Hadj KADRI

162 Politiol térhálósító szert tartalmazó vízbázisú epoxi utókezelési folyamatának reológiai jellemzése
Maria Myrelle S. QUIAMBAO ▪ Danilo D. LAPLANA ▪ Miguel Ibarra D. ABOBO ▪ Angelica G. JANCON ▪ Sonia D. SALVADOR ▪ Henry C. SIY ▪ David P. PENALOZA Jr.

168 Kollégium török diákok számára
MIKLÓS Gábor

173 Két eljárás a forgácsképződés modellezésére: reológiai modellek és véges elemes analízis
Jüri OLT ▪ Olga LIIVAPUU

CONTENT

144 Rheological investigation of SBR/CW/CB tricomposite used to create a sustainable procedure for idler rollers production
Mohammed H. AL-MAAMORI ▪ Abbass A. HASHIM ▪ Ali I. AL-MOSAWI ▪ Shaymaa Abbas ABDULSADA ▪ Kálmán MAROSSY

148 The effect of mechanical activation on the compressive strength of landfilled fly ash geopolymers
AMBRUS Mária

154 Rheological properties of blended metakaolin self-compacting concrete containing recycled CRT funnel glass aggregate
Younes OULDKHAOUA ▪ Benchaa BENABED ▪ Rajab ABOUSNINA ▪ El-Hadj KADRI

162 Rheological characterization of the curing process for a water-based epoxy added with polythiol crosslinking agent
Maria Myrelle S. QUIAMBAO ▪ Danilo D. LAPLANA ▪ Miguel Ibarra D. ABOBO ▪ Angelica G. JANCON ▪ Sonia D. SALVADOR ▪ Henry C. SIY ▪ David P. PENALOZA Jr.

168 Student hostel for Turkish students
Gábor MIKLÓS

173 Two approaches to the modelling of chip formation: rheological models and finite element analysis
Jüri OLT ▪ Olga LIIVAPUU

A finomkerámia-, üveg-, cement-, mész-, beton-, tégla- és cserép-, kő- és kavics-, tűzállóanyag-, szigetelőanyag-iparágak szakmai lapja
Scientific journal of ceramics, glass, cement, concrete, clay products, stone and gravel, insulating and fireproof materials and composites

A folyóiratot referálja · The journal is referred by:

A folyóiratban lektorált cikkek jelennek meg.
All published papers are peer-reviewed.
Kiadó · Publisher: Szilikátipari Tudományos Egyesület (SZTE)
Elnök · President: ASZTALOS István
1034 Budapest, Bécsi út 122–124.
Tel.: +36-1/201-9360 ▪ E-mail: epitoanyag@szte.org.hu
Tördelő szerkesztő · Layout editor: NÉMETH Hajnalka
Címlapfotó · Cover photo: GYURKÓ Zoltán

WWW.EPITOANYAG.ORG.HU
EN.EPITOANYAG.ORG.HU

Online ISSN: 2064-4477
Print ISSN: 0013-970x
INDEX: 2 52 50 ▪ 71 (2019) 143–178

Rheological investigation of SBR/CW/CB tricomposite used to create a sustainable procedure for idler rollers production

Mohammed H. AL-MAAMORI ▪ College of Materials Engineering, University of Babylon, Iraq
Abbass A. HASHIM ▪ Professor, Director, Power of Technology Company, Sheffield, UK
▪ Engineering and Technology Department, University Campus, North Lincolnshire, UK
Ali I. AL-MOSAWI ▪ University of Miskolc, Miskolc, 3515 Egyetemváros, Hungary
▪ qkoali76@uni-miskolc.hu
Shaymaa Abbas ABDULSADA ▪ University of Miskolc, Miskolc, 3515 Egyetemváros, Hungary
Kálmán MAROSSY ▪ University of Miskolc, Miskolc, 3515 Egyetemváros, Hungary

Érkezett: 2019. 09. 17. ▪ Received: 17. 09. 2019. ▪ https://doi.org/10.14382/epitoanyag-jsbcm.2019.25

Abstract

The concept of sustainability is now considered as the key of the future, not just for industry but also for all resources on this planet. The real guarantee for the continuation of life is by recycling all types of industrial waste using a method that combines a high level of efficiency and environmental pollution protection. This will create a sustainable resource that keeps earth's natural resources from depletion. In this study, we introduce a technological procedure for the use of cement waste in manufacturing engineering parts with high efficiency. Rheological analysis for styrene butadiene rubber has been investigated as function percentages additives (10-35 pphr) of cement waste (CW) and carbon black (CB). The rheological properties include torque and thermos-plasticity measured at temperature ranges of 165 °C, 175 °C and 185 °C. The tests showed that the cement waste has the ability and efficiency for improving the rheological properties of styrene butadiene rubber.

Keywords: SBR, cement waste, carbon black, rheological properties, sustainability
Kulcsszavak: SBR, cementhulladék, szénfekete, reológiai tulajdonságok, fenntarthatóság

Mohammed H. AL-MAAMORI
Professor of Rubber Technology at Faculty of Materials Engineering, University of Babylon, IRAQ. Research Interests: Rubber Technology, Materials Testing, Materials Processing.

Abbass A. HASHIM
Director at Power of Technology Company, Sheffield, UK. Professor at Engineering and Technology Department, University Campus, North Lincolnshire, UK. Research Interests: Polymers and Composite, Rubber Technology, Materials Testing and Processing.

Ali I. AL-MOSAWI
PhD Student at Institute of Ceramic and Polymer Engineering, Faculty of Materials Science and Engineering, University of Miskolc, Hungary. Research Interests: Polymers, Composite Materials, Rubber Technology, Flame Retardants, Materials Testing, Materials Processing.

Shaymaa Abbas ABDULSADA
PhD Student at Institute of Metallurgy, Faculty of Materials Science and Engineering, University of Miskolc, Hungary. Research Interests: Materials Testing and Processing, Engineering of Metallurgy, Corrosion Engineering, Heat Treatment of Metals, Casting of Metals.

Kálmán MAROSSY
Professor of Polymer Engineering at Institute of Ceramic and Polymer Engineering, University of Miskolc, Hungary. Research Interests: Polymer Blends, Multiphase polymer systems, Relaxation phenomenon, Thermally stimulated discharge, Polymer degradation, Composite materials, Rubber.

1. Introduction

Rubber has been used for a long time in many important industrial applications, because of its distinctive characteristics [1-3]. Researchers over the years conducted studies to develop its structure and characteristics not only by creating a new types of rubber, but also develop the existing types by adding fillers or changing processing conditions and study how its properties are affected. Rheological properties are greatly affected by the processing method and additives [4-8]. Because of rubber is a viscoelastic material, its rheological properties will change during processing. In addition, the presence of fillies within rubber composition such as carbon black or silicon dioxide will change the rheological behaviour of rubber making it more complex. The degree of change in processing conditions depends on the amount of the fillers [9-11]. When studying the rheological behaviour of rubber it is important to calculate the rate of flow at different conditions in terms of stress, applied time of stress, temperature and resilience [12-17].

Iraq's environmental regions near cement factories suffers from high concentrations of pollution [18-19]. This is due to the use of old cement factorization techniques and non-compliance with environmental standards and safety requirements. The use of filters to remove suspended dust in the air - which is a result of crushing raw materials - reduces gases emission throughout the process and dust coming out of the oven during the burning stage of raw materials and clinker crushing, are safe methods for disposal from this waste. All these environmental issues caused a significant damage for the surrounding areas of cement factories and travel to far areas by dust particles volatilization [20-21]. Therefore, it is necessary to provide an appropriate technological procedure to safely dispose the wastes for all types of industrial waste not just for cement waste, to be incorporate into useful engineering applications, where it can be used as fillers for rubber and polymers composition [22-36]. The main aim of this research is the use of cement waste as filler for styrene butadiene rubber (SBR) and to study the effect of this additive on the rheological properties in order to prove that these wastes are useful for manufacturing of idler rollers used in chain conveyors and elevators at grain silos of Iraqi State Trade Company.

2. Methodology

2.1 Materials

Styrene butadiene rubber type KER 1502 containing 23.5% Styrene supplied by Synthos S.A., Poland; Carbon black type N375 supplied by Sullivan Qiao Shanghai King Chemicals Co., Ltd., China; Zinc oxide with supplied by Saha Metal San. Tic. Ltd. Şti, Turkey; Stearic acid supplied by Hefei TNJ Chemical Industry Co.,Ltd, China; Antioxidant 6PPD supplied by Flexsys Rubber Chemicals Ltd, Belgium; Accelerator MBS supplied by Richest Group, China. Paraffin Wax supplied by Kerax Limited, England; Sulfur supplied by

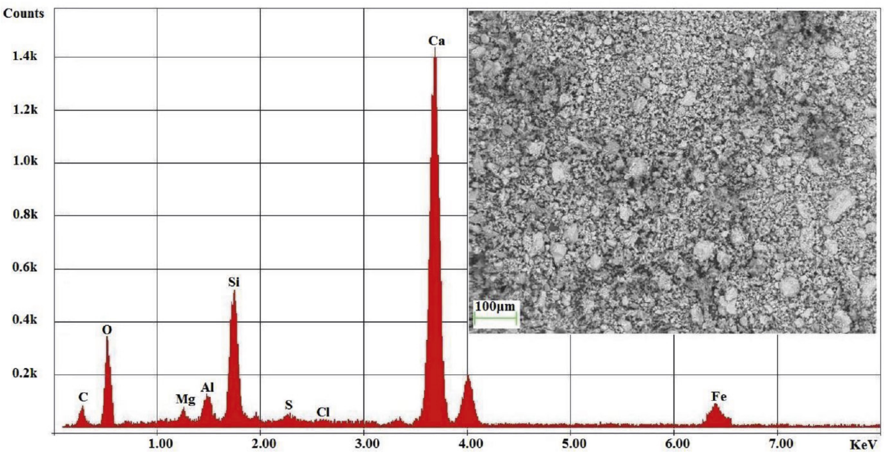

Fig. 1 SEM - energy dispersive X-ray microanalysis for cement waste
1. ábra A cement pásztázó elektronmikroszkóppal végzett energia-diszperzív röntgen mikroanalízise

Leader Technologies Co.,Ltd, China; Processing oil supplied by Shell oil company; and Cement waste (Kiln dust) which results from Portland cement manufacturing at Kufa cement plant, Iraq which using the wet process for producing cement . The chemical composition of cement waste shown in *Table 1*, and scanning electron microscopy (SEM) was used for structural analysis of cement waste as shown in *Fig. 1*.

Material	wt.%
SiO_2	11.11
Al_2O_3	2.38
Fe_2O_2	2.55
CaO	46.29
MgO	1.12
SO_3	0.59
Cl	0.12

Table 1 Chemical composition of cement waste
1. táblázat A cement hulladék kémiai összetétele

Material	Batches composition ratio, pphr			
	C_1	C_2	C_3	C_4
SBR type KER 1502 (23.5% Styrene)	100	100	100	100
Zinc oxid	5	5	5	5
Stearic acid	2	2	2	2
Paraphinic wax	2	2	2	2
Processing oil	5	5	5	5
Antioxidant 6PPD	0.5	0.5	0.5	0.5
Accelerator MBS	1	1	1	1
Sulfur	1.5	1.5	1.5	1.5
Carbon black (CB)	10	20	30	35
Cement waste (CW)	10	20	30	35

Table 2 Samples' ingredients
2. táblázat A minták összetétele

2.2 Sample preparation and testing

The raw material batches illustrated in *Table.2* had been processed by roll mill machine type Comerio Ercole Busto Avsizo with 20 rpm rotating speed, which contains two rolls with 150 mm diameter and 300 mm length rotating with 24 rpm speed. The cure characteristics for the four batches samples were evaluated according to the standard ASTM D2705 by using micro vision enterprises (MV-ODR) devise [37]. The test was done at temperature 165, 175 and 185 °C and 12 min for each sample.

3. Results and discussion

The rheological behaviour of SBR/CW/CB tricomposite at different temperature ranges and percentages of CW/CB additives are shown in *Figs. 2, 3* and *4* respectively. From these figures we can see that the deviations in rheological properties are dependent on the amount of CW/CB additives. At the initial stage of processing, the rubber is primarily heated where the viscosity is decreased and the torque is decreased consequently. In this earlier phase, the rubber compound begins to vulcanize and transform to elastic solid and the torque starts recovering. The minimum shear stress can be recorded also where the molecular chain scission may be occurred. The torque continues to rise up which proves that the crosslinking has been occurred and dominates the rubber structure [38].

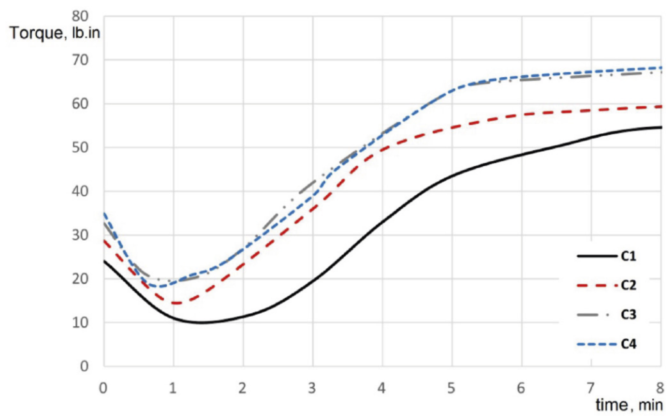

Fig. 2 Rheograph of SBR/CW/CB tricomposite at 165 °C with different percentages additives of CW/CB (C1, C2, C4 and C4 batches)
2. ábra SBR/CW/CB háromkomponensű rendszer Rheograph nyomaték görbéje 165 °C-on különböző CW/CB adagolás esetén (C1, C2, C3 és C4 minták)

Figs. 5, 6 and *7* shows the variation in τ_i,τ_{min}, and τ_{max} due to CW/CB additives and temperatures. From *Fig. 5* we can observe that the increase of initial torque (τ_i) was linear as the percentage of additives increases. It was 0.44 at 165 °C and 175 °C. After that it increased to 0.54 at 185 °C. This is an early indication that the SBR/CW/CB tricomposite is behaving differently at this particular temperature, where is some sort of internal structural changes have been occurred like crosslinking as we mentions above.

Fig. 6 shows that the highest τ_{min} and τ_{max} values were at 30 pphr CW/CB, where the SBR/CW/CB tricomposite has reached the optimum torque improvement. The rate of linear trend in *Fig. 7* for all CW/CB filler percentages is 0.82. Overall torque values obtained from rheographs increase positively with the increasing of the CW/CB additives percentage. This behavior is due to the performance and density of crosslinking inside rubber chains structure and that leads to increase vulcanization efficiency and rubber viscosity [39].

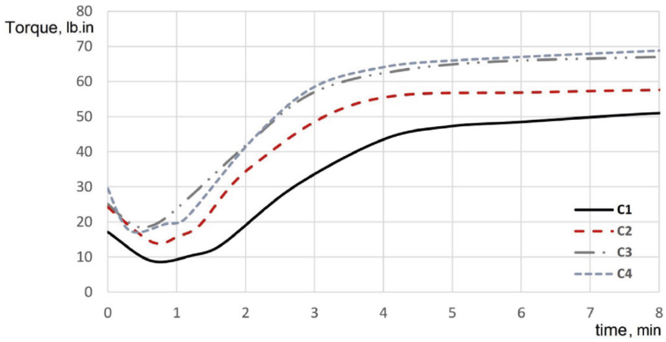

Fig. 3 *Rheograph of SBR/CW/CB tricomposite at 175 °C with different percentages additives of CW/CB (C1, C2, C4 and C4 batches)*
3. ábra *SBR/CW/CB háromkomponensű rendszer Rheograph nyomaték görbéje 175 °C-on különböző CW/CB adagolás esetén (C1, C2, C3 és C4 minták)*

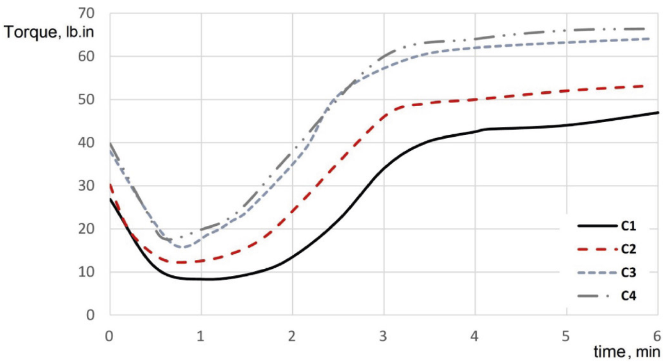

Fig. 4 *Rheograph of SBR/CW/CB tricomposite at 185 °C with different percentages additives of CW/CB (C1, C2, C4 and C4 batches)*
4. ábra *SBR/CW/CB háromkomponensű rendszer Rheograph nyomaték görbéje 185 °C-on különböző CW/CB adagolás esetén (C1, C2, C3 és C4 minták)*

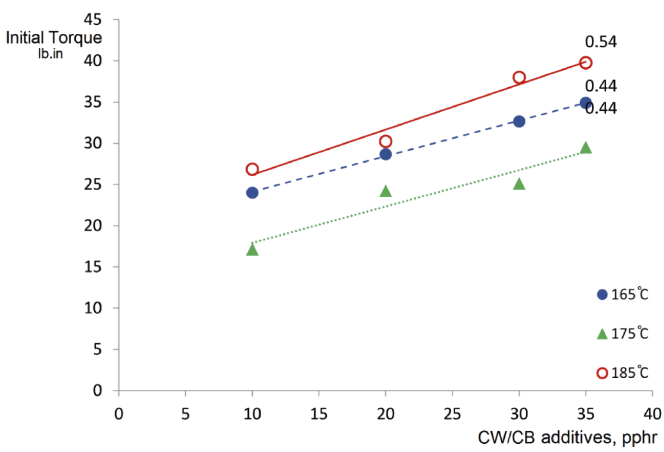

Fig. 5 *Initial torque of SBR/CW/CB tricomposite as a function of CW/CB additions at 165 °C, 175 °C and 185 °C temperature ranges*
5. ábra *SBR/CW/CB háromkomponensű rendszer kezdeti nyomatéka 165 °C, 175 °C és 185 °C-on a CW/CB adagolás függvényében*

4. Conclusions

1. The success of cement waste as an effective filler for improving the rheological properties of SBR has been proven by rheological tests.
2. The optimum of the rheological properties were obtained with CW/CB 30 pphr addition.
3. As a result of crosslinking enhancing for the interior structure of SBR tricomposite by CW/CB additives, the torque values (τ_i, τ_{min} and τ_{max}) has been refined.

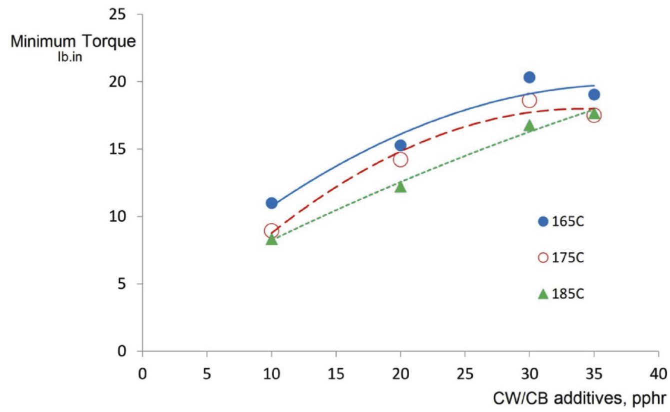

Fig. 6 *Minimum torque SBR/CW/CB tricomposite as a function of CW/CB additions at 165 °C, 175 °C and 185 °C temperature ranges*
6. ábra *SBR/CW/CB háromkomponensű rendszer minimális nyomatéka 165 °C, 175 °C és 185 °C-on a CW/CB adagolás függvényében*

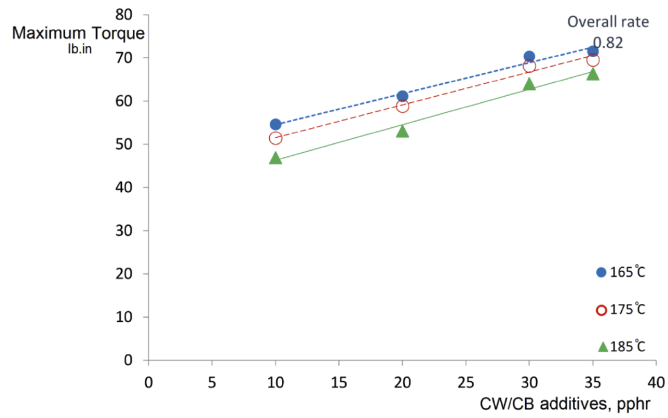

Fig. 7 *Maximum torque SBR/CW/CB tricomposite as a function of CW/CB additions at 165 °C, 175 °C and 185 °C temperature ranges*
7. ábra *SBR/CW/CB háromkomponensű rendszer maximális nyomatéka 165 °C, 175 °C és 185 °C-on a CW/CB adagolás függvényében*

References

[1] Al-Maamori, M. H., – Al-Mosawi, A. I. (2013): Rubber technology: experimental studies, 1st edition, LAP Lambert Academic Publishing, Germany. ISBN:978-3659393105
[2] White, J. L. (1995): Rubber processing: technology, materials, and principles, 1st edition, Hanser Publisher. ISBN: 978-1569901656
[3] Al-Mosawi, A. I. (2015): Experimental data: Polymers and rubber, 1st edition, United States: Createspace Independent Publishing Platform. ISBN: 978-1514657461
[4] Montes, S., – White, J. L. – Nakajima, N. (1988): Rheological behavior of rubber carbon black compounds in various shear flow histories, *Journal of Non-Newtonian Fluid Mechanics*, Vol.28, Issue.2, pp.183-212. https://doi.org/10.1016/0377-0257(88)85039-0
[5] Roland, C. M. (2013): Rheological behavior and processing of unvulcanized rubber, in James E. Mark, Burak Erman and C. Michael Roland (authors) the science and technology of rubber, 4th edition, pp.285-336. https://doi.org/10.1016/B978-0-12-394584-6.00006-6
[6] Song, Y. – Zeng, L. – Zheng, Q. (2017): Reconsideration of the rheology of silica filled natural rubber compounds, *The Journal of Physical Chemistry B*, Vol.121, Issue.23, pp 5867-5875. https://doi.org/10.1021/acs.jpcb.7b02760
[7] Zaeimoedin, T. Z. – Kamal, M. M. – Aziz, A. K. C. (2016): Rheological properties and extrusion performance evaluation of silica filled epoxidized

natural rubber (ENR) compounds as compared to natural rubber/butadiene rubber (NR/BR) compound, *Advanced Materials Research*, Vol.1133, pp.236-240.
https://doi.org/10.4028/www.scientific.net/AMR.1133.236

[8] Yaacob, H. – Mughal, M. A. – Jaya, R. P. – Hainin, M. R. – Jayanti, D. S. – Wan. C. N. C. (2016): Rheological properties of styrene butadiene rubber modified bitumen binder, *Jurnal Teknologi*, Vol.78, No.7-2, pp. 121-126. https://doi.org/10.11113/jt.v78.9503

[9] Wiessner, S. (2015): Rheological behavior and rubber processing, in S. Kobayashi, K. Müllen (eds.) Encyclopedia of Polymeric Nanomaterials, Springer, Berlin, Heidelberg, pp.1-10.
https://doi.org/10.1007/978-3-642-29648-2

[10] Crié, A. – Baritaud, C. – Valette, R. – Vergnes, B. (2015): Rheological behavior of uncured styrene-butadiene rubber at low temperatures, pure and filled with carbon black, Polymer engineering and Science, Vol.55, Issue.9, pp.2156-2162. https://doi.org/10.1002/pen.24090

[11] Al-Maamori, M. H. (2006): Mechanical properties of polymeric composite materials, Ph.D thesis, UOT, IRAQ.

[12] White, J. L. (2005): Rheological behavior and processing of unvulcanized rubber, Chapter 6 in James E. Mark, Burak Erman and Frederick R. Eirich (eds.) Science and Technology of Rubber, 3rd edition, pp.237-319. https://doi.org/10.1016/B978-012464786-2/50009-2

[13] Mostafa, A. – Abouel-Kasem, A. – Bayoumi, M. – El-Sebaie, M. (2010): Rubber-filler interactions and its effect in rheological and mechanical properties of filled compounds, *Journal of Testing and Evaluation*, Vol.38, No.3, pp.347-359. https://doi.org/10.1520/JTE101942

[14] Al-Maamori, M. H. – Al-Mosawi, Ali I. – Abdulsada, S. A. (2016): Rheological behavior of Rubber Blends», 2nd International conference on innovative trends in Engineering, Science and Management (ICITESM-16), YMCA , Jai Singh Road, Delhi, India.

[15] Boochathum, P. (2014): Rheological Behaviour of Natural Rubber Based Blends, Chapter 18 in S. Thomas, C.H. Chan, L. Pothen, Rajisha K. R., H. Maria (eds), Natural rubber materials: volume 1: Blends and IPNs, pp. 394 - 440 . https://doi.org/10.1039/9781849737647-00394

[16] Münstedt, H. (1981): Rheology of rubber-modified polymer melts, *Polymer engineering and Science*, Vol.21, Issue.5, pp.259-270. https://doi.org/10.1002/pen.760210503

[17] Gömze, L. A. (2015): Compilation of Scientific Papers I, GREX Engineering Service Ltd. publisher, Hungary. ISBN: 978-963-12-3088-8

[18] Al-Mosawi, A. I. – Hashim, A. A. – Al-Maamori, M. H. (2019): Production of high performance mountings by using rubber-polymer waste, *Open Access Library Journal*, Vol.6, No.4, pp. 1-6.
https://doi.org/10.4236/oalib.1105368

[19] Al-Mosawi, A. I. (2013): Environmental impact study for the establishment of an investment project to process the palms agricultural waste , *Journal of University of Babylon* , Special Issue for 5th International conference of environmental science, Environmental research center , University of Babylon , IRAQ.

[20] Al-Maamori, M. H. – Al-Mosawi, A. I. (2014): Manufacturing of composite rubber material for the manufacturing of rubber rubbles and other reinforced by a brass Bushes used in mechanical and electrical couplings, Central Organization for Standardization and Quality Control (COSQC), Patent No.3913, International Classification (C08C19/42), Iraqi Classification (4), IRAQ.

[21] Al-Mosawi, A. I. – Al-Maamori, M. H. – Abdulsada, S. A. (2015): Mechanical Properties of Acrylonitrile - Butadiene Rubber Reinforced by Cement Waste, *Journal of Thin Films, Coating Science Technology and Application*, Vol.2, No.2, pp. 13–16.

[22] Al-Salem, S. M. – Lettieri, P. – Baeyens, J. (2009): Recycling and recovery routes of plastic solid waste (PSW): A review, *Waste Management*, Vol.29, Issue.10, pp.2625-2643. https://doi.org/10.1016/j.wasman.2009.06.004

[23] Al-Mosawi, A. I. – Abdulsada, S. A. – Hashim, A. A. (2018): Sustainable Procedure for Using Waste of Date Seeds as a Reinforcement Material for Polymeric Composites, *Open Access Library Journal*, Vol. 5, Issue. e4384, pp.1-8. https://doi.org/10.4236/oalib.1104384

[24] Al-Mosawi, A. I. – Abdulsada, S. A., and Rijab, M.A. (2017) Recycling Procedure of Plant Waste for Manufacturing Green Composite Material, *Journal of Catalyst and Catalysis*, Vvol. 5, Issue. 4, pp.211-214..

[25] Malik, N. – Kumar, P. – Shrivastava, S. – Ghosh, S. B. (2017): An overview on PET waste recycling for application in packaging, *International Journal of Plastics Technology*, Vol. 21, Issue.1, pp.1-24. https://doi.org/10.1007/s12588-016-9164-1

[26] Al-Mosawi, A. I. – Abdulsada, S. A. – Kónya, C. – Szemere, G. (2017): Orange Peel Waste as a Reinforcing Material for Plasticised PVC, *GRANT journal*, Vol. 6, Issue. 2, pp.88-91.

[27] Al-Mosawi, A. I. – Al-Maamori, M. H. – Marossy, K. (2019): Rheological properties of NBR/CR blends as a function of silicon dioxide grain size gradation, *Építőanyag-Journal of Silicate Based and Composite Materials*, Vol.71, No.2, pp.43-45. https://doi.org/10.14382/epitoanyag-jsbcm.2019.8

[28] Abdulsada, S. A. – Al-Mosawi, A. I. – Hadi, A. A. A. – Saad, K. – Samir, H. (2017): Waste Plants as a Green Inhibitor for Reinforced Concrete, *Recent Trends in Civil Engineering & Technology*, Vol. 7, Issue. 3, pp.53-58.

[29] Al-Mosawi, A. I. – Abdulsada, S. A. (2015): Recycling of waste materials: a review. 1st edition, LAP Lambert Academic Publishing, Germany. ISBN: 978-3659695308

[30] Bolden, J. – Abu-Lebdeh, T. – Fini, E. (2013): Utilization of recycled and waste materials in various construction applications, *American Journal of Environmental Science*, Vol.9, Issue.1, pp.14-24.
https://doi.org/10.3844/ajessp.2013.14.24

[31] Abdulsada, S. A. – Al-Mosawi, A. I. (2015): Tensile strength of a new recyclable and environment friendly composite material, *Ciência e Técnica Vitivinícola*, Vol.30, Issue.1, pp. 32-40.

[32] Ondrušová, D. – Domčeková, S. – Pajtášová, M. – Dubec, A. – Mičicová, Z. – Pecušová, B. (2017): Alternative filler based on the waste from glass production and its effect on the rubber properties, *Procedia Engineering*, Vol.177, pp. 462-469. https://doi.org/10.1016/j.proeng.2017.02.246

[33] Moreira, V. X. – Soares, B. G. (2002): Study of Utilization of Ground EVA Waste as Filler in NBR Vulcanizates, Polymers and Polymer Composites, Vol.10, Issue.5, pp. 381-390. https://doi.org/10.1177/096739110201000505

[34] Ahmeda, K. – Nizamib, S. S. – Riza, N. Z. (2014): Reinforcement of natural rubber hybrid composites based on marble sludge/Silica and marble sludge/rice husk derived silica, *Journal of Advanced Research*, Vol.5, Issue.2, pp. 165-173. https://doi.org/10.1016/j.jare.2013.01.008

[35] Rattanapan, A. – Paksamut, J. – Pakeyangkoon, P. – Tuampoemsab, S. (2014): Waste silicon carbide as filler for natural rubber compounds, *Advanced Materials Research*, Vol. 979, pp. 155-158.
https://doi.org/10.4028/www.scientific.net/AMR.979.155

[36] Martín-Cortés, G. R. – Esper, F. J. – de Araujo, A. J. S. – Hennies, W. T. – Valenzuela, M. G. S. – Valenzuela-Díaz, F. R. (2016) Replacement of carbon black on natural rubber composites and nanocomposites - part 1, In: Carpenter J.S. et al. (eds.) Characterization of Minerals, Metals, and Materials 2015. Springer, Cham, pp. 145-152.
https://doi.org/10.1007/978-3-319-48191-3_18

[37] ASTM D2084-17 (2017): Standard test method for rubber property-vulcanization using oscillating disk cure meter, ASTM International, West Conshohocken, PA. https://doi.org/10.1520/D2084-17

[38] Demirhana, E. – Kandemirlib, F. – Kandemirli, M. (2007): The effects of furnace carbon blacks on the mechanical and the rheological properties of SBR1502 styrene butadiene rubber, *Materials and Design*, Vol.28, Issue.4, pp.1326-1329. https://doi.org/10.1016/j.matdes.2006.01.002[39] Zhang, A. – Wang, L. – Zhou, Y. (2003): A study on rheological properties of carbon black extended powdered SBR using a torque rheometer, *Polymer Testing*, Vol.22, Issue.2, pp.133-141.
https://doi.org/10.1016/S0142-9418(02)00061-2

Ref.:
Al-maamori, Mohammed H. – **Hashim**, Abbass A. – **Al-Mosawi**, Ali I. – **Abdulsada**, Shaymaa Abbas – **Marossy**, Kálmán: *Rheological investigation of SBR/CW/CB tricomposite used to create a sustainable procedure for idler rollers production*
Építőanyag – Journal of Silicate Based and Composite Materials, Vol. 71, No. 5 (2019), 144–147. p.
https://doi.org/10.14382/epitoanyag-jsbcm.2019.25

Mechanikai aktiválás hatása deponált pernye alapú geopolimerek nyomószilárdságára

AMBRUS MÁRIA ▪ Miskolci Egyetem, Nyersanyagelőkészítési és Környezeti Eljárástechnikai Intézet
▪ maria.ambrus@uni-miskolc.hu
Érkezett: 2019. 07. 30. ▪ Received: 30. 07. 2019. ▪ https://doi.org/10.14382/epitoanyag-jsbcm.2019.26

Kivonat

Az elsődleges nyersanyagforrások növekvő felhasználása és folyamatos csökkenése miatt a pernye napjaink egyik meghatározó nyersanyagává vált többek között cement- és betonipari, mezőgazdasági stb. felhasználásra. A pernye geopolimer alapanyagként való felhasználása már évtizedek óta foglalkoztatja a kutatókat. Jó reakcióképessége és a termékek kiváló mechanikai tulajdonságai mellett alkalmazása környezeti szempontból is előnyös. Kísérleteim során tatabányai, deponált barnaszén pernye őrlésének hatását vizsgáltam az ezekből készült geopolimerek nyomószilárdságára. A pernye főbb tulajdonságainak meghatározása után 5, 10, 20, 30, 60 és 120 perces őrleményeket készítettem, melyekből geopolimer próbatesteket állítottam elő. Az őrlési idő növelésének hatására nőtt a próbatestek testsűrűségének értéke, azonban az egytengelyű nyomószilárdság esetén nem volt megfigyelhető egyértelmű trend: kezdeti növekedés után a geopolimerek nyomószilárdsága csökkent, majd ismét megnövekedett. Annak érdekében, hogy feltárjam a változások okát az alapanyag és a próbatestek vizsgálata mellett eredményeimet összehasonlítottam korábbi deponált pernyéből (tiszaújvárosi) előállított geopolimerek tulajdonságaival. Az eddig elvégzett vizsgálatok alapján látható, hogy minden pernye esetében van egy optimális őrlési finomság.
Kulcsszavak: deponált pernye, geopolimer, mechanikai aktiválás, nyomószilárdság
Keywords: compressive strength, geopolymer, landfilled fly ash, mechanical activation

AMBRUS Mária
Tanszéki mérnök a Miskolci Egyetem Nyersanyagelőkészítési és Környezeti Eljárástechnikai Intézeténél 2018 óta. Angol nyelvű környezetmérnöki MSc tanulmányait 2019 februárjában kezdte. Eddig összesen 9 folyóirat cikkel és konferencia kiadványban megjelent tanulmánnyal rendelkezik, amelyek többnyire angol nyelven kerültek kiadásra. Több jelenleg futó kutatási projektben közreműködik az ipari hulladékok geopolimerizációja témakörében.

Mária AMBRUS
She is a research engineer at the Institute of Raw Material Preparation and Environmental Processing at the University of Miskolc since 2018. She started her Environmental Engineering MSc studies in February 2019. So far, she has 9 articles published in journals and conference proceedings, mostly in English. Currently, she is involved in several research projects in the field of the geopolymerisation of industrial wastes.

1. Bevezetés

Világviszonylatban a cement az egyik legnagyobb mennyiségben használt alapanyag. Felhasználása a társadalmi-gazdasági fejlődés elengedhetetlen velejárója, azonban előállítása nagy mennyiségű CO_2 kibocsátással jár (pl. kemencefűtés, mészkő kalcinálás, alapanyag szállítás stb.), ezért az utóbbi évtizedek során világszerte kutatásokat végeznek környezetbarát, alternatív építőanyagok kifejlesztésére [1, 2]. A geopolimerek szervetlen, polimer szerkezetű anyagok, melyek szilárd alumino-szilikát-oxidok és alkáli-szilikátok lúgos vagy savas közegben történő aktiválásával állíthatók elő. Energiahatékony és környezetbarát előállításuk, kiváló mechanikai tulajdonságaik, bizonyított sav- és tűzállóképességük miatt ideális építőipari alapanyagnak bizonyultak. Szerkezetük az alábbi képlettel jellemezhető:

$$Mn\{-(Si-O_2)z-Al-O\}n \cdot wH_2O$$

ahol „M” a töltéskiegyenlítéshez szükséges kation, leggyakrabban Na^+, K^+, az „n” a polikondenzációs fok, „z” jelöli a Si/Al moláris arányt, ami 1, 2 vagy 3 lehet, illetve „w” a kapcsolódó vízmolekulák számára utal [2-4].

A pernye a széntüzelésű erőművekben keletkező, finom szemcseméretű, világszerte nagy mennyiségben fellelhető ipari melléktermék. Miután a szén elégetése után a füstgázzal távozik a kazánból, a pernyét különböző porleválasztók segítségével (elektrosztatikus porleválasztó, mechanikai szűrő, vagy ciklon) eltávolítják a rendszerből. Ezt követően hasznosítható pl. talajjavítóként vagy cement- és betonipari alapanyagként, de legnagyobb mennyiségbe lerakásra/tárolásra kerül. Kémiai és ásványos összetétele alapján megfelelő geopolimerizációs alapanyag, felhasználása környezeti és gazdasági szempontból is előnyös [1, 5, 6].

Az elmúlt évtizedekben elvégzett, pernye-alapú geopolimer gyártásra irányuló kísérletek során kezeletlen, osztályozott (pl. szitálással, légosztályozóval) és mechanikailag aktivált pernye alkalmazását is vizsgálták [7, 8, 9], azonban a szakirodalom kis hányada foglalkozik a deponált pernye felhasználásának lehetőségeivel.

Kusnierová és szerzőtársai deponált feketeszén pernye amorf fázis tartalmának változását vizsgálták az eltelt idő függvényében és megállapították, hogy a pernye jelentős devitrifikáción ment keresztül, azaz csökkent az üveges fázis aránya [10]. Yehevis et al. kutatásuk során a deponált pernye kémiai, ásványtani és geokémiai változásait elemezték. A minták eltérő ideig, különböző mélységekben voltak deponálva, így az erózió hatását is megfigyelhették. Eredményeik alapján elmondható, hogy a pernye ásványos összetétele és mikroszerkezete megváltozott a deponálás hatására [11]. Peterová et al. deponált és friss pernye anyagtulajdonságait hasonlították össze, hogy megállapítsák, alkalmas-e a több évtizede tárolt pernye betonipari hasznosításra. Vizsgálataikkal kimutatták, hogy a különböző mélységben vett deponált pernye minták szemcseméret-eloszlásai tág határok közt mozogtak, így felhasználás előtt szükséges annak osztályozása vagy őrlése [12].

Tennakoon et al. ausztrál deponált és friss barnaszén pernye felhasználási lehetőségeit vizsgálták. Megállapították, hogy a pernyék önmagukban nem alkalmazhatók jó minőségű geopolimer előállítására az alacsony SiO_2/Al_2O_3 arányuk miatt, viszont feketeszén pernye és salak hozzáadásával akár 30 MPa feletti 7 napos nyomószilárdság is elérhető (maximum 40% barnaszén pernye használatával). Ezen keverékek esetén a deponált barnaszén pernyét tartalmazó próbatestek mikroszerkezeti vizsgálatai során kevesebb szabad pernye és salak szemcse volt megfigyelhető, mint friss pernye használata esetén [13]. Saxena et al. kísérleteik során arra következtetett, hogy a deponált pernye alkalmas jó minőségű geopolimer előállítására, továbbá megállapították, hogy 1 órás mikrohullámú hőkezelést alkalmazva magasabb szilárdságú geopolimerek állíthatók elő, mint amit kemencében 80 °C-os, 12 órás hőkezeléssel tudtak elérni [14].

A termikus kezelés mellett fontos az alapanyagok mechanikai előkészítése. Mechanikai aktiválás hatására csökken a szemcseméret és megváltozik szemcsék morfológiája, ezáltal nő a pernye reakcióképessége és nő az előállított geopolimerek nyomószilárdsága [7, 9, 15]. Kwasny et al. nedves, szárított és szitált, szárított és őrölt deponált, valamint silóban tárolt pernye alapú geopolimerek nyomószilárdságát hasonlították össze. Szárított és őrölt deponált pernye használatával közel azonos nyomószilárdságú geopolimereket sikerült készíteniük, mint a silóban tárolt pernye alkalmazásával, azonban előkezelés nélkül a reakcióképessége nem volt megfelelő [16]. A Miskolci Egyetem Nyersanyagelőkészítési és Környezeti Eljárástechnikai Intézetében már 10 éve folynak deponált pernye mechanikai aktiválására és hasznosítására irányuló kutatások. Tiszaújvárosi deponált pernye keverőmalommal történő őrléseik során Molnár et al. (2014) az őrlési idő növelésével a szemcsék agglomerálódását és a fajlagos felület csökkenését, a szubmikronos szemcsék alakjának változását tapasztalták [17]. Mucsi et al. tiszaújvárosi deponált pernyével folytatott kísérleteik során szintén a szemcsék finomodását, majd agglomerálódását figyelték meg az őrlési idő növelésével, ami a fajlagos felület kezdeti növekedését, majd csökkenését eredményezte. Ez a geopolimer próbatestek testsűrűség és nyomószilárdság értékeinél is megfigyelhető volt: kezdeti növekedés után az optimális őrlési időt túllépve mind a nyomószilárdság, mint a testsűrűség csökkenni kezdett. Kísérleteik során több malomtípussal is kísérleteztek, ezek közül keverőmalmi őrléssel sikerült a legfinomabb szemcseméretű pernyét előállítaniuk [18, 19]. Szabó et al. a pernye őrlés geopolimer habokra gyakorolt hatását vizsgálták, tiszaújvárosi pernye használatával. Kutatásaik során sikerült összefüggést felállítaniuk a geopolimer paszta folyási tulajdonsága és a pernye szemcsefinomsága között. Az előállított geopolimer habok nyomószilárdsága és testsűrűsége eleinte nőtt az őrlési idő növelésével, majd csökkenni kezdett [20].

Kísérleteim során golyósmalmi őrlés hatását vizsgáltam tatabányai deponált barnaszén pernyéből készült geopolimerek nyomószilárdságára.

2. Anyagok, vizsgálati módszerek

A geopolimerizációs kísérletekhez tatabányai deponált barnaszén pernyét (FA1) használtam, és az elért eredményeket hasonló körülmények közt őrölt, tiszaújvárosi deponált barnaszén pernye (FA2) geopolimerek vizsgálati eredményeivel vetettem össze.

A pernyék kémiai összetételének meghatározása röntgenfluoreszcens spektroszkópia segítségével (XRF) történt, mely eredményét az *1. táblázat* foglalja össze. Az XRF eredmények alapján megállapítható, hogy FA2 SiO_2 tartalma közel 15%-kal magasabb, azonban Al_2O_3 tartalma közel azonos, mint az FA1 mintáé. Ebből adódóan az FA1 minta esetén a SiO_2/Al_2O_3 arány jóval alacsonyabb (1,69), mint az FA2 minta esetén (2,3). Összetételük alapján FA1 és FA2 is F típusú pernye, azonban FA1 lényegesen magasabb CaO tartalommal rendelkezett, mint FA2.

Komponens	FA1	FA2
	Alkotó mennyisége, m/m%	
SiO_2	46,40	61,32
Al_2O_3	27,40	26,71
CaO	7,04	1,50
Fe_2O_3	6,96	4,27
MgO	2,23	0,89
K_2O	1,65	1,72
Egyéb	8,32	3,59
LOI*	0,75	1,92

**Izzítási veszteség 950 °C-on (Loss on ignition at 950 °C).*

1. táblázat A pernyék kémiai összetétele
Table 1 The chemical composition of the fly ash samples, FA1=Tatabánya fly ash, FA2=Tiszaújváros fly ash

A pernyék izzítási vesztesége fontos tulajdonság geopolimer előállítás szempontjából. Ha magas a pernye szervesanyag-tartalma, nagyobb mennyiségű aktiváló oldat használata szükséges, ami a geopolimer alacsonyabb nyomószilárdságát eredményezi. A két deponált pernyeminta LOI értéke igen alacsony, az FA1 értéke 1% alatti, míg az FA2 értéke közel 2%.

A pernyék mechanikai aktiválása a Nyersanyagelőkészítési és Környezeti Eljárástechnikai Intézet sima falú páncélzattal ellátott, Ø305×305 mm-es golyósmalmában történt. FA1 esetén 5, 10, 20, 30, 60 és 120 perces őrlést alkalmaztam. Az FA2 minták esetén az őrlés 5, 10, 20, 30 és 60 perces volt [19]. Az FA1 őrlése során acél őrlőtesteket használtam, melyek össztömege 36 kg volt 30%-os töltési fok mellett, a maximális golyóméret pedig 40 mm volt. A pernyét 110% anyagtöltési fok és 70 1/min fordulatszám alkalmazásával őröltem. az FA2 minta őrlése azonos körülmények között történt.

Az FA1 geopolimer keverékek szilárd anyag/aktiváló oldat aránya 0,82 volt. Az aktiváló oldat 75 m/m% Betol SB típusú vízüveget (25,3% SiO_2; 13,7% Na_2O; 2,7% K_2O) és 25 m/m% 8M-os NaOH-t tartalmazott. Az FA2 próbatestek 0,65 szilárd anyag/aktiváló oldat (NaOH oldat) aránnyal készültek [19].

A geopolimer próbatestek előállításához először összekevertem a pernyét és az aktiváló oldatot, amit 35 mm belső átmérőjű, formaelválasztó olajjal bekent, hengeres sablonokba töltöttem. Ezután a próbatesteket vibrációs asztal segítségével 1 percig tömörítettem. A tömörített próbatesteket 24 órán át levegőtől elzártan, állandó hőmérsékleten pihentettem, majd a 24 óra eltelte után következett a próbatestek hőkezelése 1 órás felfűtési idővel, 50 °C-on, 6 órán keresztül. Ezt követően a hőkezelt geopolimereket lehűlés után további 5 napig levegőtől elzártan, állandó hőmérsékleten pihentettem. A próbatestek tömegének, magasságának és átmérőjének mérésével meghatároztam az átlagos testsűrűség értékeket, majd ezután történt a próbatestek egytengelyű nyomószilárdság-vizsgálata.

A nyers és őrölt pernyék szemcseméret-eloszlás méréséhez laboratóriumi HORIBA LA950-V2 típusú lézeres szemcseméretelemző készüléket használtam, nedves közegű diszpergálással. A szemcseméret eloszlás meghatározása mellett a szoftver segítségével lehetséges a mért anyag fajlagos felületének (geometriai), darab-, ill. felületi eloszlásának a meghatározása is. A fajlagos felület számítása 1,75-ös alaktényezővel történt.

A geopolimerek szerkezetének vizsgálatához Jasco FT-IR 4200 típusú Fourier transzformációs infravörös spektrométert használtam.

3. Eredmények

3.1 Pernye őrlés

Az őrlések során az őrlési energia mérésére is sor került, mely egyenes arányosságban nőtt az őrlés időtartamával. Az FA1 minta 5, 10, 20, 30, 60 és 120 perces őrlése után mért nevezetes szemcseméretek (x_{10}, x_{50}, x_{90}: azok a szemcseméretek, amelynél a szemcsék 10, 50, illetve 90 %-a kisebb) változását az *1. ábra* mutatja. Az őrlemények x_{10} értéke kis mértékben folyamatosan csökkent az őrlés hatására, a 120 perces őrlés végére 1,76 µm-re csökkent. A medián szemcseméret 20 perc után jelentősen csökkent (51,12 µm-ről 17,5 µm-re), majd további őrlés hatására ~10 µm-re csökken. Az x_{90} szemcseméret 156,03 µm-ről 25,38 µm-re csökkent a 120 perces őrlés végére. A szemcseméret-elemzés során a szemcsék agglomerálódása nem volt megfigyelhető.

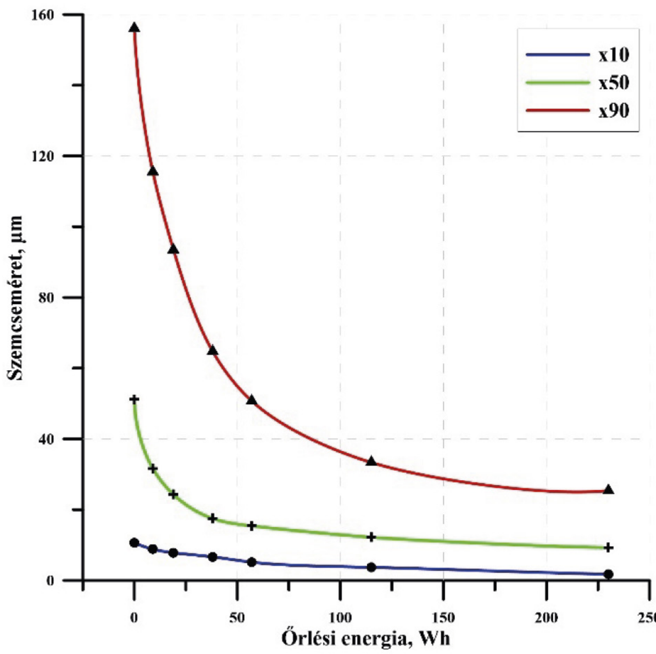

1. ábra Az FA1 őrlemények nevezetes szemcseméret értékei
Fig. 1 Characteristic particle size data of the ground FA1 samples

Az őrlemények geometriai fajlagos felület értéke az őrlési idő függvényében exponenciálisan növekedett. A fajlagos felület változása R^2=0,985 korrelációs együtthatóval az alábbi függvénnyel jellemezhető:

$$\ln(Y) = 0{,}0161\,X + 7{,}821 \qquad (1)$$

3.2 Geopolimerek nyomószilárdsága, testsűrűsége

A pernye mechanikai aktiválása előtt a nyers pernye reakcióképességének vizsgálata céljából geopolimer próbatesteket állítottam elő 6 M koncentrációjú NaOH oldat használatával. A nyers pernye alkalmazásával a geopolimer próbatestek nem voltak alkalmasak a nyomószilárdsági kísérletek elvégzésére, mivel nem rendelkeztek megfelelő mechanikai stabilitással (kézzel könnyen morzsolhatók voltak).

Az őrölt pernye finomságának és a fajlagos felület növekedésének hatására változik a keverék reológiai tulajdonsága [20], amely megfigyelhető volt a próbatestek előállítása során. A hosszabb őrlési idővel előállított őrleményekből készült geopolimer paszták hígan folyós állagúak voltak, ellentétben a rövidebb ideig őrölt pernyékből készült keverékek.

A próbatestek nyomószilárdság értékei és a kapcsolódó őrlemények fajlagos felületének változását összehasonlítva *(2. ábra)* eltérő trend figyelhető meg. Habár az FA1 őrlemény fajlagos felülete nőtt, az egytengelyű nyomószilárdság értéke 10 perc őrlés után drasztikusan lecsökkent, 23,3 MPa-ról 12 MPa alá, majd az őrlési idő 120 percre való növelésével ismét 22 MPa fölé nőtt a próbatestek szilárdsága. Az FA2 őrleményből előállított próbatestek esetén megállapítható, hogy a fajlagos felület emelkedésével kezdetben jelentős szilárdság növekedés volt tapasztalható, azonban a fajlagos felület 3000 cm²/g fölé növelésével a nyomószilárdság értéke stagnált (*3. ábra*). Azonban a nagyobb fajlagos felület nem feltétlenül jár a geopolimer próbatestek nagyobb nyomószilárdságával [21, 22].

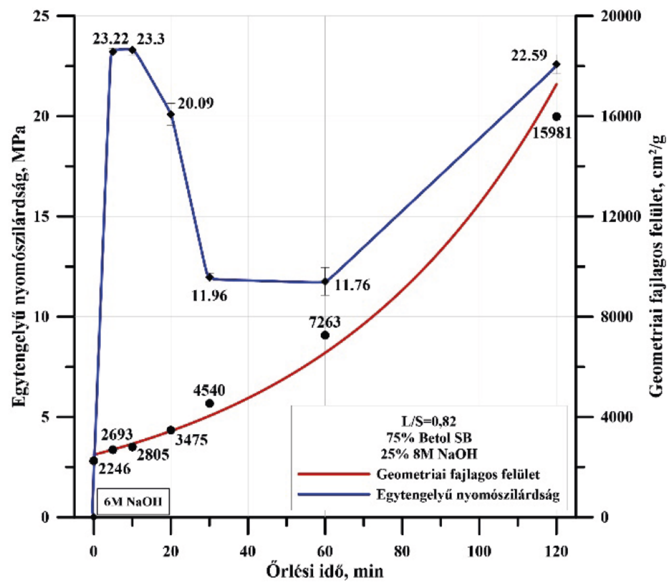

2. ábra Az FA1 próbatestek átlagos nyomószilárdság és fajlagos felület értékei
Fig. 2 The average compressive strength and specific surface area values of FA1 specimens

A próbatestek testsűrűségét megvizsgálva *(2. táblázat)* a kezdeti 1,63 g/cm³ testsűrűség a 60 perces őrlés eredményeképp 1,71 g/cm³-re emelkedett, majd 120 perces őrlés hatására 1,68 g/cm³-re csökkent, tehát az elért nyomószilárdság és a testsűrűség értékek között sincs korreláció.

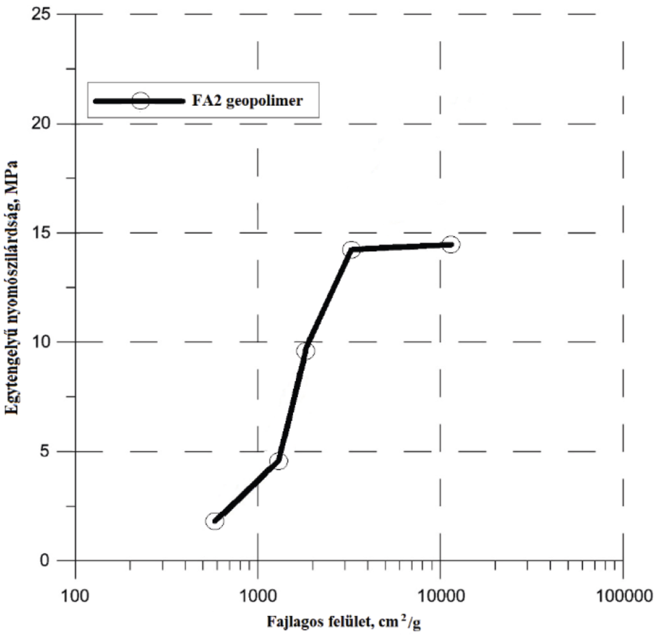

3. ábra Az FA2 próbatestek átlagos nyomószilárdsága a fajlagos felület függvényében [19]
Fig. 3 The average compressive strength of FA2 specimens in relation to specific surface area

Őrlési idő, min	5	10	20	30	60	120
Testsűrűség, g/cm³	1,63	1,65	1,65	1,68	1,71	1,68

2. táblázat Őrölt FA1 geopolimerek testsűrűség értékei
Table 2 Specimen densities of ground FA1 geopolymers

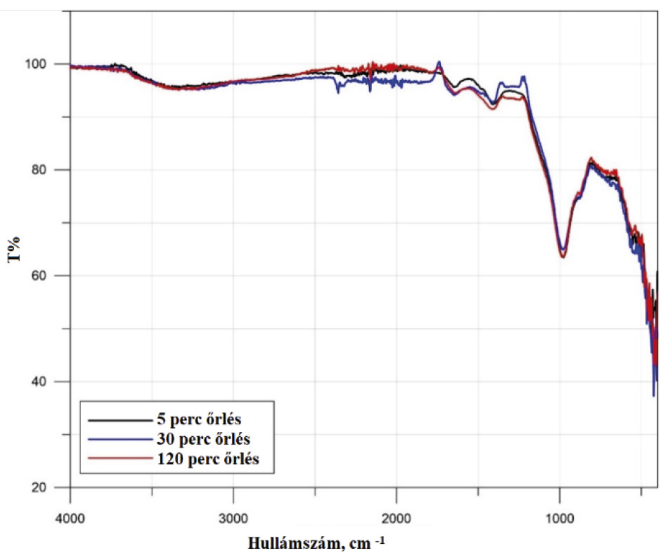

4. ábra Az 5, 30 és 120 perces FA1 őrleményből készült geopolimer próbatestek FT-IR spektrumai
Fig. 4 The FT-IR spectra of geopolymers from FA1 ground for 5, 30 and 120 minutes

3.3 FT-IR vizsgálatok

Az 5, 30 és 120 perces FA1 őrleményekből készült geopolimer próbatestek FT-IR spektrumait a *4. ábra* mutatja.

A ~3400 cm^{-1} hullámszámnál megfigyelhető széles csúcsok az –OH és HOH kötések nyújtó rezgései, míg az 1650-1630 cm^{-1} hullámszámnál megjelenők a hajlító rezgései közel azonosak, ezeket a felszínen vagy a pórusokban megkötött vízmolekulák okozhatnak. Az 1400 cm^{-1} körül megjelenő csúcsok az O–C–O kötések nyújtó rezgései, melyek jelenléte a geopolimer szilárdságának csökkenését okozhatja [23, 24], azonban a vizsgált próbatestek esetén nem volt számottevő eltérés a csúcsok intenzitása között. A 990 cm^{-1} hullámszámnál látható csúcsok az Si–O–Si és Si–O–Al kötések aszimmetrikus nyújtó rezgései, melyek a geopolimerizáció fokára utalnak, azonban ezen csúcsok intenzitása is közel azonos [25, 26, 27].

A vizsgált próbatestek FT-IR spektrumai szinte azonos lefutásúak, így a szerkezeti vizsgálatok alapján nem mutatható ki számottevő eltérés, mely magyarázatot adna a nyomószilárdság abnormális változására.

4. Megállapítások

Kísérleteim során deponált barnaszén pernye golyósmalmi őrlésével foglalkoztam. A 120 perces őrlés eltelte után sem volt megfigyelhető az őrlemények szemcseméretének növekedése, sem a fajlagos felület csökkenése, azaz a pernye szemcseméretének folyamatos csökkenését tapasztaltam. A minták őrlése után geopolimer próbatesteket készítettem, hogy az őrlés nyomószilárdságra gyakorolt hatását vizsgáljam. A próbatestek nyomószilárdság értéke és a testsűrűsége között nem állapítható meg egyértelmű kapcsolat, valamint a próbatestek FT-IR vizsgálata sem mutatott ki jelentős különbséget a geopolimerek szerkezetében. A próbatestek további vizsgálata szükséges (pl. XRD) a nyomószilárdság szabálytalan változásának megértéséhez.

Köszönetnyilvánítás

A cikkben ismertetett kutató munka az EFOP-3.6.1-16-2016-00011 jelű „Fiatalodó és Megújuló Egyetem – Innovatív Tudásváros – a Miskolci Egyetem intelligens szakosodást szolgáló intézményi fejlesztése" projekt részeként – a Széchenyi 2020 keretében – az Európai Unió támogatásával, az Európai Szociális Alap társfinanszírozásával valósul meg. A szerző köszönetét fejezi ki Dr. Debreczeni Ákosnak és Köteles Lászlónak (ME, Bányászati és Geotechnikai Intézet) az egytengelyű nyomószilárdsági mérések biztosításában és elvégzésében nyújtott segítségéért, Dr. Kristály Ferencnek (ME, Ásványtani - Földtani Intézet) az XRD vizsgálat elvégzéséért, valamint Dr. Mucsi Gábornak és Szabó Rolandnak (ME, Nyersanyagelőkészítési és Környezeti Eljárástechnikai Intézet) a témában való iránymutatásukért.

Irodalomjegyzék

[1] Nath, S.K. – Kumar, S. (2019): Reaction kinetics of fly ash geopolymerization: Role of particle size controlled by using ball mill. Advanced Powder Technology 30 (5), pp. 1079–1088. http://dx.doi.org/10.1016/j.apt.2019.02.003
[2] Mucsi, G. – Csőke, B. – Erdős, Gy. (2011): Erőműi pernyehasznosítás kutatási tapasztalatai: hidraulikus kötőanyag és geopolimer előállítása. Bányászati és Kohászati Lapok – BÁNYÁSZAT 144 (3), pp. 13–20.
[3] Davidovits, J. (2011): Geopolymer chemistry and application. Institut Geopolimére, ISBN: 9782951482050 pp. 286.
[4] Kumar, R. – Kumar, S. – Mehrotra, S. P. (2007): Towards sustainable solutions for fly ash through mechanical activation. Resources, Conservation and Recycling 52 (2), pp. 157–179. https://doi.org/10.1016/j.resconrec.2007.06.007

[5] Bokányi L., Csőke B., Debreczeni Á., Gáspár L., Gombkötő I., Horváth R., Less Gy., Mucsi G., Molnár Z., Rácz Á. (2014): Erőműi pernye komplex hasznosítása (Milagrossa Kft., Miskolc, 2014).

[6] Kumar Sharma, P. – Prasad Singh, J. – Kumar, A. (2019): Effect of Particle Size on Physical and Mechanical Properties of Fly Ash Based Geopolymers. Transactions of the Indian Institute of Metals. https://doi.org/10.1007/s12666-019-01628-w

[7] Kumar, S. – Kristály, F. – Mucsi, G. (2014): Geopolymerisation behaviour of size fractioned fly ash. Advanced Powder Technology 26 (1), pp. 24–30. http://dx.doi.org/10.1016/j.apt.2014.09.001

[8] Temuujin, J. – Williams, R. P. – van Riessen, A. (2009): Effect of mechanical activation of fly ash on the properties of geopolymer cured at ambient temperature. Journal of Materials Processing Technology 209 (12-13), pp. 5276–5280. http://dx.doi.org/10.1016/j.jmatprotec.2009.03.016

[9] Marjanović, N. – Komljenović, M. – Baščarević, Z. – Nikolić, V. (2014): Improving reactivity of fly ash and properties of ensuing geopolymers through mechanical activation, Construction and Building Materials 57, pp. 151–162. https://doi.org/10.1016/j.conbuildmat.2014.01.095

[10] Kusnierová, M. – Slesárová, A. – Prascáková, M. (2005): The significance of fly ash for their processing and utilization. In. Proc. Waste Recycling – IX. Krakow, pp. 17–19.

[11] Yeheyis, M. B. – Shang, J. Q. – Yanful, E. K. (2009): Chemical and Mineralogical Transformations of Coal Fly Ash after Landfilling, Előadás, World of Coal Ash Conference (WOCA), May 4-7, 2009. Lexington, Kentucky, USA. https://pdfs.semanticscholar.org/cbd5/45b35c33e8887885e26f9dcaec451b0ba036.pdf

[12] Peterová, A. – Škvára, F. – Šídlová, M. – Šulc, R. – Sokolová, K. – Snop, R. (2019): Can Czech Stockpiled Fly Ash be Used in the Production of Concrete? In: McCarthy, M. J. – Newlands, M. D. –Jones, M. R. – Dyer, T. D. – Csetenyi, L. J. – Zheng, L. (szerk.): EuroCoalAsh 2019 Proceedings, University of Dundee: Dundee, Egyesült Királyság/Skócia (2019), pp. 123–130.

[13] Tennakoon, C. – Sagoe-Crentsil, K. – San Nicolas, R. – Sanjayan, J. G. (2015): Characteristics of Australian brown coal fly ash blended geopolymers. Construction and Building Materials 101, pp. 396–409. http://dx.doi.org/10.1016/j.conbuildmat.2015.10.089

[14] Saxena, S. K. –Kumar, M. – Singh, N. B. (2018): Effect of Alccofine powder on the properties of Pond fly ash based Geopolymer mortar under different conditions. Environmental Technology & Innovation 9, pp. 232–242. https://doi.org/10.1016/j.eti.2017.12.010

[15] Diaz, E. I. – Allouche, E. N. – Eklund, S. (2010): Factors affecting the suitability of fly ash source material for geopolymers. Fuel 89, pp. 992–996. http://dx.doi.org/10.1016/j.fuel.2009.09.012

[16] Kwasny, J. – McGrath, T. – Lawther, S. – Soutsos, M. – Sha, W. – Cox, S. – Chen, J. F. (2019): Lagoon Fly Ash: A Potential Source of the Precursor for Geopolymer. In: McCarthy, M. J. – Newlands, M. D. –Jones, M. R. – Dyer, T. D. – Csetenyi, L. J. – Zheng, L. (szerk.): EuroCoalAsh 2019 Proceedings, University of Dundee: Dundee, Egyesült Királyság/Skócia (2019), pp. 322–333.

[17] Molnár, Z. – Kristály, F. – Mucsi, G. (2014): Mechanical activation of deposited brown coal fly ash in stirred media mill, Acta Physica Polonica A 126 (4), pp. 988–993. https://doi.org/10.12693/APhysPolA.126.988

[18] Mucsi, G. – Gombkötő, I. – Molnár, Z. – Osváth, I. – Kumar, S. (2016): Effect of mechanical activation of fly ash on geopolymer properties, In: Finch, J. – O'Connor, C. – Leroux, D. – Stubina, N. – Polin, G. (szerk): IMPC 2016: XXVIII International Mineral Processing Congress Proceedings, pp. 1–9.

[19] Mucsi, G. –Kumar, S. – Csőke, B. – Kumar,R. –Molnár, Z. – Rácz, Á. – Mádai, F. – Debreczeni, Á. (2015): Control of geopolymer properties by grinding of land filled fly ash. International Journal of Mineral Processing 143, pp. 50–58. http://dx.doi.org/10.1016/j.minpro.2015.08.010

[20] Szabó, R. – Gombkötő, I. – Svéda, M. – Mucsi, G. (2017): Effect of grinding fineness of fly ash on the properties of geopolymer foam, Arch. Metall. Mater 62 (2B), pp. 1257–1231. http://dx.doi.org/10.1515/amm-2017-0188

[21] Kumar, S. – Kumar, R. – Alex, T. C. – Bandopadhyay, A. – Mehrotra, S. P. (2007): Influence of reactivity of fly ash ongeopolymerisation. Advances in Applied Ceramics 106 (3), pp. 120–127. http://dx.doi.org/10.1179/174367607X159293

[22] Mádai, F. – Kristály, F. – Mucsi, G. (2015): Microstructure, mineralogy and physical properties of ground fly ash based geopolymers. Ceramics – Silikáty 59 (1), pp. 70–79. http://www.ceramics-silikaty.cz/2015/pdf/2015_01_70.pdf

[23] Panias, D. – Giannopoulou, I. P. – Perraki, T. (2007): Effect of synthesis parameters on the mechanical properties of fly ash-based geopolymers. Colloids and Surfaces A: Physicochemical and Engineering Aspects, 301 (1-3), pp. 246–254. http://doi:10.1016/j.colsurfa.2006.12.064

[24] Szabó, R. (2019): Lignit pernye alapú geopolimerek mechanikai tulajdonságainak szabályozása vibrációs tömörítéssel. Építő anyag – Journal of Silicate Based and Composite Materials, 71 (2), pp. 66–71. https://doi.org/10.14382/epitoanyag-jsbcm.2019.12

[25] Kumar, S. – Kumar, R. (2011): Mechanical activation of fly ash: Effect on reaction, structure and properties of resulting geopolymer. Ceramics International, 37 (2), pp. 533–541. http://dx.doi.org/10.1016/j.ceramint.2010.09.038

[26] Hamdi, N. – Messaoud, B. I. – Srasra, E. (2018): Production of geopolymer binders using clay minerals and industrial wastes. Comptes Rendus Chimie 22 (2-3), pp. 220–226. http://dx.doi.org/10.1016/j.crci.2018.11.010

[27] Yaseri, S. – Hajiaghei, G. – Mohammadi, F. – Mahdikhani, M. – Farokhzad, R. (2017): The role of synthesis parameters on the workability, setting and strength properties of binary binder based geopolymer paste, Construction and Building Materials, 157, 2017, pp 534–545. https://doi.org/10.1016/j.conbuildmat.2017.09.102

Ref.:
Ambrus, Mária: *Mechanikai aktiválás hatása deponált pernye alapú geopolimerek nyomószilárdságára*
Építőanyag – Journal of Silicate Based and Composite Materials, Vol. 71, No. 5 (2019), 148–152. p.
https://doi.org/10.14382/epitoanyag-jsbcm.2019.26

E-MRS

European Materials Research Society

E-MRS now has more than 4,000 members from industry, government, academia and research laboratories, who meet regularly to debate recent technological developments of functional materials. The E-MRS differs from many single-discipline professional societies by encouraging scientists, engineers and research managers to exchange information on an interdisciplinary platform, and by recognizing professional and technical excellence by promoting awards for achievement from student to senior scientist level. As an adhering body of the International Union of Materials Research Societies (IUMRS), the E-MRS enjoys and benefits from very close relationships with other Materials Research organizations elsewhere in Europe and around the world.

23 RUE DU LOESS, BP 20 - 67037
STRASBOURG CEDEX 02, FRANCE
EMRS@EUROPEAN-MRS.COM
WWW.EUROPEAN-MRS.COM

Rheological properties of blended metakaolin self-compacting concrete containing recycled CRT funnel glass aggregate

Younes Ouldkhaoua
PhD student at the Department of Civil Engineering, University of Laghouat, Algeria, His research interests include self-compacting concrete and reuse of waste.

Dr. Benchaa Benabed
Associate professor at the Department of Civil Engineering, University of Laghouat, Algeria. His research interests include self-compacting concrete, rheology and durability of cement-based materials.

Dr. Rajab Abousnina
Research fellow and teaching assistance, in Civil Engineering School of Engineering, Faculty of Science and Engineering, University of Waikato, New Zealand. His principal research interests focus on concrete technology, waste materials, geopolymer concrete, Oily produced water, analytical modelling and simulation.

Prof. El-Hadj Kadri
Professor at Laboratory of Mechanics and Materials of Civil Engineering, University of Cergy-Pontoise, France. His research interests include high-strength concrete and self-compacting concrete.

Younes Ouldkhaoua ▪ Civil engineering laboratory, University of Laghouat 03000, Algeria
Benchaa Benabed ▪ Civil engineering laboratory, University of Laghouat 03000, Algeria ▪ b.benchaa@lagh-univ.dz
Rajab Abousnina ▪ School of Engineering, Faculty of Science and Engineering, University of Waikato, Hamilton 3216, New Zealand
El-Hadj Kadri ▪ L2MGC laboratory, University of Cergy-Pontoise 95000, France

Érkezett: 2019. 07. 15. ▪ Received: 15. 07. 2019. ▪ https://doi.org/10.14382/epitoanyag-jsbcm.2019.27

Abstract

Rheology is a field of fluid mechanics that studies the flow of materials and the interaction between stress states and deformation according to their viscosity, elasticity and plasticity and with the appearance of new materials and the complex behaviour of concrete pumpability, since the field of civil engineering is interested in the study of concrete flow. This work will examine how the use of catodique ray tube (CRT) glass as sand replacement in proportions of 0, 10, 20, 30, 40 and 50%, and metakaolin (MK) powder in proportions of 5, 10 and 15% will affect the rheological properties of self-compacting concrete (SCC). In this investigation, the flow ability of SCC was evaluated by slump flow, L-Box, and V-funnel tests. Its resistance to segregation was measured by the sieve stability test and the yield stress and plastic viscosity was determined by a modified slump test. This investigation concluded that CRT glass improved the rheological properties and minimised the dosage of superplasticiser (SP); the best results came from concrete with 50% of CRT sand glass. This improvement helps to overcome the negative effect of MK in SCC pumpability and reduces the time of casting. An acceptable relationship between rheological properties shows that a modified slump test can be used to evaluate yield stress and viscosity.

Keywords: CRT, metakaolin, rheological properties, self-compacting concrete
Kulcsszavak: CRT, metakaolin, reológiai tulajdonságok, öntömörödő beton

1. Introduction

The advent of SCC marks a new stage in the history of concrete materials [1], and as such has several technical interests in the field of civil construction and building (pumpability, easiness and speed of implementation) [2]. The specificity of SCC lies in its fresh state behaviour, and therefore this type of concrete must be characterised by high workability and deformability while remaining stable [3-5]. These properties contribute to ensuring durable and quality structures [6, 7]. However, since the variations of chemical admixtures and supplementary materials will complicate its rheological properties, particularly its shear thickening and shear thinning behaviour [8]. Many researchers are turning to the science of rheology to design better tools to understand the workability of concrete. The most used method for placing concrete is pumping, but to determine whether concrete is pumpable or not, its rheological properties such as yield stress and plastic viscosity must be known [9]. There are two ways to evaluate its rheological properties; the first way is to use a rheometer, but its high cost means it will not be available to everyone [10]; the second way is based on the modified slump test developed by Larrard and Ferraris [11], which is simple, inexpensive, easy to implement and can be used on site.

The accumulation of waste materials is becoming more uncontrollable and is occupying more public space. This has highlighted the use of these materials for construction purposes to preserve the natural resources of aggregates, while improving the performance and durability of cementitious composites and protecting the environment against the CO_2 emissions and polluted industrial sites [12-14]. It is important to recycle television and computer monitors equipment waste because it can pose serious environmental health problems [15], particularly the chemical structure of glass that contains lead oxide (PbO) [16]. Ling and Poon [17] can treat this glass by immersing it in a bath of 5% nitric acid (HNO_3) solution for 3 hours, which will satisfy the limits of the toxicity characteristic leaching procedure (TCLP) test [18]. Hui and Sun [19] studied the use of CRT glass on the workability of mortar and found that its slump diameter increases as the glass levels of CRT increased.

MK is a pozzolanic material that can be added to a cementitious material and may improve the performance of concrete [20], however it can have a negative effect on its rheology at fresh state [21]. Many investigators showed that metakaolin affects the rheological property of SCC; the irregular shape of MK enabled it to show a shear thickening behaviour and increase the viscosity of the mixture [22-25].

This study will assess the use of CRT glass and MK powder as a substitute in sand and cement respectively on the rheological properties of SCC with a low environmental impact.

2. Materials and experimental program

2.1 Materials

Ordinary Portland cement (CEMI 42.5) was used in all SCC mixes. Metakaolin, which is used as cement replacement, was obtained from kaolin calcination at 850°C for 3 hours [26]. The chemical and physical properties of cement and MK are given in *Table 1*. X-ray diffraction (XRD) analysis and scanning electron microscopy (SEM) images of MK are also provided in *Fig. 1* and *Fig. 2* respectively. The superplasticizer (SP) used is a powerful water reducing agent based polycarboxlic-ether type with a density of 1.07 and a solid matter content of 30%.

Chemical properties Oxide content (%)	Cement	Metakaolin
SiO_2	20.83	50.30
Al_2O_3	4.13	41.81
Fe_2O_3	5.58	1.5
CaO	62.19	0.08
MgO	1.42	0.4
K_2O	2.30	0.81
Na_2O	0.38	0.09
TiO_2	0.028	0.024
Loss on ignition	2.04	5.77
Physical properties		
Specific gravity (g/cm³)	3.12	2.45
Blain fineness (cm²/g)	3300	7000

Table 1 *Chemical and physical properties of cement and metakaolin*
1. táblázat *Cement és metakaolin kémiai és fizikai tulajdonságai*

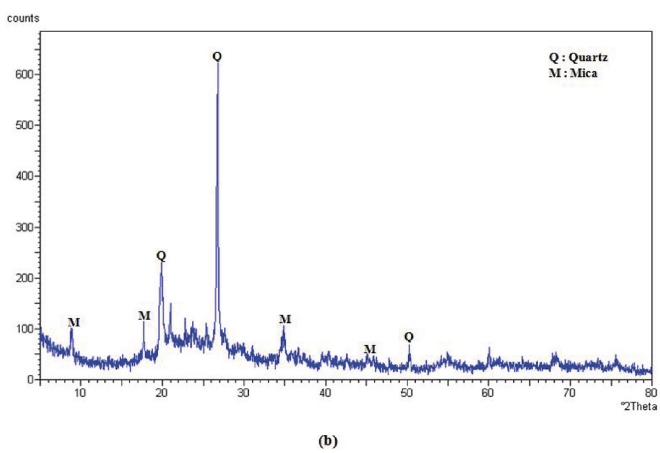

Fig. 1 X-ray diffraction of MK
1. ábra Metakaolin röntgendiffraktogramja

River sand is used as a natural fine aggregate. Waste CRT funnel glass was treated with 5% nitric acid (HNO_3) for 3 hours to remove the lead oxide, and then is used as sand replacement at levels of 0, 10, 20, 30, 40 and 50%. Two types of gravels from limestone crushing (G 3/8 and G 8/15) are used in this study. The physical properties and the particle size distribution of the used aggregates are presented in *Table 2* and *Fig. 3* respectively.

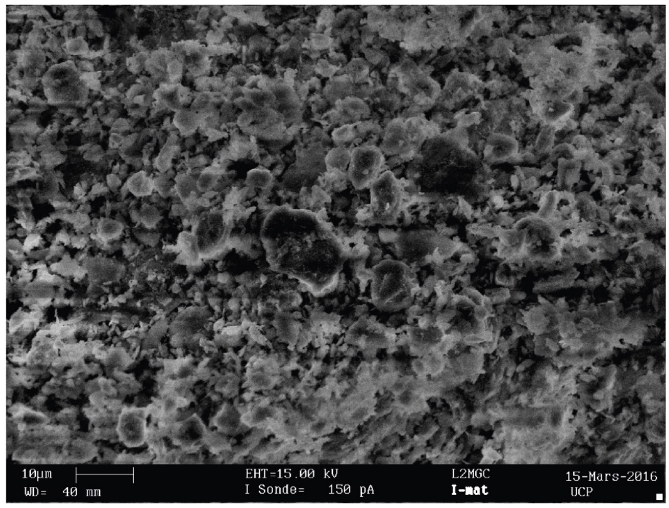

Fig. 2 Scanning electron microscope (SEM) of MK
2. ábra Metakaolin pásztázó elektronmikroszkópos felvételen

Properties	Type of aggregates			
	Fine aggregates		Coarse aggregates	
	Sand	CRT glass	Gravel 3/8	Gravel 8/15
Specific density (g/cm³)	2.7	2.75	2.69	2.68
Fineness modulus	2.44	2.16	-	-
Sand equivalent (%)	81	-	-	-
Water absorption (%)	0.83	0	3.2	3.5
Los Angeles coefficient (%)	-	-	13	15

Table 2 *Physical properties of the used aggregates*
2. táblázat *Az alkalmazott adalékanyagok fizikai tulajdonságai*

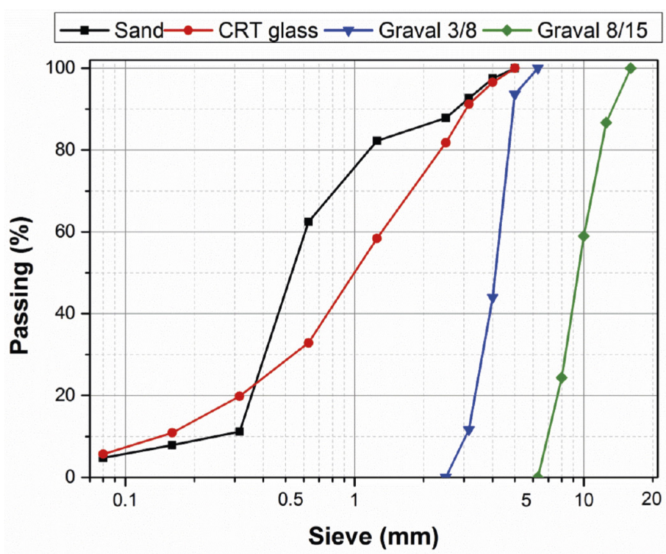

Fig. 3 Particle size distribution of fine and coarse aggregates
3. ábra A finom és durva adalékanyag szemeloszlás görbéi

2.2 Mixture proportions

To investigate how a combination of MK and CRT glass would affect the rheological properties of all the SCC mixtures, nineteen mixtures were prepared. The control mixture was made with Portland cement as a binder and natural sand as

Mix ID	Binder (OPC+MK)		W/B	Coarse aggregates (kg/m³)	Sand (kg/m³)	CRT glass (kg/m³)	SP (%)
	OPC (kg/m³)	MK (kg/m³)					
Control	469.59	0	0.4	823.24	909.78	0	0.8
MK5+CRT0	446.11	18.68	0.4	823.24	909.78	0	0.85
MK5+CRT10	446.11	18.68	0.4	823.24	818.80	90.98	0.85
MK5+CRT20	446.11	18.68	0.4	823.24	727.82	181.96	0.85
MK5+CRT30	446.11	18.68	0.4	823.24	636.85	272.93	0.83
MK5+CRT40	446.11	1868	0.4	823.24	545.87	363.91	0.83
MK5+CRT50	446.11	18.68	0.4	823.24	454.89	454.89	0.8
MK10+CRT0	422.63	37.35	0.4	823.24	909.78	0	1.1
MK10+CRT10	422.63	37.35	0.4	823.24	818.80	90.98	1.1
MK10+CRT20	422.63	37.35	0.4	823.24	727.82	181.96	1.1
MK10+CRT30	422.63	37.35	0.4	823.24	636.85	272.93	1.05
MK10+CRT40	422.63	37.35	0.4	823.24	545.87	363.91	1
MK10+CRT50	422.63	37.35	0.4	823.24	454.89	454.89	0.95
MK15+CRT0	399.15	56.03	0.4	823.24	909.78	0	1.2
MK15+CRT10	399.15	56.03	0.4	823.24	818.80	90.98	1.2
MK15+CRT20	399.15	56.03	0.4	823.24	727.82	181.96	1.2
MK15+CRT30	399.15	56.03	0.4	823.24	636.85	272.93	1.15
MK15+CRT40	399.15	56.03	0.4	823.24	545.87	363.91	1.15
MK15+CRT50	399.15	56.03	0.4	823.24	454.89	454.89	1.1

Table 3 Mix proportions of different SCC mixtures
3. táblázat A különböző SCC keverékek összetételei

fine aggregate, while in the remaining mixtures the cement was partially replaced by MK at 5, 10 and 15% and sand was replaced by CRT glass at levels of 0, 10, 20, 30, 40 and 50%. This step would determine the quantity required for each material in the batch to obtain a concrete with the desired properties, the Okamura's method [27] was used to determine mixture proportions of SCC. The proportions of all the SCC mixtures are given in *Table 3*.

2.3 Mixing procedure

The mixing procedure was as follows: the powder and aggregates were mixed together for half a minute (30 s), then 70% of the mixing water was added and mixed for 1 min. The remaining 30% of water containing the superplasticiser and the concrete was added and mixed for 1 min. This procedure continued for another 5 minutes and then stopped for 2 minutes. The concrete was mixed again for 30 seconds to ensure the properties of self-compacting concrete [28].

2.4 Test methods

According to EFNARC guidelines for SCC committee [29], the slump flow diameter and time required to reach a slump diameter of 500 mm (EN 12350-8), the V-funnel flow time (EN 12350-9), the L-box height ratio (EN 12350-10) and sieve stability (EN 12350-11) were carried out to characterise the filling, passage, and segregation of the fresh concrete.

A modification to the slump flow test allowed the rheological characteristics of fresh concrete, the yield stress (τ_0), and the viscosity (μ) to be evaluated (*Fig. 4*) [11].

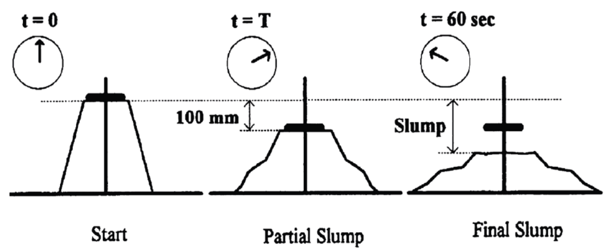

Fig. 4 Description of modified slump test
4. ábra A módosított roskadási terülés vizsgálat leírása

The yield stress was associated to the final slump (S) and the plastic viscosity was related to the time (T) to slump down to a height of 100 mm. The rheological parameters were calculated using the following empirical equations:

$$\tau_0 = \frac{\rho}{347}(300 - S) + 21 \quad (1)$$

$$\mu = \rho.T.1{,}08.10^{-5}(S - 175) \quad (2)$$

τ_0: yield stress (Pa);
μ: plastic viscosity (Pa.s);
S: final slump (mm);
ρ: specific gravity of fresh SCC (kg/m³);
T: time of partial slump (s).

3. Results and discussion

3.1 Slump flow and T_{500} time test

Fig. 5 shows the fresh properties of all the SCC, where the flow time T_{500} was less than 2.25 s and the slump flow diameters of all SCC mixes groups are 700 and 800 mm; this indicates good deformability and comply with the EFNARC recommendations [29]. These results indicate that MK reduces the slump flow diameter, unlike the control concrete. This decrease with 15% of MK is quite remarkable. There was an increase in slump flow and flow time (T_{500}) in SCC when the mixture contained CRT glass. This increase was significant compared to natural sand, particularly when the percentage of CRT glass reached 50%. This improvement may be due to differences in texture between sand and glass, which better fill the space between the coarse aggregates, and furthermore, glass sand has low water absorption and a smooth surface [30-32]. It can be concluded that combining CRT glass with MK had a beneficial effect on the spread of slump.

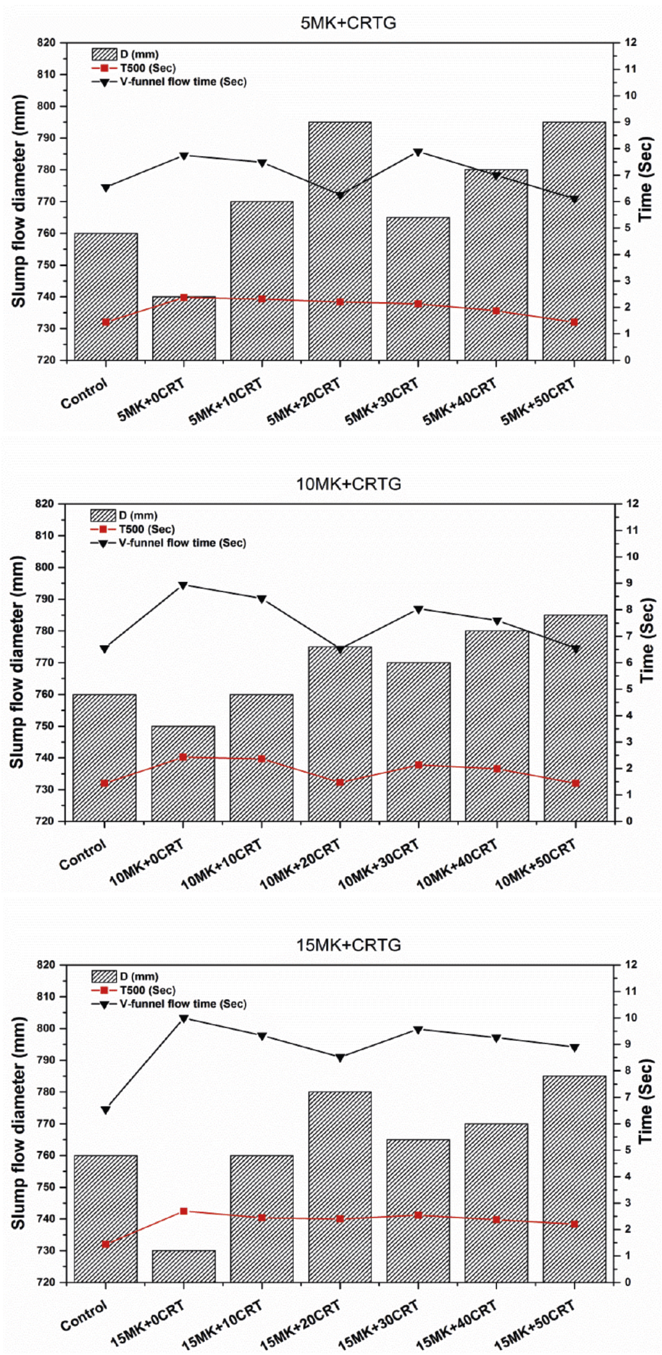

Fig. 5 Slump flow diameter and V-funnel time of different SCC mixes
5. ábra A különböző öntömörödő keverékek roskadási terülési átmérője és V-tölcsér kifolyási ideje

3.2 V-funnel flow time

Based on the results of the V-funnel test, all SCC mixtures were very stable because their flow times were less than the recommended value (12 s). *Fig. 5* shows that the addition of MK increases the flow time and viscosity by up to 15%, but it needed water and a superplasticiser to have desired self-compacting properties due to the high specific surface area of MK [33]. Rahmat and Yasin, [34] studied the fresh properties of SCC with MK and noted that the flow time increased as the amount of MK increased with a higher dose of SP. Moreover, substituting sand with CRT glass reduced the flow time so that it converged more rapidly towards the lower threshold. The best flow times occurred by adding 50% glass into all the group mixes, this and a low dose of SP reduced the viscosity also facilitated the pumpability of concretes in confined areas. *Fig. 6* plots the relationships between the V-funnel flow times and T_{500} slump flow for all groups and shows that the coefficient of correlation (R^2 superior of 0.8) has an acceptable linear correlation between the two variables.

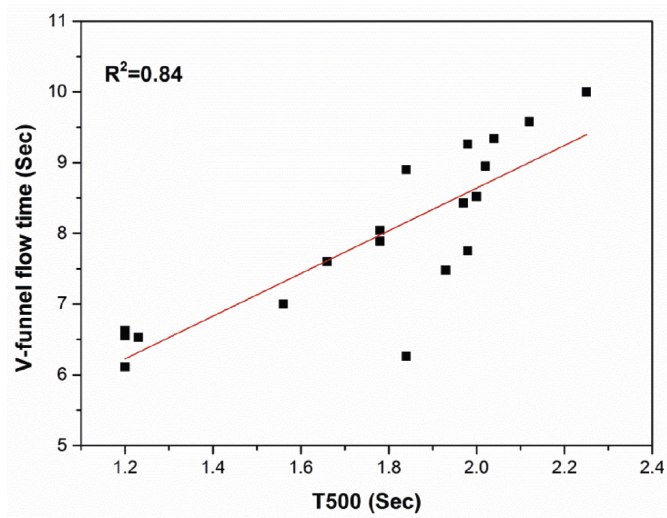

Fig. 6 Relationship between V-funnel time and slump flow time T500
6. ábra V-tölcsér kifolyási idő és roskadási terülési idő (T500) kapcsolata

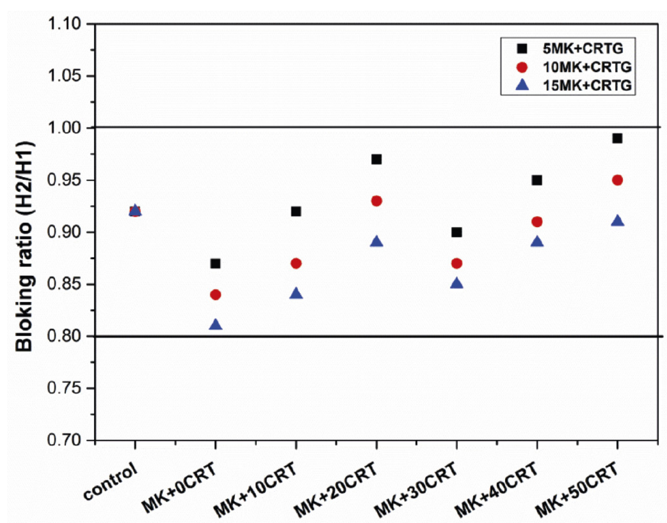

Fig. 7 Blocking ratio of different SCC mixes
7. ábra Különböző SCC-keverékek blokkolódási aránya

3.3 L-box test

With respect to the filling capacity estimated by the H_2 / H_1 ratio measured by the L-box test; all the SCC groups had a ratio H_2 / H_1> 0.8 which is in accordance with the EFNARC limitations [29]. *Fig. 7* shows that the introduction of CRT glass gave a good filling capacity, mobility, and the passage of SCC through heavily scrapped areas. Kou and Poon [35] studied the properties of SCC prepared with recycled glass aggregate and found that the ability to fill in L-box improved when the amount of recycled glass increased.

3.4 Sieve stability test

The results presented in *Fig. 8* show that all SCC had the highest stability, whereas the low milt value was due to the lack of paste that can stick to the aggregates. However, there is an optimal dosage of around 50%, beyond which stability decreases as the volume concentration of CRT glass increases because the less viscous concrete makes it easier to pass through the sieve. Umehara et al [36] reported that this decrease in the viscosity of concrete is consistent with a reduction in stability. These results will be confirmed later through the results of viscosity.

3.5 Yield stress

Fig. 9 shows the evolution of yield stress of all the SCC mixes; note that mixtures containing MK without CRT sand glass showed a shear-thickening fluid effect due to the increase in yield stress. The optimal dose was 15% MK. Parviz et al [37] reported that the rheological properties of SCC mixes with partial replacement of metakaolin reached a higher yield stress than with other mineral admixtures. Hassan and Lachemi [38] studied the effect that metakaolin had on the rheology of SCC and found that the yield stress increased as the percentage of MK increased. The incorporation of CRT sand glass helps to reduce the yield stresses, which results in a shear thinning effect, but beyond the optimal dosage of 50%, the yield stress decreased due to the effect of increasing the volume of CRT sand glass.

3.6 Plastic viscosity

The plastic viscosity of SCC containing different dose of CRT glass and MK are shown in *Fig. 10*; it shows that the viscosity increased by 36% when 15% MK was added. Güneyisi and Gesoğlu [39] investigated the effect that MK had on the viscosity of self-compacting mortar and concluded that mortars with 15% MK required a higher viscosity; nevertheless an increase in CRT sand glass reduced the plastic viscosity. The combined use of CRT sand glass has important benefits in terms of the negative effect of MK on the pumpability of concrete and the casting time.

3.7 Correlation between rheological properties

Fig. 11 highlights the relationship between yield stress and slump flow for all the SCC mixtures. Note that the yield stress decreased as the slump flow diameters increased, but the relationship between slump flow and yield stress obtained by the modified slump test showed a good correlation with the

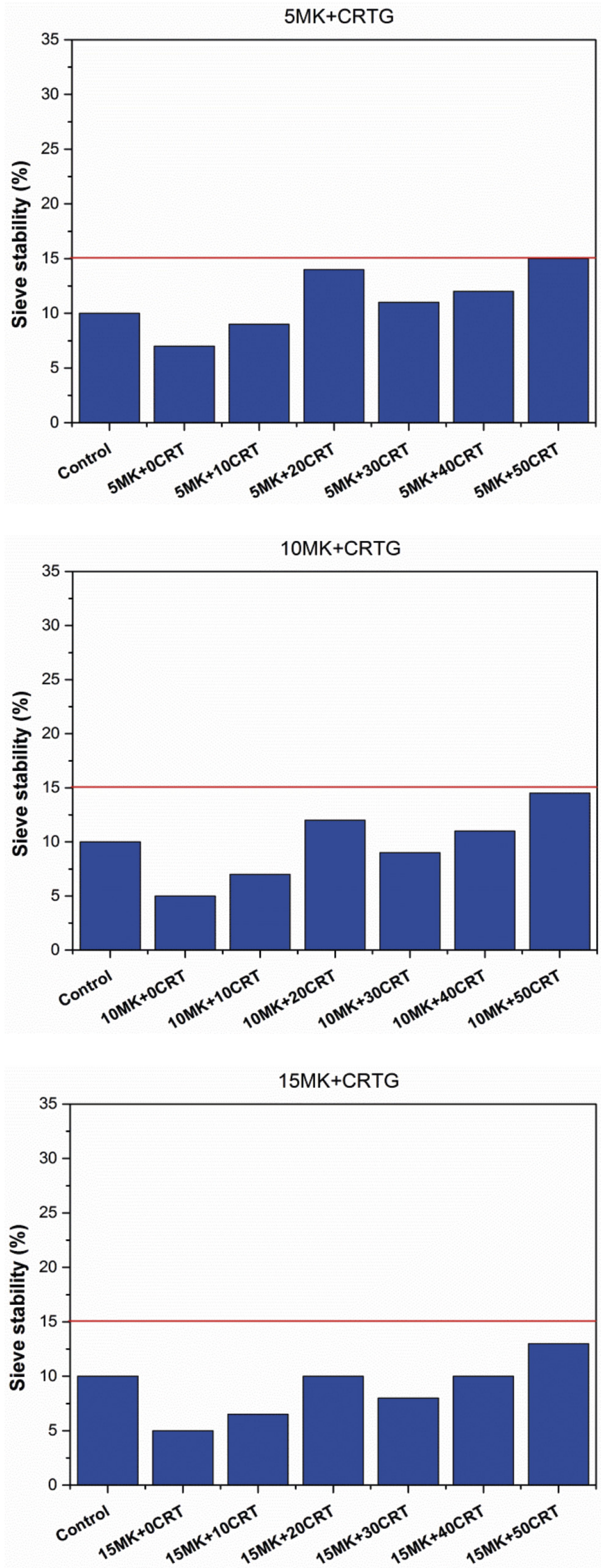

Fig. 8 Sieve stability segregation of different SCC mixes

8. ábra Különböző SCC-keverékek szitás szétosztályozódási hányada

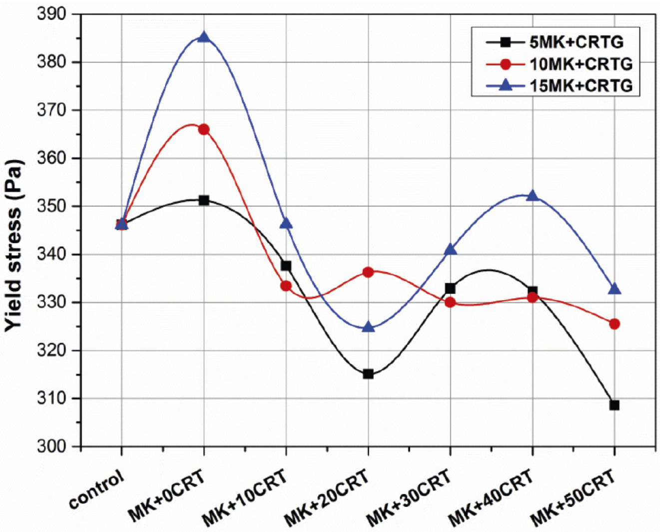

Fig. 9 Yield stress of different SCC mixes
9. ábra Különböző SCC-keverékek folyási feszültsége

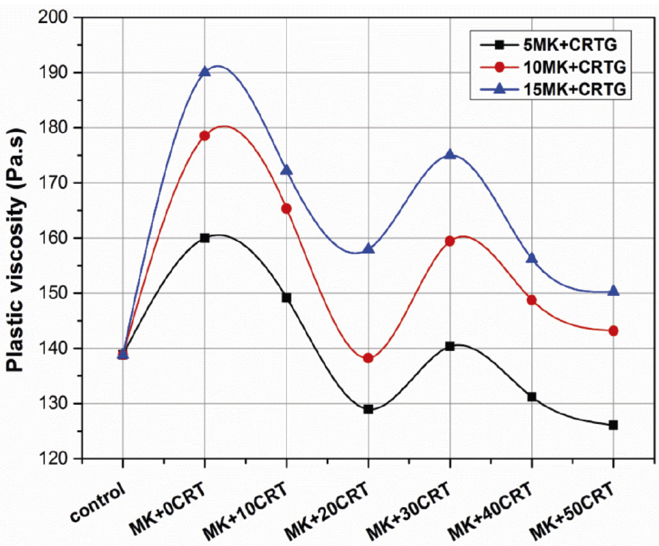

Fig. 10 Plastic viscosity of different SCC mixes
10. ábra Különböző SCC-keverékek plasztikus viszkozitása

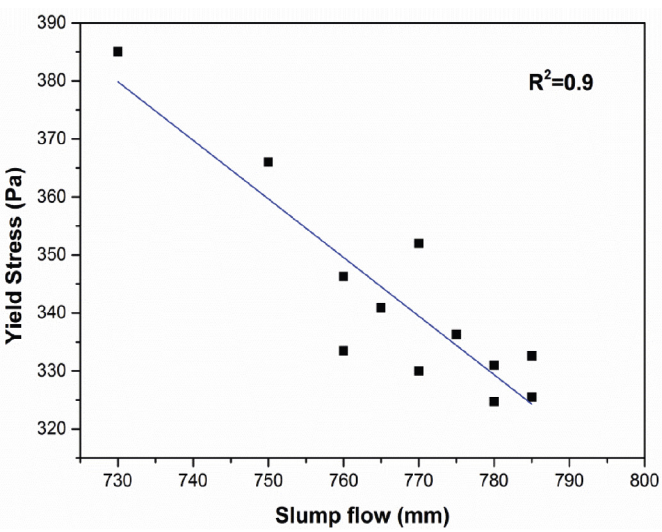

Fig. 11 Relationship between yield stress and slump flow of different SCC mixes
11. ábra SCC keverékek folyási feszültség és roskadási terülés közötti kapcsolata

coefficient R^2= 0.9. The trend of yield stress obtained by the modified slump test confirmed those found by the spreading test; this proves the relevance of this method. As *Fig. 12* shows, the plastic viscosity was proportional to the V-funnel flow times, which corroborates well with of the V-funnel time (R^2= 0.89). The obtained results are similar to those achieved by Boukendakji et al [40] and Boukhelkhal et al [41].

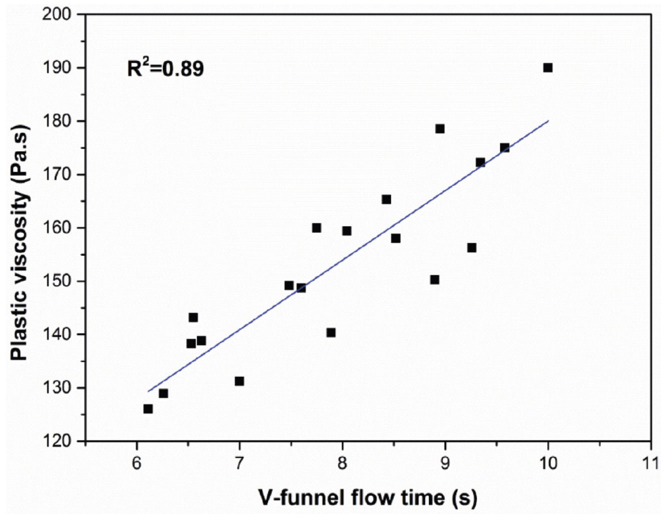

Fig. 12 Relationship between plastic viscosity and V-funnel time of different SCC mixes
12. ábra Különböző SCC-keverékek plasztikus viszkozitásának és V-tölcsér kifolyási idejének összefüggése

4. Conclusions

The use of CRT glass as fine aggregate and MK powder in SCC would not only treat the rheology of SCC (spreading, filling rate, yield stress and viscosity), it would also result in the best environmental practices by optimising and managing the waste materials, energy, and CO_2 emissions. To address these concerns, an experimental program has been set up to understand and provide answers to the questions posed in this work. The conclusions are as follows:

- The incorporation of 50% CRT glass by the mass of sand improved the workability of SCC, while low doses of superplasticiser maintained the same fresh properties; this reduction helps to lower the cost of SCC.
- An increase of 50% in CRT glass reduced sieve stability because it is related to the low viscosity of concrete that makes it easier to pass through the sieve; this leads to an increase in the segregation of SCC.
- With regard to the rheological parameters of SCC, the increase of CRT glass reduced the yield stress and plastic viscosity; the mixture with 15MK+0CRT had the highest yield stress and plastic viscosity.
- The rheological parameters and the yield stress and plastic viscosity can be evaluated using the modified slump test. An acceptable relationship between the rheological properties with the coefficient R^2 superior than 0.9, which indicates the relevance of this method.
- The combined use of CRT sand glass would have important benefits in terms of the negative effect that MK has on the pumpability and the implementation of SCC and the casting time.

References

[1] A.S. Gill, R. Siddique, (2018) Durability properties of SCC incorporating metakaolin and rice husk ash. Construction and Building Materials. 176, 2018, pp. 323-332. https://doi.org/10.1016/j.conbuildmat.2018.05.054.

[2] F. Aslani, G. Ma, (2018) Normal and High-Strength Lightweight SCC Incorporating Perlite, Scoria, and Polystyrene Aggregates at Elevated Temperatures. Journal of Materials in Civil Engineering. 30 (12), 2018, 04018328 https://doi.org/10.1061/(ASCE)MT.1943-5533.0002538.

[3] W. Cui, W.-s. Yan, H.-f. Song, X.-l. Wu, (2018) Blocking analysis of fresh SCC based on the DEM. Construction and Building Materials. 168, 2018, pp. 412-421. https://doi.org/10.1016/j.conbuildmat.2018.02.078.

[4] H. Qasrawi, (2018) Fresh Properties of Green SCC Made with Recycled Steel Slag Coarse Aggregate Under Normal and Hot Weather. Journal of Cleaner Production. 204, 2018, pp. 980-991. https://doi.org/10.1016/j.jclepro.2018.09.075.

[5] B. Benabed, (2018) Effect of combined use of crushed sand and Algerian desert dune sand on fresh properties and strength of SCC. Epitoanyag-Journal of Silicate Based & Composite Materials. 70(5), 2018, pp. 155-166. https://doi.org/10.14382/epitoanyag-jsbcm.2018.29

[6] C. Karakurt, A.O. Çelik, C. Yılmazer, V. Kiriççi, E. Özyaşar, (2018) CFD simulations of SCC with discrete phase modeling. Construction and Building Materials. 186, 2018, pp. 20-30. https://doi.org/10.1016/j.conbuildmat.2018.07.106.

[7] A.M. Matos, L. Maia, S. Nunes, P. Milheiro-Oliveira, (2018) Design of self-compacting high-performance concrete: Study of mortar phase. Construction and Building Materials. 167, 2018, pp. 617-630. https://doi.org/10.1016/j.conbuildmat.2018.02.053.

[8] F. Huang, H. Li, Z. Yi, Z. Wang, Y. Xie, (2018) The rheological properties of SCC containing superplasticizer and air-entraining agent. Construction and Building Materials. 166, 2018, pp. 833-838. https://doi.org/10.1016/j.conbuildmat.2018.01.169

[9] P.R. de Matos, A.L. de Oliveira, F. Pelisser, L.R. Prudêncio Jr, (2018) Rheological behavior of Portland cement pastes and SCC containing porcelain polishing residue. Construction and Building Materials. 175, 2018, pp. 508-518. https://doi.org/10.1016/j.conbuildmat.2018.04.212.

[10] T.Y. Shin, J.H. Kim, S.H. Han, (2017) Rheological properties considering the effect of aggregates on concrete slump flow, Materials and Structures. 50: 239, 2017. https://doi.org/10.1617/s11527-017-1104-9.

[11] C.F. Ferraris, F. de Larrard, (1998) Modified slump test to measure rheological parameters of fresh concrete. Cement, Concrete and Aggregates. 20(2), 1998, pp. 241-247. https://doi.org/10.1520/CCA10417J.

[12] O. Aksogan, R. Resatoglu, H. Binici, (2018) An environment friendly new insulation material involving waste newsprint papers reinforced by cane stalks. Journal of Building Engineering. 15, 2018, pp. 33-40. https://doi.org/10.1016/j.jobe.2017.10.011.

[13] A. Briga-Sa, D. Nascimento, N. Teixeira, J. Pinto, F. Caldeira, H. Varum, A. Paiva, (2013) Textile waste as an alternative thermal insulation building material solution. Construction and Building Materials. 38, 2013, pp. 155-160. https://doi.org/10.1016/j.conbuildmat.2012.08.037.

[14] W. Cai, C. Liu, C. Zhang, M. Ma, W. Rao, W. Li, K. He, M. Gao, (2018) Developing the ecological compensation criterion of industrial solid waste based on emergy for sustainable development. Energy. 157, 2018, pp. 940-948. https://doi.org/10.1016/j.energy.2018.05.207.

[15] W.-J. Long, Y.-c. Gu, D. Zheng, N. Han, (2018) Utilization of graphene oxide for improving the environmental compatibility of cement-based materials containing waste cathode-ray tube glass. Journal of Cleaner Production. 192, 2018, pp. 151-158. https://doi.org/10.1016/j.jclepro.2018.04.229.

[16] X. Lu, X.-a. Ning, D. Chen, K.-H. Chuang, K. Shih, F. Wang, (2018) Lead extraction from Cathode Ray Tube (CRT) funnel glass: Reaction mechanisms in thermal reduction with addition of carbon (C). Waste Management. 76, 2018, pp. 671-678. https://doi.org/10.1016/j.wasman.2018.04.010.

[17] T.C. Ling, C.S. Poon, (2011) Utilization of recycled glass derived from cathode ray tube glass as fine aggregate in cement mortar. Journal of Hazardous Materials. 192(2), 2011, pp. 451-456. https://doi.org/10.1016/j.jhazmat.2011.05.019.

[18] W. Mcdonnel, (1989) Toxicity characteristic leaching procedure (TCLP), AMER ELECTROPLATERS SOC INC 12644 RESEARCH PKWY, ORLANDO, FL 32826-3298, 1989.

[19] Z. Hui, W. Sun, (2011) Study of properties of mortar containing cathode ray tubes (CRT) glass as replacement for river sand fine aggregate. Construction and Building Materials. 25(10), 2011, pp. 4059-4064. https://doi.org/10.1016/j.conbuildmat.2011.04.043.

[20] M. Sarıdemir, M. Çiflikli, F. Soysat, (2018) Mechanical and microstructural properties of HFRHSCs containing metakaolin subjected to elevated temperatures and freezing-thawing cycles. Construction and Building Materials. 158, 2018, pp. 11-23. https://doi.org/10.1016/j.conbuildmat.2017.10.014.

[21] E. Vejmelková, M. Keppert, S. Grzeszczyk, B. Skaliński, R. Černý, (2011) Properties of SCC mixtures containing metakaolin and blast furnace slag. Construction and Building Materials. 25(3), 2011, pp. 1325-1331. https://doi.org/10.1016/j.conbuildmat.2010.09.012 .

[22] J. L. Provis, P. Duxson, J.S. van Deventer, (2011) The role of particle technology in developing sustainable construction materials. Advanced Powder Technology. 21(1), 2010, pp. 2-7 https://doi.org/10.1016/j.apt.2009.10.006.

[23] F.N. Santos, S.R.G. de Sousa, A.J.F. Bombard, S.L. Vieira, (2017) Rheological study of cement paste with metakaolin and/or limestone filler using mixture design of experiments. Construction and Building Materials. 143, 2017, pp. 92-103. https://doi.org/10.1016/j.conbuildmat.2017.03.001.

[24] I.P. Sfikas, E.G. Badogiannis, K.G. Trezos, (2014) Rheology and mechanical characteristics of SCC mixtures containing metakaolin. Construction and Building Materials. 64, 2014, pp. 121-129. https://doi.org/10.1016/j.conbuildmat.2014.04.048.

[25] B. Sabir, S. Wild, J. Bai, (2001) Metakaolin and calcined clays as pozzolans for concrete: a review. Cement and concrete composites. 23(6), 2001, pp. 441-454. https://doi.org/10.1016/S0958-9465(00)00092-5.

[26] M. Said-Mansour, E.-H. Kadri, S. Kenai, M. Ghrici, R. Bennaceur, (2011) Influence of calcined kaolin on mortar properties. Construction and building Materials. 25(5), 2011, pp. 2275-2282. https://doi.org/10.1016/j.conbuildmat.2010.11.017.

[27] H. Okamura, M. Ouchi, (2003) Self-compacting concrete. Journal of advanced concrete technology. 1(1), 2003, pp. 5-15.

[28] B. Benabed, E.-H. Kadri, L. Azzouz, S. Kenai, (2012) Properties of self-compacting mortar made with various types of sand. Cement and Concrete Composites. 34(10), 2012, pp. 1167-1173. https://doi.org/10.1016/j.cemconcomp.2012.07.007.

[29] EFNARC, (2002) Specifications and Guidelines for SCC. Association House London, UK. 2002, p. 32.

[30] T.-C. Ling, C.-S. Poon, (2013) Feasible use of recycled CRT funnel glass as heavyweight fine aggregate in barite concrete. Journal of cleaner production. 33, 2012, pp. 42-49. https://doi.org/10.1016/j.jclepro.2012.05.003.

[31] T.-C. Ling, C.-S. Poon, (2012) Effects of particle size of treated CRT funnel glass on properties of cement mortar. Materials and Structures. 46(1-2), 2012, pp. 25-34. https://doi.org/10.1617/s11527-012-9880-8.

[32] H. Zhao, C.S. Poon, T.C. Ling, (2013) Utilizing recycled cathode ray tube funnel glass sand as river sand replacement in the high-density concrete. Journal of cleaner production. 51, 2013, pp. 184-190. https://doi.org/10.1016/j.jclepro.2013.01.025.

[33] K.A. Melo, A.M.P. Carneiro, (2010) Effect of Metakaolin's finesses and content in SCC. Construction and Building Materials. 24(8), 2010, pp. 1529-1535. https://doi.org/10.1016/j.conbuildmat.2010.02.002.

[34] R. Madandoust, S.Y. Mousavi, (2012) Fresh and hardened properties of SCC containing metakaolin. Construction and Building Materials. 35, 2012, pp. 752-760. https://doi.org/10.1016/j.conbuildmat.2012.04.109.

[35] S. Kou, C. Poon, (2009) Properties of SCC prepared with recycled glass aggregate. Cement and Concrete Composites. 31(2), 2009, pp. 107-113 https://doi.org/10.1016/j.cemconcomp.2008.12.002.

[36] H. Umehara, T. Uehara, Y. Enomoto, S. Oka, (1994) Development and usage of lightweight high performance concrete. Proceedings of International Conference on high Performance Concrete (supplementary papers). Singapore, American Concrete Institute, Detroit, MI, USA, 1994, pp. 339-353.

[37] P. Ghoddousi, A.A.S. Javid, J. Sobhani, (2014) Effects of particle packing density on the stability and rheology of SCC containing mineral admixtures. Construction and building materials. 53, 2014, pp. 102-109. https://doi.org/10.1016/j.conbuildmat.2013.11.076.

[38] A. Hassan, M. Lachemi, K. Hossain, (2010) Effect of metakaolin on the rheology of SCC. In Design, production and placement of SCC, Springer 2010, pp. 103-112 https://doi.org/10.1007/978-90-481-9664-7_9.

[39] E. Güneyisi, M. Gesoğlu, (2008) Properties of self-compacting mortars with binary and ternary cementitious blends of fly ash and metakaolin. Materials and Structures. 41(9), 2008, pp. 1519-1531. https://doi.org/10.1617/s11527-007-9345-7.

[40] O. Boukendakdji, E.-H. Kadri, S. Kenai, (2012) Effects of granulated blast furnace slag and superplasticizer type on the fresh properties and compressive strength of SCC. Cement and concrete composites. 34(4), 2012, pp. 583-590. https://doi.org/10.1016/j.cemconcomp.2011.08.013.

[41] A. Boukhelkhal, L. Azzouz, A.S.E. Belaïdi, B. Benabed, (2016) Effects of marble powder as a partial replacement of cement on some engineering properties of SCC. Journal of adhesion science and Technology 30(22), 2016, pp. 2405-2419. https://doi.org/10.1080/01694243.2016.1184402.

Ref.:
Ouldkhaoua, Younes – **Benabed**, Benchaa – **Abousnina**, Rajab – **El-Kadri**, Hadj: *Rheological properties of blended metakaolin self-compacting concrete containing recycled CRT funnel glass aggregate*
Építőanyag – Journal of Silicate Based and Composite Materials, Vol. 71, No. 5 (2019), 154–161. p.
https://doi.org/10.14382/epitoanyag-jsbcm.2019.27

Rheological characterization of the curing process for a water-based epoxy added with polythiol crosslinking agent

Maria Myrelle S. Quiambao ▪ Chemrez Technologies Inc., Quezon City, Philippines
Danilo D. Laplana ▪ Chemrez Technologies Inc., Quezon City, Philippines
Miguel Ibarra D. Abobo ▪ Chemrez Product Solutions Inc., Quezon City, Philippines ▪ Chemistry Department, College of Science, De La Salle University, Manila, Philippines
Angelica G. Jancon ▪ Chemrez Technologies Inc., Quezon City, Philippines
Sonia D. Salvador ▪ D&L Industries Inc., Quezon City, Philippines
Henry C. Siy ▪ Chemrez Product Solutions Inc., Quezon City, Philippines
David P. Penaloza Jr. ▪ D&L Industries Inc., Quezon City, Philippines ▪ Chemistry Department, College of Science, De La Salle University, Manila, Philippines ▪ david.penaloza.jr@dlsu.edu.ph

Érkezett: 2019. 09. 04. ▪ Received: 04. 09. 2019. ▪ https://doi.org/10.14382/epitoanyag-jsbcm.2019.28

Maria Myrelle S. QUIAMBAO
Design and Development (D&D) specialist, Chemrez Technologies Inc., Quezon City, Philippines

Danilo D. LAPLANA
Design and Development (D&D) technologist, Chemrez Technologies Inc., Quezon City, Philippines

Ibarra Miguel D. ABOBO
MS Chemistry graduate of De La Salle University, Manila, Philippines

Angelica G. JANCON
Design and Development (D&D) manager, Chemrez Technologies Inc., Quezon City, Philippines

Sonia D. SALVADOR
Consultant, D&L Industries, Inc., Quezon City, Philippines

Henry C. SIY
General Manager, Chemrez Product Solutions Inc., Quezon City, Philippines

David P. PENALOZA Jr.
Associate professor in the Chemistry Department, College of Science, De La Salle. University., Manila, Philippines. His research interests focus on self-assembled systems and nanostructured materials.

Abstract
This work presents a rheological investigation of the curing process of a water-based epoxy system by characterizing the efficiency of polythiols as crosslinking agents. Measurements using an oscillatory rheometer equipped with a parallel geometry determined that the rheological profiles (e.g. storage modulus and sol-gel transition - aka gelation, etc.) of the epoxy resins were affected by the number of thiols and the concentration of the added crosslinking agents. A strong correlation between the number of thiols and the storage modulus of the epoxy material was observed. These results enable improvement in epoxy curing process by providing a thorough understanding of the interrelationship of these variables.

Keywords: rheology, curing, epoxy, gel time
Kulcsszavak: reológia, utókezelés, epoxi, gélesedési idő

1. Introduction

Network materials based on crosslinked polymers (thermosets) are specific materials of interest from both basic and applied points of view. A common example of thermosets is epoxies [1-5]. We usually know epoxies as adhesives. A usual chemistry would involve the reaction of 1 mole of amine with 2 moles of epoxides. This will form three-dimensional crosslinks, and the degree of crosslinking determines the curing process (*Fig. 1*).

Usually comprised of a group of crosslinkable resin (epoxide) that when reacted with a curing agent - sometimes referred to as the hardener – resulted in a cured thermoset [6-11]. Combining the epoxy resin and hardener initiates a chemical reaction that converts the initially low molecular weight liquid resin into its thermoset form (solid) characterized by highly crosslinked network structure. This is process is called curing [12-15]. The time it takes for this conversion from liquid to solid is called gel time [4, 16-18]. Understanding the curing reaction is very important in the safe and efficient utilization of epoxies as commercial and technological products.

Introduced in the 1940s, the combination of valuable properties of epoxies such as high toughness [19-23], good adhesion to many substrates [24-29] and remarkable chemical resistance [30-33] and low shrinkage [34-37] and their good processing characteristics had led to their wide utilization in the coatings industry. They are extensively used in plant maintenance, automotive primers, can and drum coatings, appliance finishes, pipe coatings and trade-sales paints [38-48].

A good majority of epoxy materials require high temperature conditions to effect curing. If epoxies are not heated enough, chemical, mechanical and heat-resistance properties of which epoxies are known for consequently suffer [49-52]. It is therefore desired to achieve ease with which the curing process can be fine tuned to suit the fabricating process.

In this work, we used rheology to characterize the curing reaction of an epoxy-amine system modified with polythiol agents. The rheological properties as affected by change in the number of thiol groups as well as varying concentrations were investigated.

2. Experimental methods

Our material of interest is a two-part water-based epoxy system provided by Chemrez, Inc. We decided to add polythiols into the system to give an opportunity to have more crosslinking points that may significantly affect the curing process. Polythiol crosslinking agents having (a) three thiol groups, represented here as $R(SH)_3$; (b) four thiols, $R(SH)_4$ and (c) six thiols, $R(SH)_6$ were used. These thiols are commercially available and hence, from an industrial point of view, are more practical to be used. Thiols were chosen because they are known to react with a lot of functional groups like epoxides inducing a curing reaction [53-57], and we can use a rheometer to follow this curing behaviour [58-63] (*Fig. 2*).

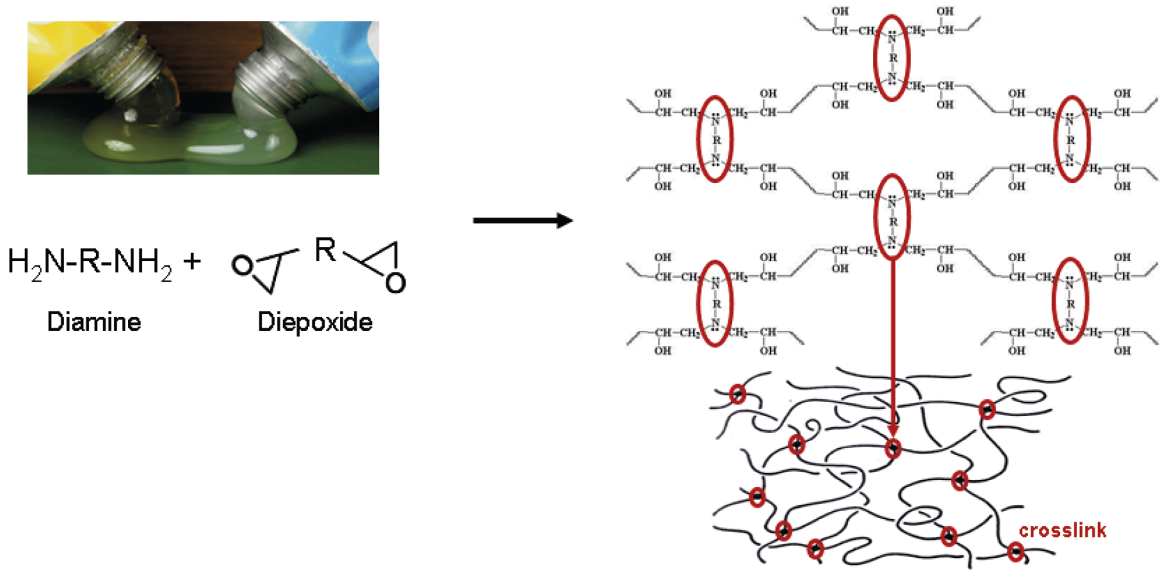

Fig. 1 *An illustration of the formation of a network system from the crosslinking reaction involving an epoxy-amine system*
1. ábra *Epoxi-amin rendszert tartalmazó térhálósodási reakcióból létrejövő hálózati rendszer kialakulásának illusztrációja*

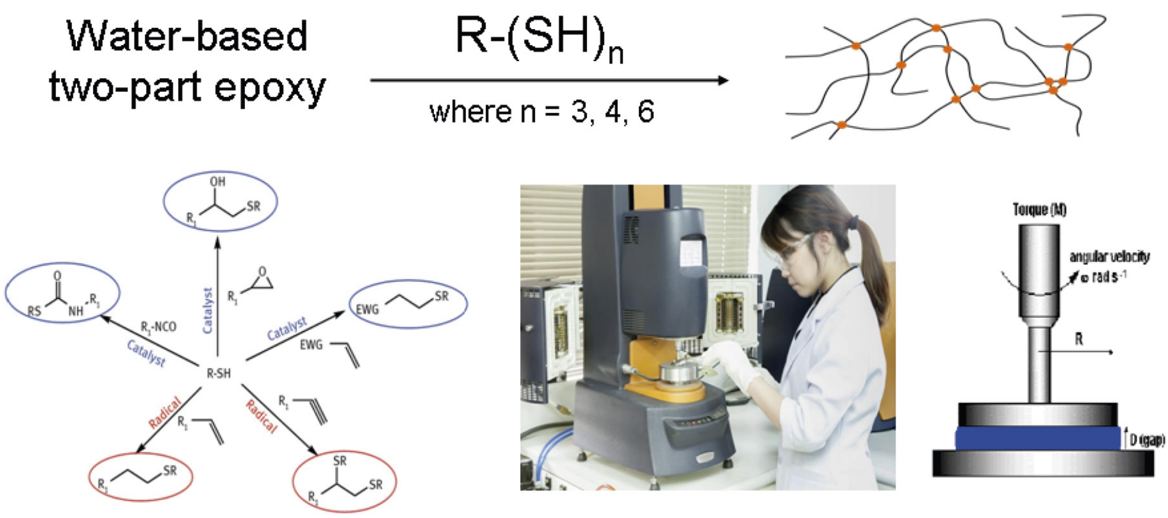

Fig. 2 *Rheological study of the curing process of a water-based epoxy with polythiol additives using a rheometer*
2. ábra *Víz alapú epoxi politiol-adalékanyagokkal való kezelési folyamatának reológiai vizsgálata reométer segítségével*

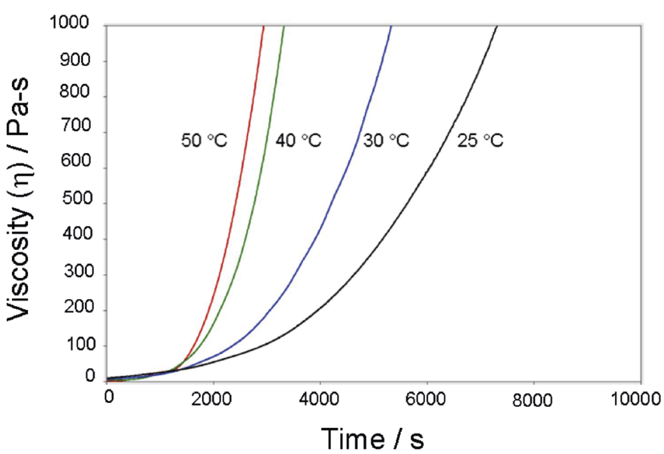

Fig. 3 *Plot of viscosity (η), in Pa-s, vs time, in s, of the epoxy samples at different temperature conditions*
3. ábra *Az epoxi minták viszkozitása (η) [Pa-s] az idő [s] függvényében különböző hőmérsékleteken*

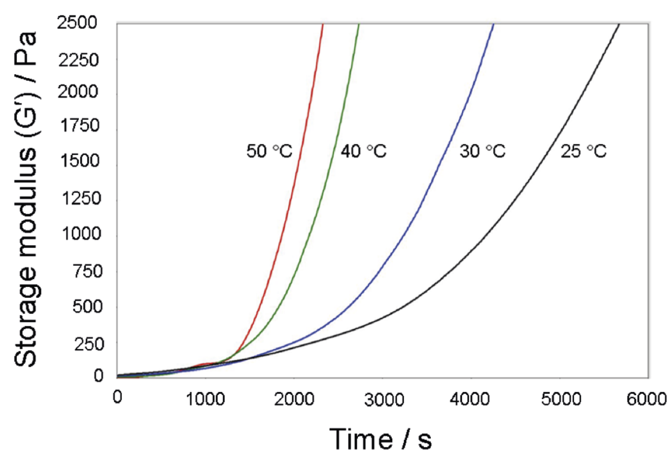

Fig. 4 *Plot of storage modulus (G'), in Pa, vs time, in s, of the epoxy samples at different temperature conditions*
4. ábra *Az epoxi minták tárolási modulusa G' [Pa] az idő [s] függvényében különböző hőmérsékleteken*

Basically, we sandwiched the samples in between two plates. The samples were then subjected to oscillations and mechanical responses during this process were obtained using TA AR3 Hybrid Rheometer. From these measurements, mechanical properties such as viscosity (η) and storage (G') and loss (G") moduli were extracted. In utilizing rheology to follow the curing process, we rely on the change of these viscoelastic parameters: G', G" and η when the material of interest is subjected to oscillations. η is the ability of the epoxy to resist flow, in a way reflects the fluidity of the epoxy material [64-65]. G' represents the elastic character (solid-like behavior) of the epoxy material and is a measure of the energy that can be recovered. On the other hand, G" reflects energy loss by the material through dissipation and represents the viscous part (liquid-like behavior) of the epoxy [4, 16, 66-69].

3. Results and discussion

To characterize the curing reaction of the epoxy material, a sinusoidal shear strain or stress is applied to the sample sandwiched between two parallel plates and the response is monitored and finally recorded: viscosity (η) and storage (G') and loss (G") moduli. We initially monitored the effect of different temperature conditions: 25, 30, 40 and 50°C on the η values of the two-part epoxy system over a period of time. As shown in *Fig. 3*, higher temperature results in a faster gelation as reflected in higher η values recorded over a shorter period of time. A case in point for instance is the higher slope of the η vs. time plot observed at 50°C than at 25°C.

Plotting G' against time – instead of η (*Fig. 4*) shows that the solid-like property of the material increases with increasing temperature. The change in these rheological parameters reflects the progress of the epoxy curing reaction: at the early stage, the epoxy resin behaves like a liquid. As the curing progresses, a crosslinking reaction occurs and this initiates network formation. This is known as the gel point [70]. During this time, epoxy behavior changes from being liquid-like to solid-like and is characterized by a significant change in η (gelation) denoting the formation of a highly crosslinked system [70]. This has a great impact on the application process of the epoxy material. However, in actual applications, increasing the temperature to hasten the curing is not very practical especially when in very wide spaces. So we came up with a solution to employ polythiol additives, in lieu of heating the epoxy to induce epoxy curing – and investigate its effect on the curing process.

At 1 %wt loading, different types of polythiol additives namely: (a) three thiol groups, represented here as $R(SH)_3$; (b) four thiols, $R(SH)_4$ and (c) six thiols, $R(SH)_6$ were used as shown in *Fig. 5*. A negative control – without $R(SH)_n$ – was also included for comparison. The polythiol with the most number of thiol reactive sites, $R(SH)_6$, exhibited the highest G' values, suggesting faster curing rate than the other polythiols used. Obviously, more reactive sites for the epoxides to crosslink offer the fastest gelation behavior the treatments considered.

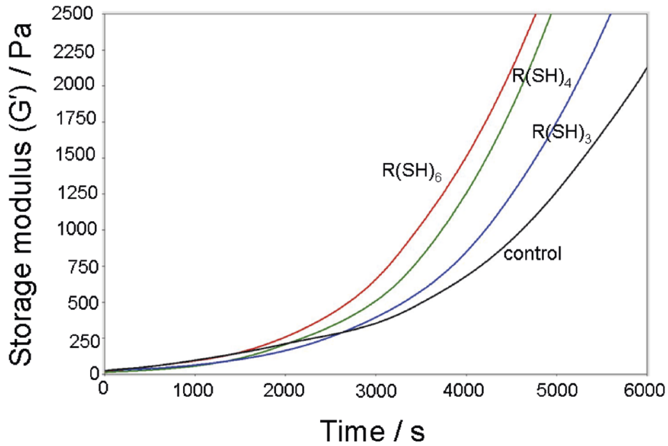

Fig. 5 Plot of storage modulus (G'), in Pa, vs time, in s, of the epoxy samples having different types of polythiol additives - $R(SH)_n$ where n=3,4,6 at 1 wt% loading - as compared to control (no additive)

5. ábra Az epoxi minták tárolási modulusa G' [Pa] az idő [s] függvényében különböző típusú politiol adalékszerekkel - $R(SH)_n$, ahol n=0,3,4,6

After identifying the polythiol additive that can provide the highest increase in G' at the shortest time, here in this case, $R(SH)_6$ – we varied the additive loading concentration: 1, 2, 3, 5 and 10 %wt. Increasing the concentration also results in a faster gelation, as observed in the significant change in G' values in much shorter time periods (*Fig. 6*).

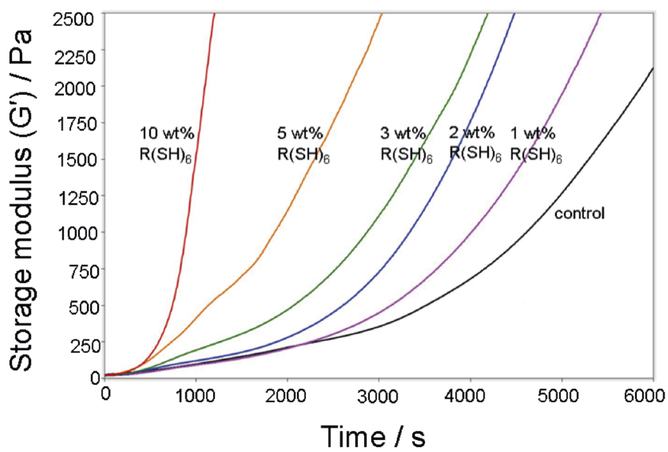

Fig. 6 Plot of storage modulus (G'), in Pa, vs time, in s, of the epoxy samples having different concentrations of $R(SH)_6$ additive as compared to control (no additive)

6. ábra Az epoxi minták tárolási modulusa G' [Pa] az idő [s] függvényében különböző koncentrációjú $R(SH)_6$ adalékszerekkel

We also determine the gel point. To do this, plot of G' and G" versus time, the time correlating to the crossover point of G' and G" corresponds to the gel point as shown in *Fig. 7*. During the initial cure period, the loss modulus is greater than storage modulus. What this means is during this stage, the liquid-like (viscous) behavior of the epoxy dominates over the solid-like (elastic) character. The crossover point is when G'=G", suggesting that a crosslinking reaction between the epoxy resin and the hardener had initiated. This is known as the gel point. This is also characterized by a significant jump in η values. In the final cure stage, G' is much greater than G" meaning the epoxy had become mostly an elastic solid.

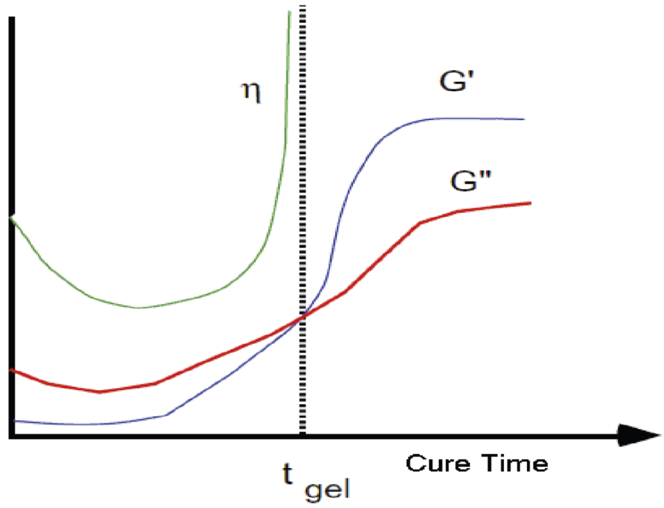

Fig. 7 Gel point is determined as the crossover point of G' and G" in the plot of these moduli values against time
7. ábra A gélpont meghatározása a G' és G" keresztezési pontjaként az idő függvényében

Getting the gel point which is the crossover points of the G' and G" at various concentrations of the $R(SH)_6$ added to the epoxy matrix tells us that increasing the additive concentration led to faster gelation (shorter gel point) as shown in *Table 1*.

Crosslinking agent	Gel point, seconds
Without (control)	4.3 x 10^3
Added with 1 %wt $R(SH)_6$ crosslinking agent	4.7 x 10^3
Added with 5 %wt $R(SH)_6$ crosslinking agent	2.2 x 10^3
Added with 10 %wt $R(SH)_6$ crosslinking agent	0.7 x 10^3

Table 1 Gel points in case of different amount of crosslinking agents
1. táblázat Gélpontok kialakulási időpontja különböző térhálósító szerek esetén

4. Conclusions

In this study, we investigated the curing of a water-based two-part epoxy system modified with polythiol additives. As shown, the curing process can be effectively characterized using rheology. By varying the type of thiol agents as well as the concentration, rheological properties such as viscosity (η), storage modulus (G'), loss modulus (G") and gel point can be fine tuned. Increasing the thiol functional groups for the added crosslinking agent and its concentration result in a faster gelation, as observed in the significant change in G' values in much shorter time periods. Also, getting the gel point which is the crossover points of the G' and G" at various concentrations of the $R(SH)_6$ added to the epoxy matrix tells us that increasing the additive concentration led to faster gelation (shorter gel point). Understanding the interrelationship of these variables is vital in epoxy formulation efforts.

Acknowledgment

We would like to acknowledge the financial grant and technical assistance provided by Chemrez, Inc. and D&L Industries, Inc.

References

[1] Enns, J.B. – Gillham, J.K. (1983): Time–temperature–transformation (TTT) cure diagram: Modeling the cure behavior of thermosets. Journal of Applied Polymer Science Vol. 28, No. 8, pp. 2567-2591. https://doi.org/10.1002/app.1983.070280810
[2] Kamal, M.R. – Sourour, S. – Ryan, M. (2017): Integrated thermo-rheological analysis of the cure of thermosets. SPE Technical Paper Vol. 19, pp. 187-191.
[3] Plazek, D.J. – Frund, Z.N. (1990): Epoxy resins (DGEBA): The curing and physical aging process. Journal of Polymer Science Part B: Polymer Physics Vol. 28, No. 4, pp. 431-448. https://10.1002/polb.1990.090280401
[4] Tung, C.M. – Dynes, P.J. (1982): Relationship between viscoelastic properties and gelation in thermosetting systems. Journal of Applied Polymer Science Vol. 27, No. 2, pp. 569-574. https://doi.org/10.1002/app.1982.070270220
[5] Varshney, V. – Patnaik, S.S. – Roy, A.K. – Farmer, B.L. (2008): A molecular dynamics study of epoxy-based networks: Cross-linking procedure and prediction of molecular and material properties. Macromolecules Vol. 41, No. 18, pp. 6837-6842. https://doi.org/10.1021/ma801153e
[6] Chern, C.S. – Poehlein, G.W. (1987): A kinetic model for curing reactions of epoxides with amines. Polymer Engineering and Science Vol. 27, No. 11, pp. 788-795. https://doi.org/10.1002/pen.760271104
[7] Dušek, K. – Bleha, M. – Luňák, S. (1977): Curing of epoxide resins: model reactions of curing with amines. Journal of Polymer Science: Polymer Chemistry Edition Vol. 15, No. 10, pp. 2393-2400. https://doi.org/10.1002/pol.1977.170151009
[8] Karkanas, P.I. – Partridge, I.K. – Attwood, D. (1996): Modelling the cure of a commercial epoxy resin for applications in resin transfer moulding. Polymer International Vol. 41, No. 2, pp. 183-191. https://doi.org/10.1002/(SICI)1097-0126(199610)41:2<183::AID-PI621>3.0.CO;2-F
[9] Mangion, M.B.M. – Johari, G.P. (1990): Relaxations in thermosets. 7. Dielectric effects during the curing and postcuring of an epoxide by mixed amines. Macromolecules Vol. 23, No. 15, pp. 3687-3695. https://doi.org/10.1021/ma00217a024
[10] Matějka, L. (2000): Amine cured epoxide networks: Formation, structure, and properties. Macromolecules Vol. 33, No. 10, pp. 3611-3619. https://doi.org/10.1021/ma991831w
[11] Ochi, M. – Okazaki, M. – Shimbo, M. (1982): Mechanical relaxation mechanism of epoxide resins cured with aliphatic diamines. Journal of Polymer Science: Polymer Physics Edition Vol. 20, No. 4, pp. 689-699. https://doi.org/10.1002/pol.1982.180200411
[12] Brewis, D.M. – Comyn, J. – Fowler, J.R. (1979): Heat distortion temperatures, glass transition temperatures and extent of chemical cure of some amine-hardened epoxide resins. Polymer Vol. 20, No. 12, pp. 1548-1552. https://doi.org/10.1016/0032-3861(79)90023-5
[13] Lin, R.H. – Hsu, J.H. (2001): In situ FT-IR and DSC investigation on the cure reaction of the dicyanate/diepoxide/diamine system. Polymer International Vol. 50, No. 10, pp. 1073-1081. https://doi.org/10.1002/pi.747
[14] Montserrat, S. – Roman, F. – Colomer, P. (2003): Vitrification and dielectric relaxation during the isothermal curing of an epoxy-amine resin. Polymer Vol. 44, No. 1, pp. 101-114. https://doi.org/10.1016/S0032-3861(02)00745-0
[15] Skladanyuk, R.V. – Zakordonskii, V.P. (2005): Influence of physical structuring on the kinetics of the epoxy-amine reaction in filled systems. Polymer Science Series A Vol. 47, No. 1, pp. 24-31.
[16] Chambon, F. – Winter, H.H. (1987): Linear viscoelasticity at the gel point of a crosslinking PDMS with imbalanced stoichiometry. Journal of Rheology Vol. 31, No. 8, pp. 683-697. https://doi.org/10.1122/1.549955
[17] Michon, C. – Cuvelier, G. – Launay, B. (1993): Concentration dependence of the critical viscoelastic properties of gelatin at the gel point. Rheologica Acta Vol. 32, No. 1, pp. 94-103. https://doi.org/10.1007/BF00396681
[18] Winter, H.H. (1987): Can the gel point of a cross-linking polymer be detected by the G' – G" crossover? Polymer Engineering and Science Vol. 27, No. 22, pp. 1698-1702. https://doi.org/10.1002/pen.760272209
[19] Benzeggagh, M.L. – Kenane, M. (1996): Measurement of mixed-mode delamination fracture toughness of unidirectional glass/epoxy composites with mixed-mode bending apparatus. Composites Science and Technology Vol. 56, No. 4, pp. 439-449. https://doi.org/10.1016/0266-3538(96)00005-X

[20] Garg, A.C. – Mai, Y.W. (1988): Failure mechanisms in toughened epoxy resins – A review. Composites Science and Technology Vol. 31, No. 3, pp. 179-223. https://doi.org/10.1016/0266-3538(88)90009-7

[21] Gojny, F.H, – Wichmann, M.H.G. – Fiedler, B. – Schulte, K. (2005): Influence of different carbon nanotubes on the mechanical properties of epoxy matrix composites – A comparative study. Composites Science and Technology Vol. 65, No. 15-16, pp. 2300-2313. https://doi.org/10.1016/j.compscitech.2005.04.021

[22] Johnsen, B.B. – Kinloch, A.J. – Mohammed, R.D. – Taylor, A.C. – Sprenger, S. (2007): Toughening mechanisms of nanoparticle-modified epoxy polymers. Polymer Vol. 48, No. 2, pp. 530-541. https://doi.org/10.1016/j.polymer.2006.11.038

[23] Rafiee, M.A. – Rafiee, J. – Wang, Z. – Song, H. – Yu, Z.Z. – Koratkar, N. (2009): Enhanced mechanical properties of nanocomposites at low graphene content. ACS Nano Vol. 3, No. 12, pp. 3884-3890. https://doi.org/10.1021/nn9010472

[24] Armelin, E. – Pla, R. – Liesa, F. – Ramis, X. – Iribarren, J.I. – Alemán, C. (2008): Corrosion protection with polyaniline and polypyrrole as anticorrosive additives for epoxy paint. Corrosion Science Vol. 50, No. 3, pp. 721-728. https://doi.org/10.1016/j.corsci.2007.10.006

[25] Dilsiz, N. – Wightman, J.P. (2000): Effect of acid-base properties of unsized and sized carbon fibers on fiber/epoxy matrix adhesion. Colloids and Surfaces A: Physicochemical and Engineering Aspects Vol. 164, No. 2-3, pp. 325-336. https://doi.org/10.1016/S0927-7757(99)00400-8

[26] Drzal, L.T. – Madhukar, M. (1993): Fibre-matrix adhesion and its relationship to composite mechanical properties. Journal of Materials Science Vol. 28, No. 3, pp. 569-610. https://doi.org/10.1007/BF01151234

[27] Ma, P.C. – Mo, S.Y. – Tang, B.Z. – Kim, J.K. (2010): Dispersion, interfacial interaction and re-agglomeration of functionalized carbon nanotubes in epoxy composites. Carbon Vol. 48, No. 6, pp. 1824-1834. https://doi.org/10.1016/j.carbon.2010.01.028

[28] Ochi, M. – Takahashi, R. – Terauchi, A. (2001): Phase structure and mechanical and adhesion properties of epoxy/silica hybrids. Polymer Vol. 42, No. 12, pp. 5151-5158. https://doi.org/10.1016/S0032-3861(00)00935-6

[29] Prolongo, S.G. – Del Rosario, G – Ureña, A. (2006): Comparative study on the adhesive properties of different epoxy resins. International Journal of Adhesion and Adhesives Vol. 26, No. 3, pp. 125-132. https://doi.org/10.1016/j.ijadhadh.2005.02.004

[30] Ahmad, S. – Gupta, A.P. – Sharmin, E. – Alam, M. – Pandey, S.K. (2005): Synthesis, characterization and development of high performance siloxane-modified epoxy paints. Progress in Organic Coatings Vol. 54, No. 3, pp. 248-255. https://doi.org/10.1016/j.porgcoat.2005.06.013

[31] Mostafaei, A. – Nasirpouri, F. (2014): Epoxy/polyaniline-ZnO nanorods hybrid nanocomposite coatings: Synthesis, characterization and corrosion protection performance of conducting paints. Progress in Organic Coatings Vol. 77, No. 1, pp. 146-159. https://doi.org/10.1016/j.porgcoat.2013.08.015

[32] Woo, R.S.C. – Chen, Y. – Zhu, H. – Li, J. – Kim, J.K. – Leung, C.K.Y. (2007): Environmental degradation of epoxy-organoclay nanocomposites due to UV exposure. Part I: Photo-degradation. Composites Science and Technology Vol. 67 No. 15-16, pp. 3448-3456. https://doi.org/10.1016/j.compscitech.2007.03.004

[33] Zhang, Z. – Breidt, C. – Chang, L. – Haupert, F. – Friedrich, K. (2004): Enhancement of the wear resistance of epoxy: short carbon fibre, graphite, PTFE and nano-TiO_2. Composites Part A: Applied Science and Manufacturing Vol. 35, No. 12, pp. 1385-1392. https://doi.org/10.1016/j.compositesa.2004.05.005

[34] Chen, M.H. – Chen, C.R. – Hsu, S.H. – Sun, S.P. – Su, W.F. (2006): Low shrinkage light curable nanocomposite for dental restorative material. Dental Materials Vol. 22, No. 2, pp. 138-145. https://doi.org/10.1016/j.dental.2005.02.012

[35] Ilie, N. – Jelen, E. – Clementino-Luedemann, T. – Hickel, R. (2007): Low-shrinkage composite for dental application. Dental Materials Journal Vol. 26, No. 2, pp. 149-155. https://doi.org/10.4012/dmj.26.149

[36] Ishida, H. – Allen, D.J. (1996): Physical and mechanical characterization of near-zero shrinkage polybenzoxazines. Journal of Polymer Science Part B: Polymer Physics Vol. 34, No. 6, pp. 1019-1030. https://doi.org/10.1002/(SICI)1099-0488(19960430)34:6<1019::AID-POLB1>3.0.CO;2-T

[37] Yarovsky, I. – Evans, E. (2001): Computer simulation of structure and properties of crosslinked polymers: application to epoxy resins. Polymer Vol. 43, No. 3, pp. 963-969. https://doi.org/10.1016/S0032-3861(01)00634-6

[38] Azeez, A.A. – Rhee, K.Y. – Park, S.J. – Hui, D. (2013): Epoxy clay nanocomposites - processing, properties and applications: A review. Composites Part B: Engineering Vol. 45, No. 1, pp. 308-320. https://doi.org/10.1016/j.compositesb.2012.04.012

[39] Bao, C. – Guo, Y. – Song, L. – Kan, Y. – Qian, X. – Hu, Y. (2011): In situ preparation of functionalized graphene oxide/epoxy nanocomposites with effective reinforcements. Journal of Materials Chemistry Vol. 21, No. 35, pp. 13290-13298. https://doi.org/10.1039/C1JM11434D

[40] Chattopadhyay, D.K. – Panda, S.S. – Raju, K.V.S.N. (2005): Thermal and mechanical properties of epoxy acrylate/methacrylates UV cured coatings. Progress in Organic Coatings Vol. 54, No. 1, pp. 10-19. https://doi.org/10.1016/j.porgcoat.2004.12.007

[41] Hughes, J.D.H. (1991): The carbon fibre/epoxy interface – A review. Composites Science and Technology Vol. 41, No. 1, pp. 13-45. https://doi.org/10.1016/0266-3538(91)90050-Y

[42] Li, Y. – Wong, C.P. (2006): Recent advances of conductive adhesives as a lead-free alternative in electronic packaging: Materials, processing, reliability and applications. Materials Science and Engineering: R: Reports Vol. 51, No. 1-3, pp. 1-35. https://doi.org/10.1016/j.mser.2006.01.001

[43] Lorenz, H. – Despont, M. – Fahrni, N. – Brugger, J. – Vettiger, P. – Renaud, P. (1998): High-aspect-ratio, ultrathick, negative-tone near-UV photoresist and its applications for MEMS. Sensors and Actuators A: Physical Vol. 64, No. 1, pp. 33-39. https://doi.org/10.1016/S0924-4247(98)80055-1

[44] Rakotomalala, M. – Wagner, S. – Döring, M. (2010): Recent developments in halogen free flame retardants for epoxy resins for electrical and electronic applications. Materials Vol. 3, No. 8, pp. 4300-4327. https://doi.org/10.3390/ma3084300

[45] Randall, J.P. – Meador, M.A.B. – Jana, S.C. (2011): Tailoring mechanical properties of aerogels for aerospace applications. ACS Applied Materials and Interfaces Vol. 3, No. 3, pp. 613-626. https://doi.org/10.1021/am200007n

[46] Rao, Y. – Ogitani, S. – Kohl, P. – Wong, C.P. (2001): Novel polymer-ceramic nanocomposite based on high dielectric constant epoxy formula for embedded capacitor application. Journal of Applied Polymer Science Vol. 83, No. 5, pp. 1084-1090. https://doi.org/10.1002/app.10082

[47] Toldy, A. – Szolnoki, B. – Marosi, G. (2011): Flame retardancy of fibre-reinforced epoxy resin composites for aerospace applications. Polymer Degradation and Stability Vol. 96, No. 3, pp. 371-376. https://doi.org/10.1016/j.polymdegradstab.2010.03.021

[48] van Westing, E.P.M. – Ferrari, G.M. – de Wit, J.H.W. (1993): The determination of coating performance with impedance measurements-I. Coating polymer properties. Corrosion Science Vol. 34, No. 9, pp. 1511-1530. https://doi.org/10.1016/0010-938X(93)90245-C

[49] Esposito, L. – Sorrentino, L. – Penta, F. – Bellini, C. (2016): Effect of curing overheating on interlaminar shear strength and its modelling in thick FRP laminates. The International Journal of Advanced Manufacturing Technology Vol. 87, No. 5-8, 2213-2220. https://doi.org/10.1007/s00170-016-8613-5

[50] Huang, Y. – Young, R.J. (1995): Interfacial behaviour in high temperature cured carbon fibre/epoxy resin model composite. Composites Vol. 26, No. 8, pp. 541-550. https://doi.org/10.1016/0010-4361(95)92619-N

[51] Kim, J. – Moon, T.J. – Howell, J.R. (2002): Cure kinetic model, heat of reaction, and glass transition temperature of AS4/3501-6 graphite-epoxy prepregs. Journal of Composite Materials Vol. 36, No. 21, pp. 2479-2498. https://doi.org/10.1177/0021998302036021712

[52] Kim, J. – Moon, T.J. – Howell, J.R. (2003): Transient thermal modeling of in-situ curing during tape winding of composite cylinders. Journal of Heat Transfer Vol. 125, No. 1, pp. 137-146. https://10.1115/1.1527912

[53] Grazú, V. – Abian, O. – Mateo, C. – Batista-Viera, F. – Fernández-Lafuente, R. – Guisán, J.M. (2003): Novel bifunctional epoxy/thiol-reactive support to immobilize thiol containing proteins by the epoxy chemistry. Biomacromolecules Vol. 4, No. 6, pp. 1495-1501. https://doi.org/10.1021/bm034262f

[54] Jin, K. – Wilmot, N. – Heath, W.H. – Torkelson, J.M. (2016): Phase-separated thiol-epoxy-acrylate hybrid polymer networks with controlled cross-link density synthesized by simultaneous thiol-acrylate and thiol-

epoxy click reactions. Macromolecules Vol. 49, No. 11, pp. 4115-4123. https://doi.org/10.1021/acs.macromol.6b00141

[55] Stuparu, M.C. – Khan, A. (2016): Thiol-epoxy "click" chemistry: Application in preparation and postpolymerization modification of polymers. Journal of Polymer Science Part A: Polymer Chemistry Vol. 54, No. 19, pp. 3057-3070. https://doi.org/10.1002/pola.28195

[56] Zhang, Y. – Li, H. – Dong, J.Y. – Hu, Y. (2014) Facile synthesis of chain end functionalized polyethylenes via epoxide ring-opening and thiol-ene addition click chemistry. Polymer Chemistry Vol. 5, No. 1, pp. 105-115. https://10.1039/C3PY00727H

[57] Zhu, D.Y. – Cao, G.S. – Qiu, W.L. – Rong, M.Z. – Zhang, M.Q. (2015): Self-healing polyvinyl chloride (PVC) based on microencapsulated nucleophilic thiol-click chemistry. Polymer Vol. 69, pp. 1-9. https://doi.org/10.1016/j.polymer.2015.05.052

[58] Khoun, L. – Centea, T. – Hubert, P. (2010) Characterization methodology of thermoset resins for the processing of composite materials – Case study: CYCOM 890RTM Epoxy Resin. Journal of Composite Materials Vol. 44, No. 11, pp. 1397-1415. https://doi.org/10.1177/0021998309353960

[59] Lange, J. – Altmann, N. – Kelly, C.T. – Halley, P.J. (2000): Understanding vitrification during cure of epoxy resins using dynamic scanning calorimetry and rheological techniques. Polymer Vol. 41, No. 15, pp. 5949-5955. https://doi.org/10.1016/S0032-3861(99)00758-2

[60] Lapique, F. – Redford, K. (2002): Curing effects on viscosity and mechanical properties of a commercial epoxy resin adhesive. International Journal of Adhesion and Adhesives Vol. 22, No. 4, pp. 337-346. https://doi.org/10.1016/S0143-7496(02)00013-1

[61] Le Pluart, L. – Duchet, J. – Sautereau, H. – Halley, P. – Gerard, J.F. (2004): Rheological properties of organoclay suspensions in epoxy network precursors. Applied Clay Science Vol. 25, No. 3-4, pp. 207-219. https://doi.org/10.1016/j.clay.2003.11.004

[62] Martinez. I – Martin, M.D. – Eceiza, A. – Oyanguren, P. – Mondragon, I. (2000): Phase separation in polysulfone-modified epoxy mixtures. Relationships between curing conditions, morphology and ultimate behavior. Polymer Vol. 41, No. 3, pp. 1027-1035. https://doi.org/10.1016/S0032-3861(99)00238-4

[63] Roller, M.B. (1986): Rheology of curing thermosets: A review. Polymer Engineering and Science Vol. 26, No. 6, pp. 432-440. https://doi.org/10.1002/pen.760260610

[64] Khayat, K.H. (1998): Viscosity-enhancing admixtures for cement-based materials - An overview. Cement and Concrete Composites Vol. 20, No. 2-3, pp. 171-188. https://doi.org/10.1016/S0958-9465(98)80006-1

[65] Pries, A.R. – Secomb, T.W. – Sperandio, M.B. – Gross, J.F. – Gaehtgens, P. (1994): Resistance to blood flow in microvessels in vivo. Circulation Research Vol. 75, No. 5, pp. 904-915. https://doi.org/10.1161/01.RES.75.5.904

[66] Almdal, K. – Dyre, J. – Hvidt, S. – Kramer, O. (1993): Towards a phenomenological definition of the term 'gel'. Polymer Gels and Networks Vol. 1, No. 1, pp. 5-17. https://doi.org/10.1016/0966-7822(93)90020-I

[67] Winter, H.H. – Chambon, F. (1986): Analysis of linear viscoelasticity of a crosslinking polymer at the gel point. Journal of Rheology Vol. 30, No. 2, pp. 367-382. https://doi.org/10.1122/1.549853

[68] Hori, K. – Penaloza, D.P. – Shundo, A. – Tanaka, K. (2012): Time-dependent heterogeneity in viscoelastic properties of worm-like micelle solutions. Soft Matter Vol. 8 No. 28, 7361-7364. https://doi.org/10.1039/C2SM25549A

[69] Shundo, A. – Penaloza Jr., D.P. – Tanaka, K. (2013): Microscopic heterogeneity in viscoelastic properties of molecular assembled systems. Chinese Journal of Polymer Science (English Edition) Vol. 31, No. 1, pp. 1-11. https://doi.org/10.1007/s10118-013-1193-z

[70] Wang, X. - Gillham, J. K. (1993): T_g-temperature property (T_gTP) diagram for thermosetting systems: anomalous behavior of physical properties vs. extent of cure. Journal of Applied Polymer Science Vol, 47, No. 3, pp. 425-446

Ref.:

Quiambao, Maria Myrelle S. – **Laplana**, Danilo D. – **Abobo**, Miguel Ibarra D. – **Jancon**, Angelica G. – **Salvador**, Sonia D. – **Siy**, Henry C. – **Penaloza**, David P. Jr.: *Rheological characterization of the curing process for a water-based epoxy added with polythiol crosslinking agent*
Építőanyag – Journal of Silicate Based and Composite Materials, Vol. 71, No. 5 (2019), 162–167. p.
https://doi.org/10.14382/epitoanyag-jsbcm.2019.28

Kollégium török diákok számára

MIKLÓS Gábor
okleveles építészmérnök, tervezői szakirány
Value4Real Kft., építész tervező

MIKLÓS Gábor ▪ Value4Real Kft. ▪ gabor.miklos.92@gmail.com

Érkezett: 2019. 08. 04. ▪ Received: 04. 08. 2019. ▪ https://doi.org/10.14382/epitoanyag-jsbcm.2019.29

Abstract

Located on the steepest street of Budapest, Student hostel for Turkish students creates a unique accommodation for those who study in the capital city of Hungary for 1 or 2 semesters. As a young architect, I wish, more and more students can have the opportunity to explore foreign countries, because these experiences can broaden their horizon. The designing area is one of the most famous historical places in Budapest, which has a romantic, mysterious atmosphere. Despite of that, Gül Baba street has a hole in the line of the historical houses, which could be closed by the designed building.

The designing process shaped to achieve two aims: connection to the atmosphere of the historical site and utilize the ancient Islamic architecture's toolbar. The first goal appears in the claddings and shape of the building mass. Ceramic surfaces can easily fit with the historical street and the environment of Gül Baba's octagonal tomb. The central organized floor plans and the interior patterns relates to the impression of the Islamic architecture.

Keywords: architecture, historical site, historic preservation, Gül Baba's octagonal tomb, ceramic cladding, Islamic architecture, architectural heritage, college, student hostel, Hungary-Turkey relations

Kulcsszavak: építészet, műemlékvédelem, műemléki környezet, Gül Baba türbéje, Gül Baba utca, kerámia burkolat, iszlám építészet, építészeti hagyományok, kollégium, diákszálló, török-magyar kapcsolatok

1. Koncepció

A Gül Baba türbéje és környezete egy különleges helyszín Budapest nagyvárosi forgatagában. A környék utcácskáiban sétálva az ember egy sokkal zártabb, rejtélyesebb, historikusabb világban találja magát, mint akár a pesti, akár a budai belváros nagy részében. Sajnos itt is találhatóak olyan hiányzó épülettömegek, amelyek csökkentik az arra járók teljességérzetét. Számomra a tervezési helyszín a foghíjtelek beépítésével és a lejtős tereppel együtt egy komplex műszaki kihívásokat igénylő feladatot is jelentett. A helyhez társított szállásfunkcióval a nemzetközi kapcsolatok erősítését, valamint a külföldi tanulók elhelyezésének segítését kívánnám elérni. Fontosnak tartom, hogy az ember már fiatalként megismerjen új kultúrákat, bővítse a látóterét, tanuljon vagy dolgozzon külföldön.

2. Elhelyezkedés

A tervezett épület Budapesten, Rózsadombon, a Gül Baba utcában két üresen álló foghíj telekre épül. Az utca Budapest legmeredekebb utcájaként ismert, közvetlen környezetében található Gül Baba türbéje, ami a 20-22. számú telkekkel is szomszédos. A türbe nemcsak hazai szinten fontos műemlék, hanem a világ legészakibb fekvésű iszlám zarándokhelye. Emiatt és az utca különleges hangulatának megőrzése érdekében a helyszín műemléki környezet alá tartozik.

2.1 Gül Baba türbéje

Gül Baba török dervis (szerzetes) volt, aki feltételezhetően Buda ostrománál szenvedett halálos sérülést. Nevét sokan Rózsa apóként fordítják magyarra, ami valószínűleg a rózsák iránti szeretetéből ered, ugyanis pontos neve sem tisztázott. Annyi azonban bizonyos, hogy köztiszteletnek örvendő személy volt, akinek koporsóját állítólag a szultán személyesen kísérte gyászmenetén, majd e koporsó felé türbét emeltetett.A történelem aztán sok nyomot hagyott az épületen és környezetében, de még így is fenn tudott maradni az eredetihez közeli állapotában.

A türbe a török-magyar kapcsolatok XX. és XXI. századi jó viszonyát is szimbolizálja, ugyanis a 2018-ban lezáruló rekonstrukciót a két nemzet közös anyagi támogatásából valósították meg. Hazai támogatásból újult meg a türbe környezete, így a Gül Baba utca is, ami új burkolatot kapott, kedvezve így a vízelvezetésnek és csúszásmentességnek.

2.2 Gül Baba utca

A meredek Gül Baba utca Budapest talán leghangulatosabb utcája. A szűk kis utcából a házak lépcsősen egymásra tapadva emelkednek, amelyekből sok még eredeti, XIX. századi állapotában maradt fent. A macskaköves burkolat szintén az utca jellegzetessége.

Az utca meredekség szempontjából három szakaszból áll, a két vége lankásabb míg a középső része a legmeredekebb, ahol az tervezési terület is található. Az utca egy forgalom elől elzárt terület, behajtás csak engedéllyel lehetséges. Még hulladék elszállítás sincs az utcában.

2.3 Telek

A 20-22 szám alatt álló telkek a zártsorú beépítés foghíjai és egyben az utcaképet is jelentősen szegényítik. A Türbe rekonstrukciójával még nagyobb igény nyílik a két telek beépítésére, mivel az északi lépcső szomszédos vele, amely a látogatók egyik gyakori útvonala is lesz. Jelenleg a telket építési törmelék borítja, illetve az egykori házakból faltest maradványok támaszkodnak a szomszédos épületre. Ezen kívül az egykori Wagner villa támfalaiból is találhatóak maradványok a kertben, amelyhez egy zsalukő fal támaszkodik. Ezek állapota igencsak megromlott, műemléki értékük nincs.

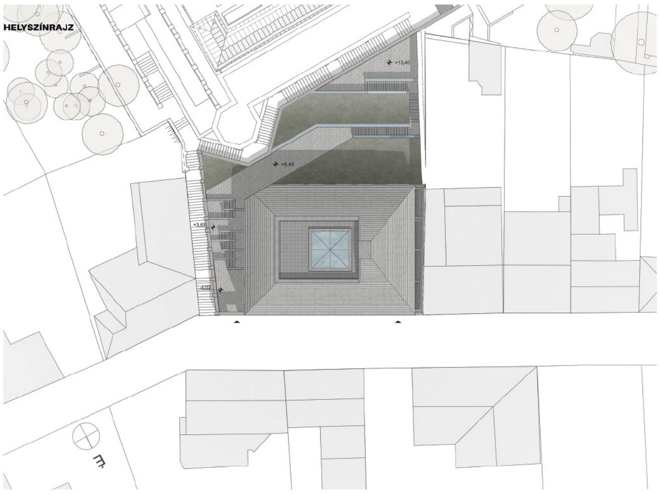

1. ábra Helyszínrajz
Fig. 1 Site plan

A telkek lakóövezetben, zártsorú beépítésben helyezkednek el. Maximális beépíthetőségük 65%, amit az építési vonal még inkább leszabályoz.

2.4 Környezeti adottságok

2.4.1 Talaj

A Rózsadomb Duna-felé eső lejtőjét eocén korú ún. „budai" márga építi fel, erre alapozták például Gül Baba sírját is Az utca egy régi vízmosás nyomvonalában halad, ezért a márgát fedő agyagösszlet vastagsága változó. Sem talaj, sem rétegvíz nem várható a terület nagyobb részén, ahol a márga felszín közelbe emelkedik és felette csak sárga mállás agyagból álló takaró van.

2.4.2 Zajhatás

A telek zárt sorú beépítésben, sarok telekként egy kétemelet plusz tetőtér beépítéses ház és az türbéből vezető északi lépcső között helyezkedik. Az utca nagyon alacsony forgalmú zsákutca, ahol leginkább az idelátogató turisták és helyi lakosok közlekednek gyalogosan. Ez feltételezhetően a jövőben se fog változni, így alacsony zajhatásnak kitett az tervezett épület.

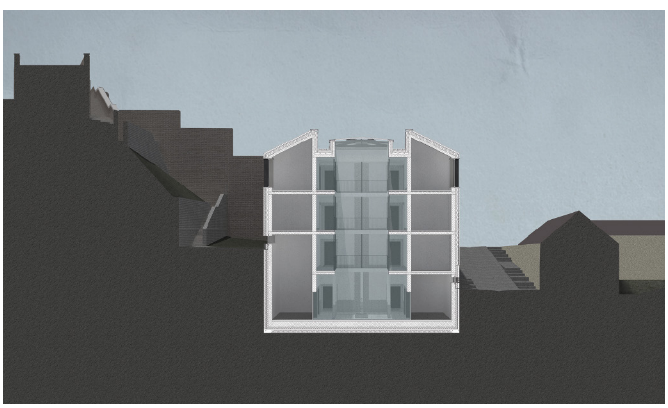

2. ábra Keresztmetszet
Fig. 2 Cross section drawing

3. Rendeltetés

A Gül Baba utca 20-22. szám alatti telkek lakó övezet alá tartoznak. A tervezett épület funkciója ehhez illeszkedően egy olyan kollégium, amely hosszútávú itt tanulásra fogad török ösztöndíjas diákokat. A létesítményt olyan tanulók fogják igénybe venni, akik egy nemzetközi szervezet által összeállított szállást és ösztöndíjat tartalmazó programban vesznek részt. Az intézmény célja továbbá a török-magyar kapcsolatok erősítése.

3.1 Török-magyar kapcsolatok

A XIX. század második felétől kezdett a történelem miatti ellenséges hangulat megváltozni a két nemzet között, főleg az értelmiségi rétegben. A századfordulón előbb Konstantinápolyban alapult Magyar Intézet, majd itthon Magyar Turáni társaság. Ezeknek és a klebelsbergi kultúrpolitikának hála például az, hogy Kós Károly ösztöndíjasként tanulmányozhatta Isztanbult és oszmán hallgatók érkeztek Budapestre.

3.2 Funkció, lehetséges megrendelő

A török-magyar kulturális kapcsolat erősítésének fontos része a fiataloknak megteremteni a lehetőséget a másik ország, másik kultúra megismerésére, illetve a közös szellemi értékek megtalálására. Ehhez nyújt lehetőséget például egy itthon is működő nemzetközi cég, amely török diákoknak biztosít külföldi tanulmányi csomagokat. Ezek a csomagok nem csak az ösztöndíjat, hanem a szálláslehetőséget is tartalmazzák, így gyorsítva az ügyintézést.

4. Építészeti koncepció

A tervezést két nagyobb cél határozta meg: a hely történeti atmoszférájára való kapcsolódás és az iszlám építészetből hozott építészeti eszköztár felhasználása. Előbbi főleg külső anyaghasználatban és a tömeg alakításban jelenik meg.

A szállásépület egy zárt belső udvar köré szerveződik, ami a legalsó szinten egy külső udvarból, recepción keresztül nyílik meg. Ezen a szinten kap helyet egy előadóterem, egy imaszoba valamint gépészeti és kiszolgáló funkciók. A felette lévő szint a meredek utca és telek viszonyai miatt még részben föld alatt van, illetve egy gazdasági bejárattal is rendelkezik. Ezenkívül itt kapnak helyett a közös használatú terek, illetve két lakószoba is. A felette lévő két szinten 8-8 lakószoba kerül kialakításra, amelyből a legfelsőbb szintiek tetőtériek. Az épület tetejét egy a kontúrtól elhúzott lapos tető fedi, amelyhez oldalanként magas tető zár fel, így kialakítva egy teknőben lévő tetőtéri helyet, ahonnan feltárul a budai hegyoldal panorámája.

4.1 Alaprajzi rendszer

Már a tervezés kezdeti fázisaitól az épület meghatározó elemét képezte az udvar, mint szervező erő használata. Az eszköz részben a környék beépítései miatt (hosszú udvaros házak), részben az iszlám építészeti vonatkozása miatt vált a terv központi részévé. A tervezett beépítés megkülönböztetett udvarok kapcsolatából jön létre.

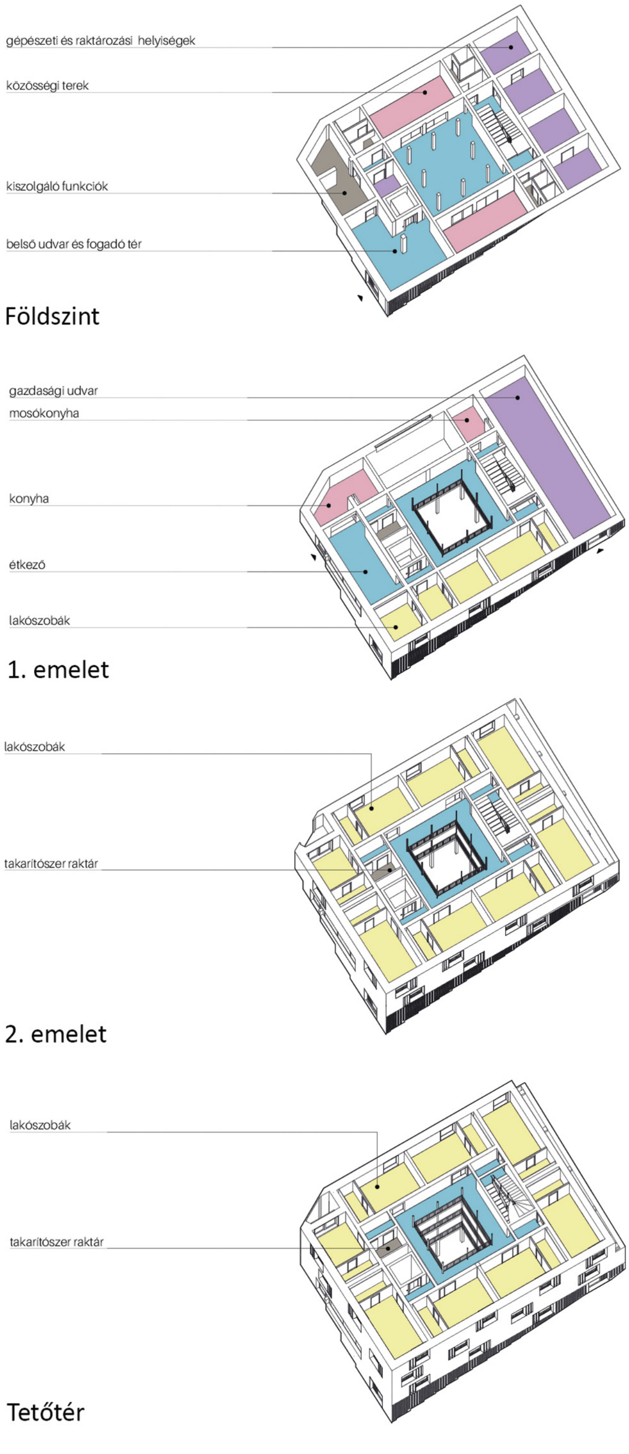

3. ábra Alaprajzi elrendezések
Fig. 3 Floor plans

Az épület fő szervező magja egy négyzet alaprajzú folyosókkal határolt, fedett belső udvar. Az iszlám építészet talán legfőbb jellemzői a szerkesztettség és a geometria. Az iszlám belső udvar köré meghatározott funkciójú terek kapcsolódtak. Érdekesség, hogy a centrális belső udvar sokszor nem középről, hanem valamelyik sarokból tárul fel. Ezen belső terek közepén sok helyen kút vagy kisebb medence áll, amely körül növényzet vagy ülő alkalmatosságok is helyet kaptak. A vízfelület jelenléte az esztétika mellett klimatikus szempontból is hasznos volt a Közel-Keleten ugyanis párolgás útján hűtötte a körülötte lévő tereket. Emellett az iszlám vallásban kulcsfontosságú szerepe van a megtisztulásnak, így például az imádkozást is megmosakodással kezdik.

4. ábra Belső látványterv – udvar
Fig. 4 Interior visualization - courtyard

A kút elhelyezésének helyi jelentés tartalma is van, ugyanis a Gül Baba utca 26. szám alatt lakott Toroczkai Wigand Ede építész, iparművész, író, akinek saját kertjében is rózsák körülvett kút állott. A Magyarság folyóiratban így értekezett a harmonikus otthon megteremtéséről:

„Ha lehet, kertre fordítsuk a dolgozószobát. Ha a viszonyok engedik, rózsás vagy medencés udvarra tekintsen, hol a víz csobogása jelezze a csendes, de örökké lüktető életet.” [1]

4.1.1 Bejárati udvar

A belső udvarhoz szervesen kapcsolódik a fogadótér, valamint a bejárati külső udvar. Az utca zártsorú egymáshoz tapadó épületfalai főleg az utca felső illetve az alsó szakaszán jellemzőek, azonban a középső szakaszon elvétve találunk példákat udvarból való megnyitásra is. Ez a megérkezés egyfelől szeretné a titokzatosságával hívogatni a látogatót, hasonlóan akár egy mediterrán szűk utcás városka sikátoraihoz. Emellett az, hogy az épülettömeg nem ér ki a lépcsőig, így az utcáról fellátni egészen a Wagner-villa rekonstruált bástyáig. Ebbe az udvarba érkezve egy titokzatos lépcsőt láthatunk, amely felvezet a hátsó kertbe, valamint az első szinti közösségi terek szintjére is bejutást enged. A lépcső szerkesztése geometrikus indíttatású volt, azzal a céllal, hogy a bejárati kapuból egy mintaként jelenjen meg.

4.1.2 Hátsó kert

A hátsó kert teraszozosan lépcsőzik fel a meredek domboldalra, hasonlóan felső szomszédok kertjéhez. Az utca felső szakaszán a telekkel megegyező oldalon ugyanis a legtöbb teleknek két utca kapcsolata is adódik a hátsó kertek fellépcsőzése miatt, így például a gépkocsi tárolást is könnyen meg tudják oldani a Turbán utca felől. A 22. számú telek azonban nem ér fel teljesen a Turbán utcáig, így innen nem közelíthető meg a ház. Azonban a hátsó kert egy nyugodt, pihenésre alkalmas helyet teremt, ahová fel tudnak sétálni a bentlakók. A kert teraszain a hely történetéhez hűen rózsákat ültethetnek.

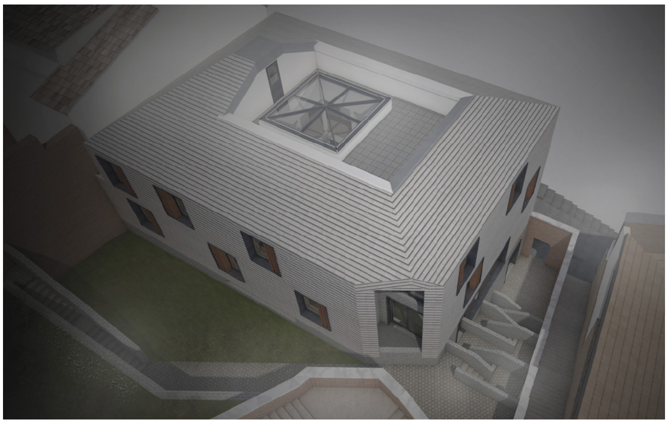

5. ábra Külső látványterv - hátsó kert
Fig. 5 Exterior visualization - backyard

4.1.3 Gazdasági udvar

Mivel az utca forgalomtól elzárt terület így a gépkocsival való megközelítés is csak engedéllyel lehetséges, emiatt az ilyen típusú forgalom nem gyakori. A tervezés korábbi fázisaiban a szomszédházhoz tapadó első emeleti udvar még gépkocsi bejáróval rendelkezett, azonban a helyi lakókkal való beszélgetés alapján megtudtam, hogy az utca ezen szakaszán a szabályos garázs kialakítása szinte lehetetlen. Így a végső döntés egy széles kapu és a mögötte található hosszúkás gazdasági udvar mellett történt, de igény esetén a garázskapu beépítésére is lenne lehetőség. Az áruszállítást az utcában megálló furgonból kipakolva tudják végezni az ottdolgozók. A belső térben rámpán keresztül lehet lejutni az 1. emelet szintjére, ahonnan lépcsőn azonnal le tudunk jutni a földszinti kiszolgáló és gépészeti helyiségekbe.

4.2 Tömegformálás

A hely adottságai miatt a tömegformálás kulcsfontosságú kérdés volt a tervezés kezdeti fázisaitól. Az utca, valamint a telek meredek emelkedése miatt a terepbe illesztés és a homlokzat lépcsőztetése sok próbálkozás árán nyerte el a tervezett formáját. A Gül Baba utcába tervezett épület a Türbéből lejövő nagyméretű tégla korlátot folytatva alakít ki egy alsó szinti foglalatot, amelyre egy egységes megjelenésű tömeg ül rá. A téglalap alaprajzú tömeg a Wagner-villa bástyájához közeli sarkon letörik, ezzel mintegy reagál a bástya által kialakított kitüremkedésre és teret ad a hátsó kertbe való átközlekedésre. Az utcafronton a gazdasági udvar felett egy légakna került kialakításra, ami által az épület kissé elhúzódik a szomszédjától ezzel is erősítve az épület befelé forduló, centrális jellegét. A telek további az utca többi házához képest ritka adottsága, hogy gyakorlatilag saroktelekként az utcából két homlokzata is megmutatkozik. A félnyeregtetőként felzáró magastetők alkalmazását azért tartottam fontosnak, hogy a ház ekképpen is illeszkedjen az utcaképbe, viszont lehetőség adódjon egy olyan tetőterasz kialakítására, ami az utcából nem látszódik.

6. ábra Külső látványterv - utcai tömeg
Fig. 6 Exterior visualization – streetview

4.3 Anyaghasználat

Az épület anyaghasználatában a környezetében lévő Türbéhez valamint az utca többi épületén is fellelhető anyaghoz kíván igazodni. Így került a választás a kerámia anyagok széleskörű alkalmazására.

7. ábra Homlokzatok
Fig. 7 Elevations

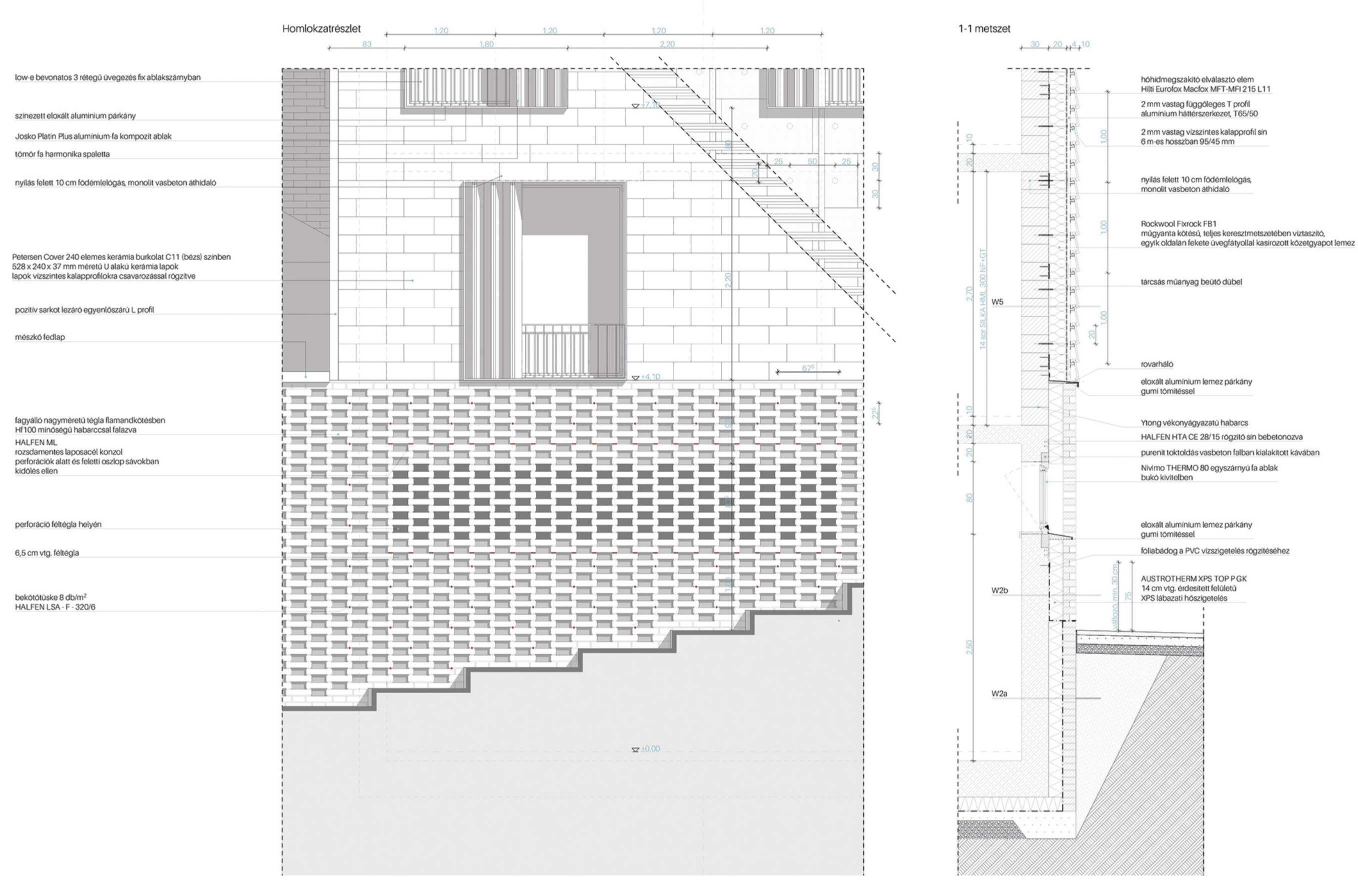

8. ábra Homlokzati részlet
Fig. 8 Elevation detail

4.3.1 Utcai homlokzat

A fentebb említett Türbéből lejövő korlát nagyméretű téglából készült, ami a házon egy perforált mintában folytatódik ugyanazon anyaggal és kötésrenddel. Az erre ráülő tömeg egységes megjelenését a Petersen Cover nevű, dán nagy elemes kerámiaburkolat biztosítja, amit fal- és tetőburkolatként is alkalmazható. Rögzítése vízszintes alumínium kalapprofilokra csavarozással történik, amik függőleges T profilú vázhoz kapcsolódnak. Ezek a bordák pontszerűen vannak a szerkezethez felfogatva hőhídmentes távtartókkal.

4.3.2 Belső udvar

A belső udvarban az iszlám építészetet idéző mázas kerámiaburkolatok jelennek meg. E minták megidézése a mai csempeburkolatokon igen népszerű. A burkolatok pozíciójuk szerint megkülönböztettek: így van türkíz lábazati, nagyelemes padló- és kiemelt szalag, illetve „terülő” burkolat. Ezek a burkolatok kifutnak a belső udvarból a fogadótérbe valamint a tetőteraszra is.

4.3.3 Kerti homlokzat

A belső tér világa a tetőn kívül a kerti homlokzatok mázas kerámia lábazatán is visszaköszön. A kerti homlokzatok emellett nagyobb megnyitásokkal teremtenek kapcsolatot a külső és belső tér között.

5. Összefoglalás

Műemlékeink és műemléki környezeteink védelme elsődleges szempont kellene legyen a hazai építész kultúrában. Tervemmel szeretném rávilágítani a figyelmet arra, hogy mennyire fontos egy ilyen különleges helyszínen a múlthoz való kapcsolódás és a modern építészeti eszközök összhangba hozása. Ez a kis szállásépület kapcsolatokat keres tömegében a környezetével, funkciójában a kultúrákkal.

Köszönetnyilvánítás

Köszönet illeti Nagy Mártont, aki diplomamunkám és több egyetemi tervezési tárgyam során építész konzulensként adta át nekem szakmai tudását.

Hivatkozások

[1] Thoroczkai Wigand Ede: „Hogyan öntsünk lelket otthonunkba. Az ízléses lakás problémája.” - Magyarság, 1923

Ref.:
Miklós, Gábor: *Kollégium török diákok számára*
Építőanyag – Journal of Silicate Based and Composite Materials, Vol. 71, No. 5 (2019), 168–172. p.
https://doi.org/10.14382/epitoanyag-jsbcm.2019.29

Two approaches to the modelling of chip formation: rheological models and finite element analysis

Jüri OLT ▪ Institute of Technology, Estonian University of Life Sciences, Estonia ▪ jyri.olt@emu.ee
Olga LIIVAPUU ▪ Institute of Technology, Estonian University of Life Sciences, Estonia ▪ olga.liivapuu@emu.ee

Érkezett: 2019. 09. 24. ▪ Received: 24. 09. 2019. ▪ https://doi.org/10.14382/epitoanyag-jsbcm.2019.30

Abstract
Metal cutting is a complex process in which several mechanisms are at work simultaneously. The mathematical modelling allows carrying out research into the optimization of machining conditions. Usually, the study of cutting process is very complicated, because the material removal process is conducted in an extremely adverse environment with high temperature and pressure in the zone of cutting. Therefore, the main goal of these studies is to establish a theory that will predict chip formation dynamics, cutting forces, temperature, tool wear, which allows to solve practical problems. This work examines the simulation of chip formation during the process of cutting. The aim of the present research is to compare models based on rheological properties of metals with 2D Finite Element Models of chip formation process.
Keywords: chip formation, elastic and plastic deformation, rheological models, finite element method
Kulcsszavak: forgácsképződés, rugalmas és képlékeny alakváltozás, reológiai modellek, véges elemek módszere

Jüri OLT, DSc.
He is a Professor at the Institute of Technology of the Estonian University of Life Sciences. His main researching area are fundamentals of production enginering, dynamics of machining technological systems, materials cutting and design of technological machinery.

Olga LIIVAPUU, PhD.
She is an Associate Professor at the Institute of Technology of the Estonian University of Life Sciences. She received Ph.D. degree in mathematics from University of Tartu in 2011. Her current research interests include applications of mathematical models to chip formation process and finite element analysis.

1. Introduction

The chip formation process proceeds with a very significant relative deformation of material, reflecting the high deformation rate in a comparatively small zone. The mathematical modelling will play very important role in increasing the awareness of the cutting process and reducing the number of experiments which are frequently used for a selection of different cutting parameters, tool design, machinability evaluation, etc. The chip formation mechanism in the orthogonal metal cutting process, is the focus in the present research. To simulate this process, we compare two approaches: description of the physical properties of the deformed metal using discrete complex mechanical (rheological) models and finite element models.

The study of the rheological properties of materials is widely used by engineers, physicists, chemists and mathematicians. The physical properties of deformed metal can be described in the form of an adequate mechanical model, constructed as a composition of mechanical elements such as elasticity, viscosity and plasticity [1]. Considering combinations of linear elastic springs, linear viscous dash-pots and elements of plasticity one can build a model which gives an observable perspective reflecting the nature of material removal process, changes in deformation and stresses of material and their dependence on the structure [2], [3], [4]. Many real metals combine behaviors of all these elements and it is possible to consider the stress-strain state of metal under the action of external loads. The rheological models in the form of non-periodic diagrams allow to describe new properties that reflect the process of deformation and destruction of a workable material in the process of cutting. Increasing number of elements will allow to construct more accurate model describing the response of real materials. But in this case there are more material parameters need to be evaluated by experiments, usually, it might be very difficult, if not an impossible, task.

Finite element method (FEM) is most frequently used in metal cutting analysis. In recent years, FEM has become the main tool for simulating metal cutting processes. It provides appropriate approach to visualize cutting process, because it allows to predict various characteristics of the metal cutting such as cutting forces, temperatures, stresses, chip types and shapes, etc. [5-8].

2. Application of rheological models to the chip formation process

Metal cutting is a complicated mechanical process, which includes plastic deformation and destruction of metal in the local zone, friction in interaction of the cutting tool with workable material. In accordance with the results of previous studies [8], this interaction accompanied with flat chip formation was examined in two stages up to the moment of the formation of shaving, i.e. the deformation to the shear plane and the shift of the element of small thickness on the plane of shift.

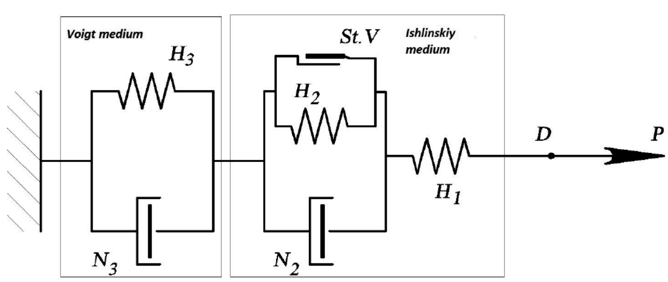

Fig. 1 The model for a mechanical system in the chip formation process
1. ábra A forgácsképződési folyamat mechanikai rendszerének modellje

We describe the process of chip formation with the help of the rheological model proposed by Veitz and Maksarov [9]. This model is constructed as combination of two rheological bodies connected in series: the elastic-ductile-plastic medium of Ishlinskiy type [2], [3], [4] and viscoelastic Voigt medium with the delay of deformation (see *Fig. 1*). The four-element rheological model of Ishlinskiy most fully reflects the dynamics of plastic deformation and destruction of a solid body in the cut off layer of metal. The force ***P*** applied to the point D imitates by the linear elastic spring element H_1 the elastic instantaneous deformation, formed in front of the area of plastic deformation in the zone of chip formation. The next part of this model imitates the prolonged viscoelastic deformation with the help of the spring H_2 and the dash-pot N_2 connected in parallel. After reaching the yield stress σ_y which imitates St. Venant element *St.V.* the instantaneous residual deformation appears. This leads to the shaping of local segments of shift in the primary deformation zone of the cut off layer. At this stage, permanent, irreversible deformation begins [10], [11]. The Voigt model, which consists of the spring H_3 and the dash-pot N_3 in parallel, describes movement of the shift of material foreword in the direction of tool movement and prolonged viscoelastic deformation.

The process describing relation of brittle and ductile fracture of material is presented in (*Fig. 1*). Indeed, we can assume that the brittle fracture corresponds to break of elastic external element H_1 and viscous fracture corresponds to the break of elastic internal element H_2 which is preceded by the relative shift of viscous element N_2 [3]. Elements of mechanical system can be considered in relation to the direction of deformation with the input and output, the direction of the pointer in the (*Fig. 1*) indicates the direction of deformation of the system.

The differential constitutive relations between stress and strain for the model describing the process of chip formation can be presented in the form of the following rheological equation [12]:

$$a_1\ddot{\sigma} + a_2\dot{\sigma} + a_3(\sigma \pm \sigma_y) = a_4\ddot{\varepsilon} + a_5\dot{\varepsilon} + a_6\varepsilon \tag{1}$$

where coefficients a_i $(i = 1, \cdots, 6)$ depend on stiffness coefficients and coefficients of linear resistance, σ_y is a yield stress.

The solutions and analysis of this rheological equation were studied in [10]. We derive the relations between coefficients of the rheological equation (1) and the stiffness and viscosity of material of the mechanical system. We write the equation (1) in the short-hand notation using integral formulation and the Laplace transform. For the Ishlinskiy model we have

$$z_I(p) = \frac{p}{c_1} + \frac{p}{\beta_2 \cdot p + c_2} = \frac{\beta_2 p^2 + (c_1 + c_2) \cdot p}{\beta_2 c_1 \cdot p + c_1 c_2}$$

where the properties of elastic elements H_1 and H_2 of the Ishlinskiy model are described by stiffness coefficients c_1 and c_2 the dash-pot element N_1 is characterized by the coefficient of linear resistance β_2 and $p^i = \frac{\partial^i}{\partial t^i}$ are the linear differential operators.

For the model of Voigt, the operator resistance takes the form

$$z_V(p) = \frac{p}{\beta_3 \cdot p + c_3}$$

where H_3 and N_3 are described by the stiffness coefficient c_3 and β_3 the coefficient of linear resistance respectively.

The entire model describing the process of chip formation can be presented in the following form

$$z(p) = p \cdot \frac{\beta_2\beta_3 \cdot p^2 + (\beta_2 c_1 + \beta_2 c_3 + \beta_3 c_1 + \beta_3 c_2) \cdot p + (c_1 c_2 + c_2 c_3 + c_1 c_3)}{\beta_2\beta_3 c_1 \cdot p^2 + (\beta_2 c_1 c_3 + \beta_3 c_1 c_2) \cdot p + c_1 c_2 c_3} \tag{2}$$

In order to simplify the calculations, we introduce the following notations for the coefficients of differential operator p and free terms in the numerator and denominator of equation (2):

$$\begin{cases} a_1 = \beta_2\beta_3 \\ a_2 = \beta_2 c_1 + \beta_2 c_3 + \beta_3 c_1 + \beta_3 c_2 \\ a_3 = c_1 c_2 + c_2 c_3 + c_1 c_3 \\ a_4 = \beta_2\beta_3 c_1 \\ a_5 = \beta_2 c_1 c_3 + \beta_3 c_1 c_2 \\ a_6 = c_1 c_2 c_3 \end{cases}$$

Then the operator resistance can be expressed in the form [3]

$$z(p) = p \cdot \frac{a_1 \cdot p^2 + a_2 \cdot p + a_3}{a_4 \cdot p^2 + a_5 \cdot p + a_6},$$

it means that returning to the space of originals we obtain the rheological equation (1), which define the relation between stress and deformation of the mechanical system.

To motivate the adequacy of the rheological model (1) we assume that the deformation in time is supposed to be known and solve this equation for the stress. We substitute σ in the equation (1) by a new variable $x = a_3(\sigma \pm \sigma_y)$ and get

$$\ddot{x} + 2\gamma\dot{x} + \omega_0^2 x = f(t), \tag{3}$$

where

$\omega_0 = \sqrt{\frac{a_3}{a_1}} = \sqrt{\frac{c_1 c_2 + c_2 c_3 + c_1 c_3}{\beta_2\beta_3}}$ is a frequency,

$\gamma = \frac{a_2}{2a_1} = \frac{\beta_2 c_1 + \beta_2 c_3 + \beta_3 c_1 + \beta_3 c_2}{2\beta_2\beta_3}$ is a dumping constant,

$f(t) = f(\varepsilon, \dot{\varepsilon}, \ddot{\varepsilon}) = \frac{a_3 a_4 \cdot \ddot{\varepsilon} + a_3 a_5 \cdot \dot{\varepsilon} + a_3 a_6 \varepsilon}{a_1}$.

Let us denote the vibration frequency by $\omega = \sqrt{\gamma^2 - \omega_0^2}$ The solution of homogeneous part of equation (3) for oscillation mode is

$$x(t) = e^{-\gamma t}(A\cos\omega t + B\sin\omega t), \qquad \text{for } \gamma^2 - \omega_0^2 < 0,$$

and for relaxation mode

$$x(t) = Ae^{(\omega-\gamma)t} + Be^{(-\omega-\gamma)t}, \qquad \text{for } \gamma^2 - \omega_0^2 > 0.$$

The general solution of equation (3) for relaxation mode is

$$x(t) = e^{-\gamma t}\left[\frac{1}{2}e^{\omega t} \cdot \int \frac{f(t)e^{(\gamma-\omega)t}}{\omega}dt - \frac{1}{2}e^{-\omega t} \cdot \int \frac{f(t)e^{(\gamma+\omega)t}}{\omega}dt + Ae^{\omega t} + Be^{-\omega t}\right] \tag{4}$$

With a fixed value of deformation $\varepsilon = \varepsilon_0 = const$ function $f(t)$ can be expressed as follows

$$f(t) = \frac{a_3 a_6 \varepsilon_0}{a_1},$$

the phenomenon of stress relaxation is characteristic for a majority of real materials, and is consisting in a gradual decrease of stress in the medium, if the deformation is invariable.

After transition from variable x to variable σ and taking into account initial conditions $\sigma(0) = \sigma_0$ and $\dot{\sigma}(0) = const$ an equation describing stress relaxation takes the following form

$$\sigma(t) = \sigma_y + \frac{a_6\varepsilon_0}{a_1(\gamma^2-\omega^2)} + \frac{1}{2\omega}\Big[(\sigma_0 - \sigma_y)\big((\gamma+\omega)e^{\omega t} + (\omega-\gamma)e^{-\omega t}\big) - -\frac{a_6\varepsilon_0}{a_1}\Big(\frac{1}{\gamma-\omega}e^{\omega t} - \frac{1}{\gamma+\omega}e^{-\omega t}\Big) + \dot{\sigma}(0)(e^{\omega t} - e^{-\omega t})\Big] \cdot e^{-\gamma t} \quad (5)$$

From equation (5) we can conclude that for our rheological model stress relaxes to its equilibrium with two relaxation times $\tau_1 = \frac{1}{\gamma-\omega}$ and $\tau_2 = \frac{1}{\gamma+\omega}$. We get the following expression for the for the rates of relaxation $\gamma - \omega$ and $\gamma + \omega$ in the terms of stiffness coefficients c_i and coefficients of linear resistance β_i:

$$\gamma \pm \omega = \frac{a_2}{2a_1} \pm \sqrt{\frac{a_2^2 - 4a_1a_3}{4a_1^2}} = \frac{1}{2a_1}\left(a_2 \pm \sqrt{a_2^2 - 4a_1a_3}\right) =$$

$$= \frac{1}{2\beta_2\beta_3}\Big[(\beta_2c_1 + \beta_2c_3 + \beta_3c_1 + \beta_3c_2) \pm$$

$$\pm \sqrt{(\beta_2c_1 + \beta_2c_3 + \beta_3c_1 + \beta_3c_2)^2 - 4\beta_2\beta_3(c_1c_2 + c_2c_3 + c_1c_3)}\Big].$$

It follows from proposed rheological model in the zone of primary plastic deformation occur processes which generate instability of chip formation. The analysis of the developed plastic deformation of metal shows that this process has wavelike nature. At the moment which corresponds to the implementation of plastic deformation in the zone of plastic contact of chip with the tool, which reflects the elastic reaction of the workable material, the cut off layer undergoes the secondary deformation. Our theoretical studies were confirmed by experimental data which were conducted in the broader band for back rake angle α from -5° to 25° and for different values of cutting speed. It was determined in [2] that the form of chip by processing steel AISI 45 is following:

- discontinuous chip for α = -5° and cutting speed 10 m/min;
- built-up edge chip for α = 25° and cutting speed 25 m/min;
- continuous chip for α = 10° and cutting speed 75 m/min.

It confirms our studies on the origin of the primary relaxation phenomena, which induce the origination of the self-oscillating process by turning materials.

3. Finite element analysis of chip formation process and description of simulation model

The basis of all finite elements methods involves dividing the body into an equivalent system of small finite elements for which the relevant variables and quantities are determined only at the nodes of the elements. This procedure is called discretization or meshing. The accuracy of the solution depends on the total number of elements used and their variation in size and type. The elements must be made small enough to give relevant results and large enough to reduce time required for the simulation. In recent years, numerous special-purpose and general-purpose finite element packages have been used for metal cutting analysis: Deform 2D/3D, MSC.Marc., Thirdwave AdvantEdge, Abaqus, Ls-Dyna, etc. In modeling the plastic material flow there are three main formulations for simulation of metal cutting Eulerian, Lagrangian and Arbitrary Lagrangian-Eulerian (ALE). The last one combines the best features of Lagrangian and Eulerian formulations [13]. In this case, the mesh is not attached to the material and it can move to avoid distortion and update the free chip geometry. The mesh follows the material flow and problem is solved for displacements in Lagrangian step, while the mesh is regenerated and problem for velocities is solved in Eulerian step.

The thermo-mechanical modeling of flow stress of workpiece material plays very important role in metal cutting simulation. In finite element models flow stress is an instantaneous yield stress which depends on strain, strain rate and temperature. To describe the material flow during the cutting process an elasto-viscoplastic description of the material behavior can be written in the form of constitutive models:

$$\sigma = f(\varepsilon, \dot{\varepsilon}, T), \quad (6)$$

where σ is the Von-Mises stress, ε is the plastic strain, $\dot{\varepsilon}$ is the generalized strain rate and T is the temperature. The most widely used is Johnson-Cook material constitutive model. This model is based on torsion and dynamic Hopkinson bar test over a wide range of strain rates and temperatures [14]. This constitutive equation has the following form:

$$\sigma = (A + B\varepsilon^n)\left(1 + C\ln\frac{\dot{\varepsilon}}{\dot{\varepsilon}_0}\right)\left(1 - \left(\frac{T - T_r}{T_m - T_r}\right)^m\right) \quad (7)$$

The elastic-plastic term representing strain hardening is in the first parenthesis. The coefficient A is the yield strength value when the stressing rate is low, B is the hardening modulus and n is the hardening coefficient. The viscosity term, where C is the strain rate sensitivity coefficient, is in the parenthesis, it shows that flow stress of material increases when material is exposed to high strain rates. The last one is temperature softening term. T is the instantaneous temperature, T_r is the room temperature, T_m is the melting temperature of a given material and m is the thermal softening coefficient. Johnson-Cook constitutive model assumes that flow stress is affected by strain, strain rate and temperature independently.

In the present research we consider the finite element model used for the plane-strain orthogonal metal cutting simulation, which is based on the Lagrangian formulation in Third Wave Systems AdvantEdge simulation software. AdvantEdge integrates finite element numerics and material modeling appropriate for metal cutting. The software has comprehensive library of materials, input interface allows to set cutting parameters (feed rate, depth of cut, length of cut, cutting speed and initial temperature of the workpiece) as well as tool and workpiece geometries. Other parameters of cutting are fixed automatically, the user control on material parameters and solver are not allowed. The material model considers elastic-plastic strains, strain rate and has an isotropic power law for strain hardening. In AdvantEdge a staggered method is utilized for the purpose of coupling the mechanical and heat transfer equations. Geometrically identical meshes for the mechanical and thermal models are used. An isothermal mechanical step is taken first, it is followed by a rigid transient thermal step with constant heating from plastic work and friction. The finite deformation formulation uses a six-noded quadratic triangle elements. As the cutting layer transforms into chip, it separates from the workpiece splitting the nodes. The separation of nodes is achieved by continuous remeshing, the software enables element distortion around the cutting edge by updating the mesh periodically both refining large elements and coarsening small elements.

4. Conclusions

The rheological model in the form of a series connection of elastic-ductile-plastic relaxing medium of Ishlinskiy and the medium of Voigt describes the mechanical properties of chip formation process, but does not contain the evaluation of cutting temperature. The analysis of rheological model shows that instability of the process of cutting is caused by the wavelike nature of the plastic deformation and destruction of metal. Within the generalized rheological model of the chip formation process, material deformed in the cut off layer reflects the relaxation effect inherent in stress. Stress relaxes to its equilibrium value not according to the simple exponential law, but with a significantly more complicated law, with two relaxation times $\tau_1 = \frac{1}{\gamma-\omega}$ and $\tau_2 = \frac{1}{\gamma+\omega}$. At the moment which corresponds to the completion of plastic deformation in the zone of plastic contact of chip with the tool and which also reflects the elastic reaction of the workable material in the process of cutting, the cut off layer undergoes a second deformation. The instability of chip formation in the primary zone of the plastic deformation process is the basic reason for the appearance of instability within the process of cutting in the closed dynamic system of a machine tool. The analysis of the rheological equation (1) proves that the model enables an adequate description of the deformation process of chip formation and determination of the criteria to its transition to a non-stable mode, provoking self-excited oscillation.

High temperature in the cutting zone hostilely affects the strength, hardness and wear resistance of the cutting tool. Therefore, estimation of cutting temperature is a decisive aspect in the study of metal cutting. The future work on the present rheological model will focus on adding the temperature parameters into the rheological equation (1) describing the process of chip formation. To this end, will use the rheological model proposed by Malyshev [15]. For this model it is assumed that the plastic deformation of the metal in the shear zone can be considered as the result of compression of the metal layer, taking into account the friction of the chips on the front surface of the tool and the cutting temperature.

With the advent of efficient software packages, FEM has become one of the most powerful tools for the simulation and analysis of cutting process. This allows studying the cutting process in greater detail than possible in experiments. FEM simulation takes into account the material properties better than analytical models. FEM models allow to simulate the interaction of chip and tool in different forms. In spite of many advantages of FEM models, it is difficult to simulate the morphology of cutting chips. The continuous chip is often considered as more preferable, because it generates stable cutting forces. Moreover, it is easiest for simulation codes, but during experiments the sharp edged continuous chip that comes out at a high speed may be dangerous to the operator and may lead to unpredictable damage of the cutting tool. The majority of finite element codes simulates only continuous chips.

References

[1] Rybin, V.V. (1986) Large plastic deformation and fracture of metals. Metallurgiya, Moscow, 318 p.

[2] Maksarov, V., Olt, J., Laatsit, T, Leemet, T. (2008) Physical argumentation of deformation process potential control while cutting heavily processed material. Proceedings of 6th International DAAAM Baltic Conference INDUSTRIAL ENGINEERING, Tallinn, pp. 263-268.

[3] Maksarov, V.; Khalimonenko, A.; Olt, J. (2017). Managing the process of machining on machines on the basis of dynamic modelling for a technological system. Építőanyag - Journal of Silicate Based and Composite Materials, 69 (2), pp. 66–71, https://doi.org/10.14382/epitoanyag-jsbcm.2017.12.

[4] Olt, J., Liyvapuu, A., Madissoo, M., Maksarov, V. (2016) Dynamic simulation of chip formation in the process of cutting. Int. J. Mater. Prod. Tec. Vol. 53, No 14, pp. 1-14, https://doi.org/10.1504/IJMPT.2016.076363

[5] Arrazola, P. J., Ugarte, D., Montoya, J., Villar, A., Marya, S. (2005) Finite element modeling of chip formation process with Abaqus/Explicit 6.3. [Performance].VIII International Conference on Computational Plasticity, Barcelona, URL: http://congress.cimne.upc.es/complas05/admin/Files/FilePaper/p173.pdf

[6] Boros, B., Csörgö, A., Hidas, A., Kotnyek, B., Szabó, A., Kossa, A., Stépán, G. (2017) Two-Dimensional Finite Element Analysis of Turning Processes. Periodica Polytechnica Mechanical Engineering. Vol. 61, No 1, pp. 44-54, https://doi.org/10.3311/PPme.9283

[7] Öpöz, T.T., Chen, X. (2016) Chip formation mechanism using finite element simulation. J.Mech.Eng. Vol. 62, pp. 312-325, https://doi.org/10.5545/sv-jme.2016.3523

[8] Watmon, T. B., Xiao, D., Peter, O.-O. (2016) Finite element analysis of orthogonal metal machining. Int. J. Sci. Res. Inn. Tech. Vol. 3, No 2, pp. 46-55.

[9] Veitz, V., Maksarov, V. (2000) Dynamics and control of the process of chip formation with cutting-edge mechanical processing. NWPI, Sant-Petersburg, 225 p.

[10] Tärgla, T., Olt, J., Liivapuu, O. (2018) Simulation of plastic deformation and destruction in the process of chip formation. Matec Web of Conferences. Vol. 211, pp. 1-5, https://doi.org/10.1051/matecconf/201821117007

[11] Liivapuu, O., Olt, J., Tärgla, T. (to appear) Comparison between finite element analysis and rheological models for chip formation. Acta et Commentationes Universitatis Tartuensis de Mathematica.

[12] Olt, J., Maksarov, V. (2015) Development of chatter-resistant system of cutting tool. Proceedings of the DAAAM symposium. pp. 0223-0228, https://doi.org/10.2507/26th.daaam.proceedings.03

[13] Hughes, T. J. R. (2000) The finite element method. Linear static and dynamic finite element analysis. Prentice-hall, New Jersey, 704. p.

[14] Johnson, G.R., Cook, W. H. (1983) A constitutive model and data for metals subjected to large strains, high strain-rates and high temperatures. Proceedings of the 7th International Symposium of Ballistics. pp. 541-547.

[15] Malyshev, V.I. (2011) Essays on the history of science on cutting materials. TGU, Tolyatti, 314 p.

Ref.:

Olt, Jüri – **Liivapuu**, Olga: *Two approaches to the modelling of chip formation: rheological models and finite element analysis*
Építőanyag – Journal of Silicate Based and Composite Materials, Vol. 71, No. 5 (2019), 173–176. p.
https://doi.org/10.14382/epitoanyag-jsbcm.2019.30

GUIDELINE FOR AUTHORS

The manuscript must contain the followings: title; author's name, workplace, e-mail address; abstract, keywords; main text; acknowledgement (optional)**; references; figures, photos with notes; tables with notes; short biography** (information on the scientific works of the authors).

The full manuscript should not be more than 6 pages including figures, photos and tables. Settings of the word document are: 3 cm margin up and down, 2,5 cm margin left and right. Paper size: A4. Letter size 10 pt, type: Times New Roman. Lines: simple, justified.

TITLE, AUTHOR

The title of the article should be short and objective.

Under the title the name of the author(s), workplace, e-mail address.

If the text originally was a presentation or poster at a conference, it should be marked.

ABSTRACT, KEYWORDS

The abstract is a short summary of the manuscript, about a half page size. The author should give keywords to the text, which are the most important elements of the article.

MAIN TEXT

Contains: materials and experimental procedure (or something similar), results and discussion (or something similar), conclusions.

REFERENCES

References are marked with numbers, e.g. [6], and a bibliography is made by the reference's order. References should be provided together with the DOI if available.

Examples:

Journals:

[6] Mohamed, K. R. – El-Rashidy, Z. M. – Salama, A. A.: In vitro properties of nano-hydroxyapatite/chitosan biocomposites. *Ceramics International.* 37(8), December 2011, pp. 3265–3271, http://doi.org/10.1016/j.ceramint.2011.05.121

Books:

[6] Mehta, P. K. – Monteiro, P. J. M.: Concrete. Microstructure, properties, and materials. *McGraw-Hill*, 2006, 659 p.

FIGURES, TABLES

All drawings, diagrams and photos are figures. The **text should contain references to all figures and tables**. This shows the place of the figure in the text. Please send all the figures in attached files, and not as a part of the text. **All figures and tables should have a title**.

Authors are asked to submit color figures by submission. Black and white figures are suggested to be avoided, however, acceptable.

The figures should be: tiff, jpg or eps files, 300 dpi at least, photos are 600 dpi at least.

BIOGRAPHY

Max. 500 character size professional biography of the author(s).

CHECKING

The editing board checks the articles and informs the authors about suggested modifications. Since the author is responsible for the content of the article, the author is not liable to accept them.

CONTACT

Please send the manuscript in electronic format to the following e-mail address: femgomze@uni-miskolc.hu and epitoanyag@szte.org.hu or by post: Scientific Society of the Silicate Industry, Budapest, Bécsi út 122–124., H-1034, HUNGARY

We kindly ask the authors to give their e-mail address and phone number on behalf of the quick conciliation.

Építőanyag – *Journal of Silicate Based and Composite Materials*, Quarterly peer-reviewed periodical of the Hungarian Scientific Society of the Silicate Industry, SZTE. http://epitoanyag.org.hu

Information for immediate release

Professionals reveal the eco-friendly building materials for 2020

- Majority of professionals believe **bamboo (74%)** is the eco-friendly building material that will **experience** the **greatest increase** in **usage** within the property industry in **2020**
- Thereafter, **69%** expect **straw bales** to have a strong inclusion in **construction projects** scheduled for **next year**
- Contrastingly, **cork (38%)** is the eco-friendly building material that the experts predict will be **utilised** the **least** in the property industry during 2020

One of the biggest developments in the property industry has been that of eco-friendly building materials. Materials which essentially reduce the harmful environmental impact of building operations.

Interested in sustainable building, Sell House Fast surveyed 582 architects, engineers and construction (AEC) professionals to identify the eco-friendly building materials they expect the property (commercial as well as non-commercial) industry to increase using in 2020.

The eco-friendly building materials AEC professionals predict will see the biggest increase in usage within the property industry during 2020	
Bamboo	**74%**
Straw Bales	**69%**
Timbercrete	**61%**
Recycled Plastics	**56%**
Ferrock	**47%**
Hempcrete	**44%**
Cork	**38%**
AEC = architects, engineers and construction professionals	

Sell House Fast found that the majority of experts believe **bamboo (74%)** is the eco-friendly building material that will **experience** the **greatest increase** in **usage** within the property industry **next year.**

Thereafter, **69%** expect **straw bales** to have a strong inclusion **in construction projects** scheduled in 2020. Whilst slightly less feel the same way about **timbercrete (61%)**.

Contrastingly, **cork (38%)** is the eco-friendly building material that experts predict will be **utilised the least** by the property industry over the course of 2020.

Robby du Toit, the Managing Director of Sell House Fast commented: "The property industry is more eco-conscious than ever before. This has led to a surge in the innovation and development of eco-friendly building materials. As professionals become better acquainted with the properties and benefits of different eco-friendly building materials, their adoption rate in construction projects can expect to see a positive increase. This research certainly highlights the eco-friendly building materials that will have a big impact in 2020".

SELLHOUSEFAST.UK

What are the eco-friendly building materials?

Bamboo: Bamboo is light-weight and has tensile strength. Bamboo is the ideal replacement for expensive and heavy imported building materials. Bamboo provides a great alternative to concrete and rebar construction.	**74%**
69%	**Straw Bales:** Straw bale is a renewable resource that can be used to replace concrete, plaster, wood, fiberglass, stone and gypsum when building walls. Straw bales naturally have high fire-retardant as well as insulating (for hot and cold climates) qualities.
Timbercrete: Timbercrete is a mix of sawdust and concrete. Timbercrete is much lighter than concrete. Also, the sawdust element replaces some of the more energy-intensive components found in normal concrete. Timbercrete is versatile and can be shaped into bricks, blocks etc.	**61%**
56%	**Recycled Plastics:** Concrete made from ground-up rubbish and recycled plastics. By doing so, reducing greenhouse gas emissions and creating a new beneficial way of utilising plastic waste that would otherwise just be left clogging up landfills.
Ferrock: Ferrock combines various recycled materials (e.g. steel dust) to create a building material that not only resembles concrete but is even stronger. Ferrock absorbs and seals carbon dioxide as part of the drying and hardening process, thus making it less CO2 intensive than concrete.	**47%**
44%	**Hempcrete:** Hempcrete (a bio-composite material) is formed from the inner fibres of hemp plants. The hemp fibres are treated with lime to create concrete-like shapes which are not only durable but super-lightweight.
Cork: Cork is made from the tree bark of cork oak. Cork does not absorb water or rot. Likewise, if left uncoated – cork is naturally fire resistant. Cork is ideal for flooring and insulation sheets due to its noise as well as shock adsorption attributes.	**38%**

Notes to editors: Please note, if you use any of this press release and/or information tables, please credit https://www.sellhousefast.uk/

Precursor-BioBased

Developing novel precursor fibre (PF) materials from blends of modified lignin and biopolymers which can be converted to carbon fibre (CF) using industry standard heating processes so that current manufacturing plant can continue to be used.

Energy efficient / cost reduction

Reducing energy consumption, including CO2 emissions, associated with the traditional manufacture of CF through the development of new low energy, cost effective biobased PF to CF conversion technologies.

Carbon Fibre

Establishing a new value chain for lignin by utilising low commercial value material to produce CF which will in turn be processed into carbon fibre reinforced polymers (CFRP).

Composites

Enabling EU based companies to build a technological lead and competitive advantage through the establishment of an indigenous capability to manufacture carbon fibre from sustainable precursors using energy efficient and cost-effective technology; this is of paramount importance for European competitiveness in the composites market.